

## 9 The strong coupling $\alpha_s$

Authors : L. Del Debbio, P. Petreczky, S. Sint

### 9.1 Introduction

The strong coupling  $\alpha_s(\mu) = \bar{g}_s^2(\mu)/(4\pi)$  defined at scale  $\mu$ , is the parameter that determines the strength of strong interactions in the Standard Model. It plays a key role in the understanding of QCD and in its application to collider physics, where it is ubiquitous in calculations of physical processes, e.g., at the LHC. For example, the parametric uncertainty from  $\alpha_s$  is one of the dominant sources of uncertainty in the Standard Model predictions for the Higgs boson [1] and top quark cross sections, see, e.g., Ref. [2]. In order to fully exploit the experimental results that will be collected during the high-luminosity run of the LHC in the near future, it is mandatory to reduce the uncertainty on  $\alpha_s$  below 1%. Similarly, high-accuracy determinations of this coupling will help in understanding the stability of the vacuum of the Standard Model and will yield one of the essential boundary conditions for completions of the Standard Model at high energies [3–10]. At this level of precision, it becomes imperative to have a robust understanding of systematic errors. Lattice simulations are ideally placed to play a central role in this quest. In the following we try to summarize the main features of the lattice approach in a way that we hope is understandable by nonexperts. For recent, complementary review articles, we refer the reader to Refs. [11, 12].

In order to determine the running coupling at scale  $\mu$

$$\alpha_s(\mu) = \frac{\bar{g}_s^2(\mu)}{4\pi}, \quad (282)$$

we should first “measure” a short-distance quantity  $\mathcal{Q}$  at scale  $\mu$  either experimentally or by lattice calculations, and then match it to a perturbative expansion in terms of a running coupling, conventionally taken as  $\alpha_{\overline{\text{MS}}}(\mu)$ ,

$$\mathcal{Q}(\mu) = c_1 \alpha_{\overline{\text{MS}}}(\mu) + c_2 \alpha_{\overline{\text{MS}}}^2(\mu) + \dots. \quad (283)$$

We note that in some cases also a lowest-order constant term,  $c_0$ , may be present; in the following, we always assume that such a term has been subtracted on both sides and absorbed in a re-definition of  $\mathcal{Q}(\mu)$ . We distinguish between phenomenological and lattice determinations of  $\alpha_s$ , the essential difference being the origin of the values of  $\mathcal{Q}$  in Eq. (283). The basis of phenomenological determinations are experimentally measurable cross sections or decay widths from which  $\mathcal{Q}$  is defined. These cross sections have to be sufficiently inclusive and at sufficiently high scales such that perturbation theory can be applied. Often hadronization corrections have to be used to connect the observed hadronic cross sections to the perturbative ones. Experimental data at high  $\mu$ , where perturbation theory is progressively more precise, usually have increasing experimental errors, not least due to the very smallness of  $\alpha_s(\mu)$ . Hence, it is not easy to find processes that allow one to follow the  $\mu$ -dependence of a single  $\mathcal{Q}(\mu)$  over a range where  $\alpha_s(\mu)$  changes significantly and precision is maintained. Note also that determinations of  $\alpha_s$  from experimental data at hadron colliders necessarily require a simultaneous fit of the Parton Distribution Functions (PDFs) [13], making the whole procedure more complicated and prone to systematic errors.

In contrast, in lattice gauge theory, one can design  $\mathcal{Q}(\mu)$  Euclidean short-distance quantities that are not directly related to experimental observables. This allows us to follow the  $\mu$ -dependence until the perturbative regime is reached and nonperturbative “corrections” are negligible. The only experimental input for lattice computations of  $\alpha_s$  are the masses or decay constants of hadrons, which fixes the overall energy scale of the theory and the quark masses. Therefore, experimental errors are completely negligible and issues such as hadronization do not occur. We can construct many short-distance quantities that are easy to calculate non-perturbatively in lattice simulations with small statistical uncertainties. We can also simulate at parameter values that do not exist in nature (for example, with unphysical quark masses between bottom and charm) to help control systematic uncertainties. These features mean that precise results for  $\alpha_s$  can be achieved with lattice-gauge-theory computations. Further, as in phenomenological determinations, the different methods available to determine  $\alpha_s$  in lattice calculations with different associated systematic uncertainties enable valuable cross-checks. Practical limitations are discussed in the next section, but a simple one is worth mentioning here. Experimental results (and therefore the phenomenological determinations) of course have all quarks present, while in lattice gauge theories in practice only the lighter ones are included and one is then forced to use the matching at thresholds, as discussed in the following subsection.

It is important to keep in mind that the dominant source of uncertainty in most present day lattice-QCD calculations of  $\alpha_s$  are from the truncation of continuum/lattice perturbation theory and from discretization errors. Perturbative truncation errors are of particular concern because they often cannot easily be estimated from studying the data itself. Perturbation theory provides an asymptotic series and the size of higher-order coefficients can sometimes turn out to be larger than suggested by naive expectations based on power counting from the behaviour of lower-order terms. We note that perturbative truncation errors are also the dominant source of uncertainty in several of the phenomenological determinations of  $\alpha_s$ .

The various phenomenological approaches to determining the running coupling constant,  $\alpha_{\overline{\text{MS}}}^{(5)}(M_Z)$  are summarized by the Particle Data Group [14]. The PDG review lists five categories of phenomenological results used to obtain the running coupling: using hadronic  $\tau$  decays, hadronic final states of  $e^+e^-$  annihilation, deep inelastic lepton–nucleon scattering, electroweak precision data, and high-energy hadron-collider data. Excluding lattice results, the PDG, in their most recent update [15], quotes the weighted average as

$$\alpha_{\overline{\text{MS}}}^{(5)}(M_Z) = 0.1175(10), \quad \text{PDG 24 [15]} \quad (284)$$

compared to  $\alpha_{\overline{\text{MS}}}^{(5)}(M_Z) = 0.1176(11)$  of the older PDG 2020 [14]. For a general overview of the various phenomenological and lattice approaches see, e.g., Ref. [2]. The extraction of  $\alpha_s$  from  $\tau$  data, which is one of the most precise and thus has a large impact on the nonlattice average in Eq. (284), is especially sensitive to the treatment of higher-order perturbative terms as well as the treatment of nonperturbative effects. This is important to keep in mind when comparing our chosen range for  $\alpha_{\overline{\text{MS}}}^{(5)}(M_Z)$  from lattice determinations in Eq. (399) with the nonlattice average from the PDG.

### 9.1.1 Scheme and scale dependence of $\alpha_s$ and $\Lambda_{\text{QCD}}$

Despite the fact that the notion of the QCD coupling is initially a perturbative concept, the associated  $\Lambda$ -parameter is nonperturbatively defined,

$$\begin{aligned}\Lambda &\equiv \mu \varphi_s(\bar{g}_s(\mu)), \\ \varphi_s(\bar{g}_s) &= (b_0 \bar{g}_s^2)^{-b_1/(2b_0^2)} e^{-1/(2b_0 \bar{g}_s^2)} \exp \left[ - \int_0^{\bar{g}_s} dx \left( \frac{1}{\beta(x)} + \frac{1}{b_0 x^3} - \frac{b_1}{b_0^2 x} \right) \right],\end{aligned}\quad (285)$$

provided that  $\beta(\bar{g}_s) = \mu \frac{\partial \bar{g}_s(\mu)}{\partial \mu}$  is the full renormalization group function in the (mass-independent) scheme which defines  $\bar{g}_s$ . The first two coefficients,  $b_0$  and  $b_1$ , in the perturbative expansion

$$\beta(x) \sim -b_0 x^3 - b_1 x^5 + \dots, \quad (286)$$

are scheme-independent (“universal”) and given by

$$b_0 = \frac{1}{(4\pi)^2} \left( 11 - \frac{2}{3} N_f \right), \quad b_1 = \frac{1}{(4\pi)^4} \left( 102 - \frac{38}{3} N_f \right). \quad (287)$$

In the  $\overline{\text{MS}}$  scheme, the coefficients of the  $\beta$ -function have been calculated up to 5-loop order, i.e.,  $b_2$ ,  $b_3$  and  $b_4$  are known [16–20].

As a renormalization-group-invariant quantity, the  $\Lambda$ -parameter is  $\mu$ -independent. However, it does depend on the renormalization scheme albeit in an exactly computable way: A perturbative change of the coupling from one mass-independent scheme  $S$  to another (taken here to be the  $\overline{\text{MS}}$  scheme) takes the form

$$g_{\overline{\text{MS}}}^2(\mu) = g_S^2(\mu) (1 + c_g^{(1)} g_S^2(\mu) + \dots), \quad (288)$$

where  $c_g^{(i)}$ ,  $i \geq 1$  are finite coefficients. Performing this change in the expression for the  $\Lambda$ -parameter at a large scale  $\mu$ , so that higher-order terms can be neglected, one obtains the exact relation between the respective  $\Lambda$ -parameters of the two schemes,

$$\Lambda_{\overline{\text{MS}}} = \Lambda_S \exp \left[ c_g^{(1)} / (2b_0) \right]. \quad (289)$$

Note that this exact relation allows us to nonperturbatively define  $\Lambda_{\overline{\text{MS}}}$ , by starting from any nonperturbatively defined scheme  $S$  for which  $c_g^{(1)}$  is known. Given the high-order knowledge (5-loop by now) of  $\beta_{\overline{\text{MS}}}$  then means that the errors in  $\alpha_{\overline{\text{MS}}}(m_Z)$  correspond almost completely with the errors of  $\Lambda_S$ . We will therefore mostly discuss them in that way. Starting from Eq. (285), we have to consider (i) the error of  $\bar{g}_S^2(\mu)$  (denoted as  $(\frac{\Delta\Lambda}{\Lambda})_{\Delta\alpha_S}$ ) and (ii) the truncation error in  $\beta_S$  (denoted as  $(\frac{\Delta\Lambda}{\Lambda})_{\text{trunc}}$ ). Concerning (ii), note that knowledge of  $c_g^{(n_1)}$  for the scheme  $S$  means that  $\beta_S$  is known to  $n_1 + 1$  loop order;  $b_{n_1}$  is known. We thus see that in the region where perturbation theory can be applied, the following errors of  $\Lambda_S$  (or consequently  $\Lambda_{\overline{\text{MS}}}$ ) have to be considered

$$\left( \frac{\Delta\Lambda}{\Lambda} \right)_{\Delta\alpha_S} = \frac{\Delta\alpha_S(\mu)}{8\pi b_0 \alpha_S^2(\mu)} \times [1 + \mathcal{O}(\alpha_S(\mu))], \quad (290)$$

$$\left( \frac{\Delta\Lambda}{\Lambda} \right)_{\text{trunc}} = k \alpha_S^{n_1}(\mu) + \mathcal{O}(\alpha_S^{n_1+1}(\mu)), \quad (291)$$

where the pre-factor  $k$  depends on  $b_{n_1+1}$  and in typical good schemes such as  $\overline{\text{MS}}$  it is numerically of order one. Statistical and systematic errors such as discretization effects contribute to  $\Delta\alpha_S(\mu)$ . In the above we dropped a scheme subscript for the  $\Lambda$ -parameters because of Eq. (289).

By convention  $\alpha_{\overline{\text{MS}}}$  is usually quoted at a scale  $\mu = M_Z$  where the appropriate effective coupling is the one in the five-flavour theory:  $\alpha_{\overline{\text{MS}}}^{(5)}(M_Z)$ . In order to obtain it from a result with fewer flavours, one connects effective theories with different number of flavours as discussed by Bernreuther and Wetzel [21]. For example, one considers the  $\overline{\text{MS}}$  scheme, matches the three-flavour theory to the four-flavour theory at a scale given by the charm-quark mass [22–24], runs with the 5-loop  $\beta$ -function [16–20] of the four-flavour theory to a scale given by the  $b$ -quark mass, and there matches to the five-flavour theory, after which one runs up to  $\mu = M_Z$  with the five-loop  $\beta$ -function. For the matching relation at a given quark threshold we use the mass  $m_\star$  which satisfies  $m_\star = \overline{m}_{\overline{\text{MS}}}^{(N_f)}(m_\star)$ , where  $\overline{m}$  is the running mass (analogous to the running coupling). Then

$$\bar{g}_{N_f-1}^2(m_\star) = \bar{g}_{N_f}^2(m_\star) \times [1 + 0 \times \bar{g}_{N_f}^2(m_\star) + \sum_{n \geq 2} t_n \bar{g}_{N_f}^{2n}(m_\star)] \quad (292)$$

with [22, 24, 25]

$$t_2 = \frac{1}{(4\pi^2)^2} \frac{11}{72}, \quad (293)$$

$$t_3 = \frac{1}{(4\pi^2)^3} \left[ -\frac{82043}{27648} \zeta_3 + \frac{564731}{124416} - \frac{2633}{31104} (N_f - 1) \right], \quad (294)$$

$$t_4 = \frac{1}{(4\pi^2)^4} [5.170347 - 1.009932(N_f - 1) - 0.021978(N_f - 1)^2], \quad (295)$$

(where  $\zeta_3$  is the Riemann zeta-function) provides the matching at the thresholds in the  $\overline{\text{MS}}$  scheme. Often the software packages **RunDec** [26, 27] or the more recent one, **REvolver** [28], are used for quark-threshold matching and running in the  $\overline{\text{MS}}$ -scheme.

While  $t_2, t_3, t_4$  are numerically small coefficients, the charm-threshold scale is also relatively low and so there are nonperturbative uncertainties in the matching procedure, which are difficult to estimate but which we assume here to be negligible. This is supported by nonperturbative tests [29], where perturbative decoupling relations in the  $\overline{\text{MS}}$  scheme were shown to quantitatively describe decoupling at the few permille level, down to the charm-quark region. Obviously there is no perturbative matching formula across the strange “threshold”; here matching is entirely nonperturbative. Model-dependent extrapolations of  $\bar{g}_{N_f}^2$  from  $N_f = 0, 2$  to  $N_f = 3$  were done in the early days of lattice gauge theory. We will include these in our listings of results but not in our estimates, since such extrapolations are based on untestable assumptions.

### 9.1.2 Overview of the review of $\alpha_s$

We begin by explaining lattice-specific difficulties in Sec. 9.2.1 and the FLAG criteria designed to assess whether the associated systematic uncertainties can be controlled and estimated in a reasonable manner. These criteria remain unchanged since the FLAG 19 report, as there has still not been sufficiently broad progress to make them more stringent. However, in this report we have implemented a systematic scale variation to help assess systematic errors due to the

truncation of the perturbative series. Scale variations are widely used in phenomenology and its application to lattice determinations has been advocated in Ref. [11]. We explain the procedure at the end of this introduction and, where possible, we will quote corresponding results.

We then discuss, in Sec. 9.3 – Sec. 9.9, the various lattice approaches and results from calculations with  $N_f = 0, 2, 2+1$ , and  $2+1+1$  flavours. For lattice approaches with neither a new result nor a result passing all FLAG criteria, we refer to the discussion in previous FLAG reports. In particular, this regards determinations of  $\alpha_s$  from QCD vertices and from the eigenvalue spectrum of the Dirac operator.

Since FLAG 21, the strategy of nonperturbative renormalization by decoupling, as introduced by the ALPHA collaboration in Ref. [30], produced a new result for  $\alpha_s$ . It is important to realize that this method shifts the perspective on results for the  $\Lambda$ -parameter with unphysical flavour numbers, in particular for  $N_f = 0$ : Such results can be related to  $N_f > 0$  results by a nonperturbative matching calculation. We therefore made an effort to review  $N_f = 0$  results, some of which are now over 20 years old. In particular, we also included a new section on the gradient-flow (GF) coupling in infinite space-time volume, even though only results for  $N_f = 0$  exist at the moment.

After the discussion of the various lattice methods, we proceed, in Sec. 9.10, with the averages together with our best estimates for  $\alpha_{\overline{\text{MS}}}^{(5)}$ . These are currently determined from three- and four-flavour QCD simulations only, however, with the decoupling result also relying on the  $N_f = 0$   $\Lambda$ -parameter as input. Therefore, we discuss results for the  $N_f = 0$   $\Lambda$ -parameter in some detail, in addition to the physical cases with  $N_f = 3, 4$  and  $5$ , where the latter is derived from  $N_f = 3$  and  $4$  results by the standard perturbative evolution across the bottom-quark threshold.

### 9.1.3 Additions with respect to the FLAG 21 report

Since the FLAG 21 report there were two new papers on  $N_f = 3$ :

Petreczky 20 [31] from heavy-quark current two-point functions (Sec. 9.8).

ALPHA 22 [32] from the decoupling method (Sec. 9.4).

In  $N_f = 0$  QCD, there are a number of additional works:

Brihan 21 [33], from step-scaling with the twisted periodic gradient-flow coupling (Sec. 9.3).

Hasenfratz 23 [34] and Wong 23 [35] from the GF scheme in infinite volume (Sec. 9.9)

Chimirri 23 [36] from heavy-quark current two-point functions (Sec. 9.8)

Brambilla 23 [37], from the force between static quarks (Sec. 9.5)

## 9.2 General issues

### 9.2.1 Discussion of criteria for computations entering the averages

As in the PDG review, we only use calculations of  $\alpha_s$  published in peer-reviewed journals, and that use NNLO or higher-order perturbative expansions, to obtain our final range in

Sec. 9.10. We also, however, introduce further criteria designed to assess the ability to control important systematics, which we describe here. Some of these criteria, e.g., that for the continuum extrapolation, are associated with lattice-specific systematics and have no continuum analogue. Other criteria, e.g., that for the renormalization scale, could in principle be applied to nonlattice determinations. Expecting that lattice calculations will continue to improve significantly in the near future, our goal in reviewing the state-of-the-art here is to be conservative and avoid prematurely choosing an overly small range.

In lattice calculations, we generally take  $\mathcal{Q}$  to be some combination of physical amplitudes or Euclidean correlation functions which are free from UV and IR divergences and have a well-defined continuum limit. Examples include the force between static quarks and two-point functions of quark-bilinear currents.

In comparison to values of observables  $\mathcal{Q}$  determined experimentally, those from lattice calculations require two more steps. The first step concerns obtaining the scale  $\mu$  in physical units (GeV), given its value,  $a\mu$ , in lattice units. Ideally one compares the lattice result for some hadron mass  $aM_{\text{had}}$  with the known experimental result for  $M_{\text{had}}$  to determine  $a$  and thus  $\mu$  in physical units. Alternatively, convenient intermediate scales such as  $\sqrt{t_0}$ ,  $w_0$ ,  $r_0$ ,  $r_1$ , [38–41] can be used if their relation to an experimental dimensionful observable is established. For more details we refer to Sec. 11 on scale setting in this FLAG report. The low-energy scale  $\mu$  needs to be computed at the same lattice spacings (i.e., the same bare couplings) where  $\mathcal{Q}$  is determined, at least as long as one does not use the step-scaling method (see below). This induces a practical difficulty given present computing resources. In the determination of the low-energy reference scale the volume needs to be large enough to avoid finite-size effects. On the other hand, in order for the perturbative expansion of Eq. (283) to be reliable, one has to reach sufficiently high values of  $\mu$ , i.e., short enough distances. To avoid uncontrollable discretization effects the lattice spacing  $a$  has to be accordingly small. This means

$$L \gg \text{hadron size} \sim \Lambda_{\text{QCD}}^{-1} \quad \text{and} \quad 1/a \gg \mu, \quad (296)$$

(where  $L$  is the box size) and therefore

$$L/a \gg \mu/\Lambda_{\text{QCD}}. \quad (297)$$

The currently available computer power, however, limits  $L/a$ , typically to  $L/a = 32 - 96$ . Unless one accepts compromises in controlling discretization errors or finite-size effects, this means one needs to set the scale  $\mu$  according to

$$\mu \lll L/a \times \Lambda_{\text{QCD}} \sim 10 - 30 \text{ GeV}. \quad (298)$$

(Here  $\lll$  or  $\ggg$  means at least one order of magnitude smaller or larger.) Therefore,  $\mu$  can be  $1 - 3 \text{ GeV}$  at most. This raises the concern whether the asymptotic perturbative expansion truncated at 1-loop, 2-loop, or 3-loop in Eq. (283) is sufficiently accurate. There is a finite-size scaling method, usually called step-scaling method, which solves this problem by identifying  $\mu = 1/L$  in the definition of  $\mathcal{Q}(\mu)$ , see Sec. 9.3.

For the second step after setting the scale  $\mu$  in physical units (GeV), one should compute  $\mathcal{Q}$  on the lattice,  $\mathcal{Q}_{\text{lat}}(a, \mu)$  for several lattice spacings and take the continuum limit to obtain the left hand side of Eq. (283) as

$$\mathcal{Q}(\mu) \equiv \lim_{a \rightarrow 0} \mathcal{Q}_{\text{lat}}(a, \mu) \quad \text{with } \mu \text{ fixed}. \quad (299)$$

This is necessary to remove the discretization error.

Here it is assumed that the quantity  $\mathcal{Q}$  has a continuum limit, which is regularization-independent. The method discussed in Sec. 9.7, which is based on the perturbative expansion of a lattice-regulated, divergent short-distance quantity  $W_{\text{lat}}(a)$  differs in this respect and must be treated separately.

In summary, a controlled determination of  $\alpha_s$  needs to satisfy the following:

1. The determination of  $\alpha_s$  is based on a comparison of a short-distance quantity  $\mathcal{Q}$  at scale  $\mu$  with a well-defined continuum limit without UV and IR divergences to a perturbative expansion formula in Eq. (283).
2. The scale  $\mu$  is large enough so that the perturbative expansion in Eq. (283) is precise to the order at which it is truncated, i.e., it has good *asymptotic* convergence.
3. If  $\mathcal{Q}$  is defined by physical quantities in infinite volume, one needs to satisfy Eq. (297).
4. Nonuniversal quantities, i.e., quantities that depend on the chosen lattice regularization and do not have a nontrivial continuum limit need a separate discussion, see Sec. 9.7.

Conditions 2. and 3. give approximate lower and upper bounds for  $\mu$  respectively. It is important to see whether there is a window to satisfy 2. and 3. at the same time. If it exists, it remains to examine whether a particular lattice calculation is done inside the window or not.

Obviously, an important issue for the reliability of a calculation is whether the scale  $\mu$  that can be reached lies in a regime where perturbation theory can be applied with confidence. However, the value of  $\mu$  does not provide an unambiguous criterion. For instance, the Schrödinger Functional, or SF coupling (Sec. 9.3) is conventionally taken at the scale  $\mu = 1/L$ , but one could also choose  $\mu = 2/L$ . Instead of  $\mu$  we therefore define an effective  $\alpha_{\text{eff}}$ . For schemes such as SF (see Sec. 9.3) or  $qq$  (see Sec. 9.5) this is directly the coupling of the scheme. For other schemes such as the vacuum polarization we use the perturbative expansion Eq. (283) for the observable  $\mathcal{Q}$  to define

$$\alpha_{\text{eff}} = \mathcal{Q}/c_1. \quad (300)$$

As mentioned earlier, if there is an  $\alpha_s$ -independent term it should first be subtracted. Note that this is nothing but defining an effective, regularization-independent coupling, a physical renormalization scheme. For ease of notation, here and in what follows we denote by  $\alpha_s$  the coupling  $\alpha_{\overline{\text{MS}}}(\mu)$  that appears in Eq. (283).

Let us now comment further on the use of the perturbative series. Since it is only an asymptotic expansion, the remainder  $R_n(\mathcal{Q}) = \mathcal{Q} - \sum_{i \leq n} c_i \alpha_s^i$  of a truncated perturbative expression  $\mathcal{Q} \sim \sum_{i \leq n} c_i \alpha_s^i$  cannot just be estimated as a perturbative error  $k \alpha_s^{n+1}$ . The error is nonperturbative. Often one speaks of “nonperturbative contributions”, but nonperturbative and perturbative cannot be strictly separated due to the asymptotic nature of the series (see, e.g., Ref. [42]).

Still, we do have some general ideas concerning the size of nonperturbative effects. The known ones such as instantons or renormalons decay for large  $\mu$  like inverse powers of  $\mu$  and are thus roughly of the form

$$\exp(-\gamma/\alpha_s), \quad (301)$$



with some positive constant  $\gamma$ . Thus we have, loosely speaking,

$$\mathcal{Q} = c_1\alpha_s + c_2\alpha_s^2 + \dots + c_n\alpha_s^n + \mathcal{O}(\alpha_s^{n+1}) + \mathcal{O}(\exp(-\gamma/\alpha_s)). \quad (302)$$

For small  $\alpha_s$ , the  $\exp(-\gamma/\alpha_s)$  is negligible. Similarly the perturbative estimate for the magnitude of relative errors in Eq. (302) is small; as an illustration for  $n = 3$  and  $\alpha_s = 0.2$  the relative error is  $\sim 0.8\%$  (assuming coefficients  $|c_{n+1}/c_1| \sim 1$ ).

For larger values of  $\alpha_s$  nonperturbative effects can become significant in Eq. (302). An instructive example comes from the values obtained from  $\tau$  decays, for which  $\alpha_s \approx 0.3$ . Here, different applications of perturbation theory (fixed order and contour improved) each look reasonably asymptotically convergent but the difference does not seem to decrease much with the order (see, e.g., the contribution by Pich to Ref. [43]; see, however, also the discussion in Refs. [44, 45]). In addition, nonperturbative terms in the spectral function may be nonnegligible even after the integration up to  $m_\tau$  (see, e.g., Refs. [46], [47]). All of this is because  $\alpha_s$  is not really small.

Since the size of the nonperturbative effects is very hard to estimate one should try to avoid such regions of the coupling. In a fully controlled computation one would like to verify the perturbative behaviour by changing  $\alpha_s$  over a significant range instead of estimating the errors as  $\sim \alpha_s^{n+1}$ . Some computations try to take nonperturbative power ‘corrections’ to the perturbative series into account by including such terms in a fit to the  $\mu$ -dependence. We note that this is a delicate procedure, as a term like, e.g.,  $\alpha_s(\mu)^3$  is hard to distinguish from a  $1/\mu^2$  term when the  $\mu$ -range is restricted and statistical and systematic errors are present. We consider it safer to restrict the fit range to the region where the power corrections are negligible compared to the estimated perturbative error.

The above considerations lead us to the following special criteria for the determination of  $\alpha_s$ :

- Renormalization scale
  - ★ all data points relevant in the analysis have  $\alpha_{\text{eff}} < 0.2$
  - all data points have  $\alpha_{\text{eff}} < 0.4$  and at least one  $\alpha_{\text{eff}} \leq 0.25$
  - otherwise
- Perturbative behaviour
  - ★ verified over a range of a factor 4 change in  $\alpha_{\text{eff}}^{n_l}$  without power corrections or alternatively  $\alpha_{\text{eff}}^{n_l} \leq \frac{1}{2}\Delta\alpha_{\text{eff}}/(8\pi b_0\alpha_{\text{eff}}^2)$  is reached
  - agreement with perturbation theory over a range of a factor  $(3/2)^2$  in  $\alpha_{\text{eff}}^{n_l}$  possibly fitting with power corrections or alternatively  $\alpha_{\text{eff}}^{n_l} \leq \Delta\alpha_{\text{eff}}/(8\pi b_0\alpha_{\text{eff}}^2)$  is reached
  - otherwise

Here  $\Delta\alpha_{\text{eff}}$  is the accuracy cited for the determination of  $\alpha_{\text{eff}}$  and  $n_l$  is the loop order to which the connection of  $\alpha_{\text{eff}}$  to the  $\overline{\text{MS}}$  scheme is known. Recall the discussion around Eqs. (290,291); the  $\beta$ -function of  $\alpha_{\text{eff}}$  is then known to  $(n_l + 1)$ -loop order.<sup>1</sup>

<sup>1</sup>Once one is in the perturbative region with  $\alpha_{\text{eff}}$ , the error in extracting the  $\Lambda$ -parameter due to the truncation of perturbation theory scales like  $\alpha_{\text{eff}}^{n_l}$ , as discussed around Eq. (291). In order to detect/control such corrections properly, one needs to change the correction term significantly; we require a factor of four for a ★ and a factor  $(3/2)^2$  for a ○. An exception to the above is the situation where the correction terms are small anyway, i.e.,  $\alpha_{\text{eff}}^{n_l} \approx (\Delta\Lambda/\Lambda)_{\text{trunc}} < (\Delta\Lambda/\Lambda)_{\Delta\alpha} \approx \Delta\alpha_{\text{eff}}/(8\pi b_0\alpha_{\text{eff}}^2)$  is reached.



- Continuum extrapolation

At a reference point of  $\alpha_{\text{eff}} = 0.3$  (or less) we require

- ★ three lattice spacings with  $\mu a < 1/2$  and full  $\mathcal{O}(a)$  improvement,  
or three lattice spacings with  $\mu a \leq 1/4$  and 2-loop  $\mathcal{O}(a)$  improvement,  
or  $\mu a \leq 1/8$  and 1-loop  $\mathcal{O}(a)$  improvement
- three lattice spacings with  $\mu a < 3/2$  reaching down to  $\mu a = 1$  and full  $\mathcal{O}(a)$  improvement,  
or three lattice spacings with  $\mu a \leq 1/4$  and 1-loop  $\mathcal{O}(a)$  improvement
- otherwise

In addition to the above criteria we have looked at scale variations as a general mean to assess perturbative behaviour (cf. subsection below). Continuum extrapolations are often not the primary concern in determinations of  $\alpha_s$ . Where appropriate we will evaluate the new FLAG data-driven criterion, by which the distance of the data to the continuum-extrapolated value is measured in units of the quoted error. If the observable is  $Q(a)$  with an extrapolated continuum value  $Q(0) \pm \Delta Q$  we look at the size of

$$\delta_{\min} = \frac{|Q(0) - Q(a_{\min})|}{\Delta Q}. \quad (303)$$

Some scepticism is warranted if  $\delta_{\min}$  exceeds 3 or so, although there may be cases where this can be justified. While we keep the core FLAG criteria unchanged, our general assessment will be informed by these measures.

We also need to specify what is meant by  $\mu$ . Here are our choices:

$$\begin{aligned} \text{step scaling} &: \mu = 1/L, \\ \text{heavy quark-antiquark potential} &: \mu = 2/r, \\ \text{observables in position space} &: \mu = 1/|x|, \\ \text{observables in momentum space} &: \mu = q, \\ \text{moments of heavy-quark currents} &: \mu = 2\overline{m}_c, \\ \text{Gradient-Flow (GF) scheme in infinite volume} &: \mu = 1/\sqrt{8t}, \end{aligned} \quad (304)$$

where  $|x|$  is the Euclidean norm of the four-vector  $x$ ,  $q$  is the magnitude of the momentum,  $\overline{m}_c$  is the heavy-quark mass (in the  $\overline{\text{MS}}$  scheme with  $N_f$  quarks, including the heavy-quark flavour) and usually taken around the charm-quark mass. The parameter  $t$  denotes the gradient-flow time. We note again that the above criteria cannot be applied when regularization-dependent quantities  $W_{\text{lat}}(a)$  are used instead of  $Q(\mu)$ . These cases are specifically discussed in Sec. 9.7.

In principle one should also account for electro-weak radiative corrections. However, both in the determination of  $\alpha_s$  at intermediate scales  $\mu$  and in the running to high scales, we expect electro-weak effects to be much smaller than the presently reached precision. Such effects are therefore not further discussed.

The attentive reader will have noticed that bounds such as  $\mu a < 3/2$  or at least one value of  $\alpha_{\text{eff}} \leq 0.25$  which we require for a ○ are not very stringent. There is a considerable difference between ○ and ★. We have chosen the above bounds, unchanged since FLAG 16, as not too many current computations would satisfy more stringent ones. Nevertheless, we

believe that the ○ criteria already give reasonable bases for estimates of systematic errors. An exception may be Cali 20 [48], which is discussed in detail in Sec. 9.6.

In anticipation of future changes of the criteria, we expect that we will be able to tighten our criteria for inclusion in the average, and that many more computations will reach the present ★ rating in one or more categories.

In addition to our explicit criteria, the following effects may influence the precision of results:

*Topology sampling:* In principle a good way to improve the quality of determinations of  $\alpha_s$  is to push to very small lattice spacings thus enabling large  $\mu$ . It is known that the sampling of field space becomes very difficult for the HMC algorithm when the lattice spacing is small and one has the standard periodic boundary conditions. In practice, for all known discretizations the topological charge slows down dramatically for  $a \approx 0.05$  fm and smaller [49–55]. Open boundary conditions solve the problem [56] but are not frequently used. Since the effect of the freezing on short-distance observables is not known, we also do need to pay attention to this issue. Remarks are added in the text when appropriate.

*Quark-mass effects:* We assume that effects of the finite masses of the light quarks (including strange) are negligible in the effective coupling itself where large, perturbative,  $\mu$  is considered.

*Scale setting:* The scale does not need to be very precise, since using the lowest-order  $\beta$ -function shows that a 3% error in the scale determination corresponds to a  $\sim 0.5\%$  error in  $\alpha_s(M_Z)$ . Since the errors of scale determinations are now typically at the 1-2 percent level or better, the corresponding error in  $\alpha_s(M_Z)$  will remain subdominant for the foreseeable future.

*Other limits/extrapolations:* Besides the continuum limit and the infinite-volume extrapolation of hadronic observables, further limits may be required, depending on the method employed. An obvious case is the large-mass extrapolation in the decoupling method. While in this case, an effective theory can be deployed to derive plausible fit functions, this is less clear in other cases. An example is the infinite space-time volume extrapolation in the GF scheme, which is needed to make contact with the available perturbative calculations. One would expect the volume dependence to be quite different at low and high energies, and there may be a complicated intermediate regime. Systematic uncertainties are then much harder to quantify and our approach necessarily is on a case-by-case basis. Data-driven criteria like the new FLAG continuum-limit criterion are considered, however, these may fail if the data does not sufficiently overlap with the true (and possibly unknown) asymptotic regime.

### 9.2.2 Physical scale

Since FLAG 19, a new FLAG working group on scale setting has been established. We refer to Sec. 11 for definitions and the current status. Note that the error from scale setting is sub-dominant for current  $\alpha_s$  determinations.

A popular scale choice has been the intermediate  $r_0$  scale, and its variant  $r_1$ , which both derive from the force between static quarks, see Eq. (335). One should bear in mind that their determination from physical observables also has to be taken into account. The phenomenological value of  $r_0$  was originally determined as  $r_0 \approx 0.49$  fm through potential models describing quarkonia [40]. Of course the quantity is precisely defined, independently of such model considerations. But a lattice computation with the correct sea-quark content is needed to determine a completely sharp value. When the quark content is not quite realistic, the value of  $r_0$  may depend to some extent on which experimental input is used to determine

(actually define) it.

The latest determinations from two-flavour QCD are  $r_0 = 0.420(14)–0.450(14)$  fm by the ETM collaboration [57, 58], using as input  $f_\pi$  and  $f_K$  and carrying out various continuum extrapolations. On the other hand, the ALPHA collaboration [59] determined  $r_0 = 0.503(10)$  fm with input from  $f_K$ , and the QCDSF collaboration [60] cites  $0.501(10)(11)$  fm from the mass of the nucleon (no continuum limit). Recent determinations from three-flavour QCD are consistent with  $r_1 = 0.313(3)$  fm and  $r_0 = 0.472(5)$  fm [61–63]. Due to the uncertainty in these estimates, and as many results are based directly on  $r_0$  to set the scale, we shall often give both the dimensionless number  $r_0\Lambda_{\overline{\text{MS}}}$ , as well as  $\Lambda_{\overline{\text{MS}}}$ . In the cases where no physical  $r_0$  scale is given in the original papers or we convert to the  $r_0$  scale, we use the value  $r_0 = 0.472$  fm. In case  $r_1\Lambda_{\overline{\text{MS}}}$  is given in the publications, we use  $r_0/r_1 = 1.508$  [63], to convert, which remains well consistent with the update [54] neglecting the error on this ratio. In some, mostly early, computations the string tension,  $\sqrt{\sigma}$  was used. We convert to  $r_0$  using  $r_0^2\sigma = 1.65 - \pi/12$ , which has been shown to be an excellent approximation in the relevant pure gauge theory [64, 65].

The more recent gradient-flow scales  $t_0, w_0$  are very attractive alternatives to  $r_0$ , as their determination is much simpler within a given simulation and most collaborations quote their values. The main downside are potentially large cutoff effects. We intend to transition from  $r_0$  to  $t_0$ . In this report we start by reporting  $N_f = 0$  results both with  $r_0$  and with  $\sqrt{8t_0}$ , where we use as conversion factor the central value of  $\sqrt{8t_0}/r_0 = 0.9435(97)$  from Dalla Brida 19 [30]. A general discussion of the various scales is given in the scale-setting section of this FLAG report, cf. Sec. 11.

### 9.2.3 Studies of truncation errors of perturbation theory

As discussed previously, we have to determine  $\alpha_s$  in a region where the perturbative expansion for the  $\beta$ -function, Eq. (286) in the integral Eq. (285), is reliable. In principle this must be checked, and is difficult to achieve as we need to reach up to a sufficiently high scale. A recipe routinely used to estimate the size of truncation errors of the perturbative series is to study the dependence on the renormalization scale of an observable evaluated at a fixed order in the coupling, as the renormalization scale is varied around some ‘optimal’ scale  $\mu_*$ , from  $\mu = \mu_*/2$  to  $2\mu_*$ . For examples, see Ref. [11].

Alternatively, or in addition, the renormalization scheme chosen can be varied, which investigates the perturbative conversion of the chosen scheme to the perturbatively defined  $\overline{\text{MS}}$  scheme and in particular ‘fastest apparent convergence’ when the ‘optimal’ scale is chosen so that the  $\mathcal{O}(\alpha_s^2)$  coefficient vanishes.

The ALPHA collaboration in Ref. [66] and ALPHA 17 [67], within the SF approach defined a set of  $\nu$ -schemes for which the 3-loop (scheme-dependent) coefficient of the  $\beta$ -function for  $N_f = 2 + 1$  flavours was computed to be  $b_2^\nu = -(0.064(27) + 1.259(1)\nu)/(4\pi)^3$ . The standard SF scheme has  $\nu = 0$ . For comparison,  $b_2^{\overline{\text{MS}}} = 0.324/(4\pi)^3$ . A range of scales from about 4 GeV to 128 GeV was investigated. It was found that while the procedure of varying the scale by a factor 2 up and down gave a correct estimate of the residual perturbative error for  $\nu \approx 0 \dots 0.3$ , for negative values, e.g.,  $\nu = -0.5$ , the estimated perturbative error is much too small to account for the mismatch in the  $\Lambda$ -parameter of  $\approx 8\%$  at  $\alpha_s = 0.15$ . This mismatch, however, did, as expected, still scale with  $\alpha_s^{n_1}$  with  $n_1 = 2$ . In the schemes with negative  $\nu$ , the coupling  $\alpha_s$  has to be quite small for scale variations of a factor 2 to correctly signal the perturbative errors.

For a systematic study of renormalization-scale variations as a measure of perturbative truncation errors in various lattice determinations of  $\alpha_s$ , we implement scale variations following the proposal in Ref. [11]. Scale variations are commonly used in phenomenology as a tool to investigate truncations errors. While they cannot give a precise estimate of the truncation errors, they provide a simple, quantitative test that can be uniformly applied to all observables. Furthermore, the implementation proposed in Ref. [11] does not rely on lattice data. The only inputs are the coefficients of the perturbative expansion of  $\alpha_{\text{eff}}$ , so that, in principle, an estimate of the truncation errors can be done *before* embarking in a numerical simulation. Here we shall summarize briefly the methodology, provide the coefficients of the perturbative expansions for the observables of interest in this review, and compute the corresponding truncation errors.

**Methodology** The use of scale variations for the determination of the missing higher-order uncertainties relies on a simple observation, namely that the scale  $\mu$  that appears on the left-hand side of Eq. (283) does not need to match the scale at which the running coupling constant is computed on the right-hand side of the same equation. Eq. (283) can be rewritten, with the same level of precision, as

$$\mathcal{Q}(\mu) = c_1 \alpha_{\overline{\text{MS}}}(\mu') + \sum_{k=2}^n c'_k(s) \alpha_{\overline{\text{MS}}}^k(\mu') + \mathcal{O}\left(\alpha_{\overline{\text{MS}}}^{n+1}(\mu')\right), \quad (s = \mu'/\mu). \quad (305)$$

The coefficients

$$c'_k(s) = \sum_{\ell=0}^{k-1} c'_{k,\ell} \log^\ell(s), \quad (306)$$

for  $k \geq 2$ , are determined from the coefficients  $c_k$  in Eq. (283) using the recursion

$$c'_{k,0} = c_k, \quad (307)$$

$$c'_{k,\ell} = \frac{2}{\ell} \sum_{j=1}^{k-1} j (4\pi)^{k-j} b_{k-j-1} c'_{j,\ell-1}, \quad (308)$$

where  $b_n$  are the coefficients of the beta function defined in Eq. (286). The dependence on  $s$ , and therefore on the scale  $\mu'$ , is entirely due to the truncation of the perturbative expansion. Denoting the truncated series by

$$\mathcal{Q}^{(n)}(\mu, \mu') = c_1 \alpha_{\overline{\text{MS}}}(\mu') + \sum_{k=2}^n c'_k(s) \alpha_{\overline{\text{MS}}}^k(\mu'), \quad (309)$$

it is possible to show that the scale-variation procedure described below yields a sensible estimate of the truncation error

$$\delta_n = \left| \mathcal{Q}(\mu) - \mathcal{Q}^{(n)}(\mu, \mu') \right|, \quad (310)$$

see, e.g., the discussion in Ref. [68]. Formally,

$$\mu' \frac{\partial}{\partial \mu'} \mathcal{Q}^{(n)}(\mu, \mu') \propto \alpha_{\overline{\text{MS}}}^{n+1}(\mu'), \quad (311)$$

showing that scale variations capture the correct size of the truncation error, at least parametrically.

**Implementation** The implementation of the scale variations proceeds as follows.

1. We assume a value for  $\Lambda_{\overline{\text{MS}}}^{(3)}$ , e.g., the current best estimate in FLAG. Given this value, we compute the corresponding value of  $\alpha_{\overline{\text{MS}}}(s_{\text{ref}}\mu)$  (at fixed  $N_f = 3$ ) where  $\mu$  is the scale associated to the observable  $\mathcal{Q}$ . Typical choices are  $s_{\text{ref}} = 1$  or  $s_{\text{ref}} = s^*$ , the latter being the scale of fastest apparent convergence. Similarly, we also compute the value of  $\alpha_{\overline{\text{MS}}}^{(5)}(M_Z)$ . All these values are computed using the running of the strong coupling, the value of  $\Lambda_{\overline{\text{MS}}}^{(3)}$  as the unique input, in addition to the  $\overline{\text{MS}}$  charm- and bottom-quark masses at their own scale,  $\bar{m}_c^{(4)}(\bar{m}_c)$  and  $\bar{m}_b^{(5)}(\bar{m}_b)$ , respectively and  $m_Z$ .
2. Using Eq. (309), we compute the value  $\mathcal{Q}_{\text{ref}}$  of the observable by imposing that it coincides with its truncated expansion,

$$\mathcal{Q}_{\text{ref}} = \mathcal{Q}^{(n)}(\mu, s_{\text{ref}}\mu), \quad (312)$$

where  $s_{\text{ref}}\mu$  is the scale associated to the observable as shown explicitly in Eq. (283). By construction, using the value  $\mathcal{Q}_{\text{ref}}$ , setting  $s = s_{\text{ref}}$ , and solving Eq. (309), we recover for  $\alpha_{\overline{\text{MS}}}(s_{\text{ref}}\mu)$  the value obtained in step 1. Hence, we interpret  $\mathcal{Q}_{\text{ref}}$  as the value of the observable that yields the value of  $\alpha_{\overline{\text{MS}}}^{(5)}(M_Z)$  in step 1, when performing the *usual* extraction of the strong coupling.

3. We use Eq. (309) again, but this time set  $s = s_{\text{ref}}/2, 2s_{\text{ref}}$ , to extract  $\alpha_{\overline{\text{MS}}}(s\mu)$  by solving

$$\mathcal{Q}_{\text{ref}} = \mathcal{Q}^{(n)}(\mu, s\mu). \quad (313)$$

Because the expansion is truncated, the value obtained here for  $\alpha_{\overline{\text{MS}}}(s\mu)$  is different from the one obtained by running the coupling from the value of  $\alpha_{\overline{\text{MS}}}(s_{\text{ref}}\mu)$  computed in step 2.

4. Using  $\alpha_{\overline{\text{MS}}}(s\mu)$  as the initial condition, we run the strong coupling constant and compute  $\alpha_{\overline{\text{MS}}}^{(5)}(M_Z)$ . The difference between this value and the value computed in step 1 is used as an estimate of the uncertainty due to the truncation of the perturbative expansion.

Typically scale variations are performed by multiplying and dividing the reference scale by a factor 2. For some determinations, where the perturbative matching is done at a few GeV, dividing the scale by a factor of 2 yields a low scale where perturbation theory is clearly no longer applicable and therefore the scale variation yields an artificially large error. In these cases, we consider only the variation obtained by multiplying the reference scale by a factor 2. To be more specific, we define the following quantities.

$\delta_{(4)}(s_{\text{ref}})$ : The renormalization scale  $s_{\text{ref}}\mu$  is multiplied and divided by a factor two. We quote a symmetric error by averaging the difference between the results obtained with the scales  $s_{\text{ref}}\mu$  and  $2s_{\text{ref}}\mu$ , and the difference between the results obtained with scales  $s_{\text{ref}}/2 \times \mu$  and  $s_{\text{ref}}\mu$ . Note however that in some cases the error is markedly asymmetric. We will quote the differences as a percentage deviation from the reference value of  $\alpha_s(m_Z)$ .

$\delta_{(2)}(s_{\text{ref}})$ : The renormalization scale is multiplied by a factor two only. The error  $\delta_{(2)}(s_{\text{ref}})$  is simply the difference between the two results obtained with the two scales, again taken as a percentage deviation from the reference value of  $\alpha_s(m_Z)$ .

We also explore two common choices, namely  $s_{\text{ref}} = 1$  and  $s_{\text{ref}} = s^*$ , the scale of fastest apparent convergence, i.e., the scale at which  $c'_2(s^*) = 0$ .

**Perturbative coefficients** The coefficients of the perturbative expansion for the observables of interest in this review are summarized in Tab. 55. For each observable we report the number of coefficients that are available for the perturbative expansion, the scale at which the perturbative matching is done, the list of coefficients and the relevant references.

Observable	$n_1$ (loops)	$\mu$ [GeV]	perturbative coefficients	References
Step-scaling	2	80	$-1.37520970, 0.57120172$	[69, 70]
	3	1.5	$-0.0485502, 0.687447, 0.818808$	[71–75]
Potential		2.5	same as line above, $\mu$ changed	
		5.0	same as line above, $\mu$ changed	
	3	2.0	$-1.4346, 0.16979, 3.21120$	[76]
Vacuum polarization		4.0		[77]
		1.3		[48]
$-\log W_{11}$	2	4.4	$-0.87811924, 4.20161085$	[78, 79]
$-\log W_{12}/u_0^6$		4.4	$0.79128076, 3.18658638$	
HQ $r_4$	2	$m_c$	$-0.07762325, 0.07957445$	[80–82]
HQ $r_4$		$2m_c$	same as line above, $\mu$ changed	
HQ $r_6$		$2m_c$	$0.77386542, -0.08560363$	
HQ $r_8$		$2m_c$	$1.08917060, 0.20034888$	
GF coupling	2	$1/\sqrt{8t}$	$1.09778674 + 0.007555192 N_f$ $-0.98225 - 0.069913N_f + 0.001872234N_f^2$	[38, 83]

Table 55: Summary of the coefficients of the perturbative expansion of the observables discussed in this review as a power series in  $\alpha_{\overline{\text{MS}}}$ . We assume that the observables are normalized so that  $c_1 = 1$  and we only quote the coefficients starting from  $c_2$ . The coefficients are computed for  $N_f = 3$ , unless the explicit dependence on the number of flavours is given. For each observable, we quote the number of coefficients that are known analytically and the scale of perturbative matching to the  $\overline{\text{MS}}$  scheme. Note that for the GF coupling there are two coefficients, reported as functions of  $N_f$ , over two separate lines.

### 9.3 $\alpha_s$ from Step-Scaling Methods

#### 9.3.1 General considerations

The method of step-scaling functions avoids the scale problem, Eq. (296). It is in principle independent of the particular boundary conditions used and was first developed with periodic boundary conditions in a two-dimensional model [84].

The essential idea of the step-scaling strategy is to split the determination of the running coupling at large  $\mu$  and of a hadronic scale into two lattice calculations and connect them by ‘step scaling’. In the former part, we determine the running coupling constant in a finite-volume scheme in which the renormalization scale is set by the inverse lattice size  $\mu = 1/L$ . In this calculation, one takes a high renormalization scale while keeping the lattice spacing sufficiently small as

$$\mu \equiv 1/L \sim 10 \dots 100 \text{ GeV}, \quad a/L \ll 1. \quad (314)$$

In the latter part, one chooses a certain  $\bar{g}_{\text{max}}^2 = \bar{g}^2(1/L_{\text{max}})$ , typically such that  $L_{\text{max}}$  is around 0.5–1 fm. With a common discretization, one then determines  $L_{\text{max}}/a$  and (in a large



volume  $L \geq 2\text{--}3\text{ fm}$ ) a hadronic scale such as a hadron mass,  $\sqrt{t_0}/a$  or  $r_0/a$  at the same bare parameters. In this way one gets numbers for, e.g.,  $L_{\text{max}}/r_0$  and by changing the lattice spacing  $a$  carries out a continuum-limit extrapolation of that ratio.

In order to connect  $\bar{g}^2(1/L_{\text{max}})$  to  $\bar{g}^2(\mu)$  at high  $\mu$ , one determines the change of the coupling in the continuum limit when the scale changes from  $L$  to  $L/s$ , where  $s$  is a scale factor, set to  $s = 2$  in most applications. Then, starting from  $L = L_{\text{max}}$  one iteratively performs  $k$  steps to arrive at  $\mu = s^k/L_{\text{max}}$ . This part of the strategy is called step scaling. Combining these results yields  $\bar{g}^2(\mu)$  at  $\mu = s^k (r_0/L_{\text{max}}) r_0^{-1}$ , where  $r_0$  stands for the particular chosen hadronic scale.

At present most applications in QCD use Schrödinger functional boundary conditions [85, 86] and we discuss this below in a little more detail. (However, other boundary conditions are also possible, such as twisted periodic boundary conditions for the gauge fields and the discussion also applies to them.) An important reason is that these boundary conditions avoid zero modes for the quark fields and quartic modes [87] in the perturbative expansion in the gauge fields. Furthermore the corresponding renormalization scheme is well studied in perturbation theory [70, 88, 89] with the 3-loop  $\beta$ -function and 2-loop cutoff effects (for the standard Wilson regularization) known.

In order to have a perturbatively well-defined scheme, the SF scheme uses Dirichlet boundary conditions at time  $t = 0$  and  $t = T$ . These break translation invariance and permit  $\mathcal{O}(a)$  counter terms at the boundary through quantum corrections. Therefore, the leading discretization error is  $\mathcal{O}(a)$ . Improving the lattice action is achieved by adding counter terms at the boundaries whose coefficients are denoted as  $c_t, \tilde{c}_t$ . In practice, these coefficients are computed with 1-loop or 2-loop perturbative accuracy. A better precision in this step yields a better control over discretization errors, which is important, as can be seen, e.g., in Refs. [64, 90].

Also computations with Dirichlet boundary conditions do in principle suffer from the insufficient change of topology in the HMC algorithm at small lattice spacing. However, in a small volume the weight of nonzero charge sectors in the path integral is exponentially suppressed [91] and in a Monte Carlo run of typical length very few configurations with nontrivial topology should appear.<sup>2</sup> Considering the issue quantitatively Ref. [92] finds a strong suppression below  $L \approx 0.8\text{ fm}$ . Therefore the lack of topology change of the HMC is not a serious issue for the high-energy regime in step-scaling studies. However, the matching to hadronic observables requires volumes where the problem cannot be ignored. Therefore, Ref. [93] includes a projection to zero topology into the *definition* of the coupling. A very interesting comparison of the step-scaling approach for a ( $Q = 0$ )-projected coupling and its unprojected version was recently carried out in Ref. [94], with  $N_f = 0$  and twisted periodic boundary conditions for the gauge field. A new parallel-tempering approach to relate systems with different boundary conditions was used. The results validate the  $Q = 0$  approach, in that step scaling in large volume (where contributions from  $Q \neq 0$  configurations are sizeable) leads, within errors, to indistinguishable results, once the couplings are properly matched. We note also that a mix of Dirichlet and open boundary conditions is expected to remove the topology issue entirely [95] and may be considered in the future.

Apart from the boundary conditions, the very definition of the coupling needs to be chosen. We briefly discuss in turn, the two schemes used at present, namely, the ‘Schrödinger

<sup>2</sup>We simplify here and assume that the classical solution associated with the used boundary conditions has charge zero. In practice this is the case.



Functional' (SF) and 'Gradient-Flow' (GF) schemes.

The SF scheme is the first one, which was used in step-scaling studies in gauge theories [85]. Inhomogeneous Dirichlet boundary conditions are imposed in time,

$$A_k(x)|_{x_0=0} = C_k, \quad A_k(x)|_{x_0=L} = C'_k, \quad (315)$$

for  $k = 1, 2, 3$ . Periodic boundary conditions (up to a phase for the fermion fields) with period  $L$  are imposed in space. The matrices

$$\begin{aligned} LC_k &= i \operatorname{diag}(\eta - \pi/3, -\eta/2, -\eta/2 + \pi/3), \\ LC'_k &= i \operatorname{diag}(-(\eta + \pi), \eta/2 + \pi/3, \eta/2 + 2\pi/3), \end{aligned}$$

just depend on the dimensionless parameter  $\eta$ . The coupling  $\bar{g}_{\text{SF}}$  is obtained from the  $\eta$ -derivative of the effective action,

$$\langle \partial_\eta S|_{\eta=0} \rangle = \frac{12\pi}{\bar{g}_{\text{SF}}^2}. \quad (316)$$

For this scheme, the finite  $c_g^{(i)}$ , Eq. (288), are known for  $i = 1, 2$  [70, 89].

More recently, gradient-flow couplings have been used frequently because of their small statistical errors at large couplings (in contrast to  $\bar{g}_{\text{SF}}$ , which has small statistical errors at small couplings). The gradient flow is introduced as follows [38, 96]. Consider the flow gauge field  $B_\mu(t, x)$  with the flow time  $t$ , which is a one-parameter deformation of the bare gauge field  $A_\mu(x)$ , where  $B_\mu(t, x)$  is the solution to the gradient-flow equation

$$\begin{aligned} \partial_t B_\mu(t, x) &= D_\nu G_{\nu\mu}(t, x), \\ G_{\mu\nu} &= \partial_\mu B_\nu - \partial_\nu B_\mu + [B_\mu, B_\nu], \end{aligned} \quad (317)$$

with initial condition  $B_\mu(0, x) = A_\mu(x)$ . The renormalized coupling is defined by [38]

$$\bar{g}_{\text{GF}}^2(\mu) = \mathcal{N} t^2 \langle E(t, x) \rangle|_{\mu=1/\sqrt{8t}}, \quad (318)$$

with  $\mathcal{N} = 16\pi^2/3 + \mathcal{O}((a/L)^2)$  and where  $E(t, x)$  is the action density given by

$$E(t, x) = \frac{1}{4} G_{\mu\nu}^a(t, x) G_{\mu\nu}^a(t, x). \quad (319)$$

In a finite volume, one needs to specify additional conditions. In order not to introduce two independent scales one sets

$$\sqrt{8t} = cL, \quad (320)$$

for some fixed number  $c$  [97]. Schrödinger functional boundary conditions [98] or twisted periodic boundary conditions [33, 99, 100] have been employed. Matching of the GF coupling to the  $\overline{\text{MS}}$ -scheme coupling is known to 1-loop for twisted boundary conditions with zero quark flavours and SU(3) group [100] and to 2-loop with SF boundary conditions with zero quark flavours [101]. The former is based on a MC evaluation at small couplings and the latter on numerical stochastic perturbation theory.<sup>3</sup>

Collaboration	Ref.	$N_f$	publication status	renormalization scale	perturbative behaviour	continuum extrapolation	scale	$\Lambda_{\overline{\text{MS}}}[\text{MeV}]$	$r_0\Lambda_{\overline{\text{MS}}}$
ALPHA 10A	[103]	4	A	★	★	★	only running of $\alpha_s$ in Fig. 4		
Perez 10	[104]	4	C	★	★	○	only step-scaling function in Fig. 4		
ALPHA 17	[105]	2+1	A	★	★	★	$\sqrt{8t_0} = 0.415 \text{ fm}$	341(12)	0.816(29)
PACS-CS 09A	[106]	2+1	A	★	★	○	$m_\rho$	371(13)(8)( $^{+0}_{-27}$ ) <sup>#</sup>	0.888(30)(18)( $^{+0}_{-65}$ ) <sup>†</sup>
			A	★	★	○	$m_\rho$	345(59) <sup>##</sup>	0.824(141) <sup>†</sup>
ALPHA 12*	[59]	2	A	★	★	★	$f_K$	310(20)	0.789(52)
ALPHA 04	[107]	2	A	■	★	★	$r_0 = 0.5 \text{ fm}^\S$	245(16)(16) <sup>§</sup>	0.62(2)(2) <sup>§</sup>
ALPHA 01A	[108]	2	A	★	★	★	only running of $\alpha_s$ in Fig. 5		
Bribian 21	[33]	0	A	★	★	★	$r_0 = 0.5 \text{ fm}$	249.4(8.0)	0.632(20)
Nada 20	[109]	0	A	★	★	★	consistency checks for [110], same gauge configurations		
Dalla Brida 19	[110]	0	A	★	★	★	$r_0 = 0.5 \text{ fm}$	260.5(4.4)	0.660(11)
Ishikawa 17	[100]	0	A	★	★	★	$r_0, [\sqrt{\sigma}]$	253(4)( $^{+13}_{-2}$ ) <sup>†</sup>	0.606(9)( $^{+31}_{-5}$ ) <sup>+</sup>
CP-PACS 04 <sup>&amp;</sup>	[90]	0	A	★	★	○	only tables of $g_{\text{SF}}^2$		
ALPHA 98 <sup>††</sup>	[111]	0	A	★	★	○	$r_0 = 0.5 \text{ fm}$	238(19)	0.602(48)
Lüscher 93	[88]	0	A	★	○	○	$r_0 = 0.5 \text{ fm}$	233(23)	0.590(60) <sup>§§</sup>

<sup>#</sup> Result with a constant (in  $a$ ) continuum extrapolation of the combination  $L_{\text{max}}m_\rho$ .

<sup>†</sup> In conversion from  $\Lambda_{\overline{\text{MS}}}$  to  $r_0\Lambda_{\overline{\text{MS}}}$  and vice versa,  $r_0$  is taken to be 0.472 fm.

<sup>##</sup> Result with a linear continuum extrapolation in  $a$  of the combination  $L_{\text{max}}m_\rho$ .

<sup>\*</sup> Supersedes ALPHA 04.

<sup>§</sup> The  $N_f = 2$  results were based on values for  $r_0/a$  which have later been found to be too small by [59]. The effect will be of the order of 10–15%, presumably an increase in  $\Lambda r_0$ . We have taken this into account by a ■ in the renormalization scale.

<sup>&</sup> This investigation was a precursor for PACS-CS 09A and confirmed two step-scaling functions as well as the scale setting of ALPHA 98.

<sup>††</sup> Uses data of Lüscher 93 and therefore supersedes it.

<sup>§§</sup> Converted from  $\alpha_{\overline{\text{MS}}}(37r_0^{-1}) = 0.1108(25)$ .

<sup>+</sup> Also  $\Lambda_{\overline{\text{MS}}}/\sqrt{\sigma} = 0.532(8)( $^{+27}_{-5}$ )$  is quoted.

Table 56: Results for the  $\Lambda$ -parameter from computations using step scaling of the SF-coupling. Entries without values for  $\Lambda$  computed the running and established perturbative behaviour at large  $\mu$ .

### 9.3.2 Discussion of computations

In Tab. 56 we give results from various determinations of the  $\Lambda$ -parameter. For a clear

<sup>3</sup>For a variant of the twisted periodic finite volume scheme the 1-loop matching has been computed analytically.

assessment of the  $N_f$ -dependence, the last column also shows results that refer to a common hadronic scale,  $r_0$ . As discussed above, the renormalization scale can be chosen large enough such that  $\alpha_s < 0.2$  and the perturbative behaviour can be verified. Consequently only ★ is present for these criteria except for early work where the  $n_l = 2$  loop correction to  $\overline{\text{MS}}$  was not yet known and we assigned a ■ concerning the renormalization scale. With dynamical fermions, results for the step-scaling functions are always available for at least  $a/L = \mu a = 1/4, 1/6, 1/8$ . All calculations have a nonperturbatively  $\mathcal{O}(a)$  improved action in the bulk. For the discussed boundary  $\mathcal{O}(a)$  terms this is not so. In most recent calculations 2-loop  $\mathcal{O}(a)$  improvement is employed together with at least three lattice spacings.<sup>4</sup> This means a ★ for the continuum extrapolation. In other computations only 1-loop  $c_t$  was available and we arrive at ○. We note that the discretization errors in the step-scaling functions of the SF coupling are usually found to be very small, at the percent level or below. However, the overall desired precision is very high as well, and the results in CP-PACS 04 [90] show that discretization errors at the below percent level cannot be taken for granted. In particular with staggered fermions (unimproved except for boundary terms) few-percent effects are seen in Perez 10 [104].

In the work by PACS-CS 09A [106], the continuum extrapolation in the scale setting is performed using a constant function in  $a$  and with a linear function. Potentially the former leaves a considerable residual discretization error. We here use, as discussed with the collaboration, the continuum extrapolation linear in  $a$ , as given in the second line of PACS-CS 09A [106] results in Tab. 56. After perturbative conversion from a three-flavour result to five flavours (see Sec. 9.2.1), they obtain

$$\alpha_{\overline{\text{MS}}}^{(5)}(M_Z) = 0.118(3). \quad (321)$$

In Ref. [105], the ALPHA collaboration determined  $\Lambda_{\overline{\text{MS}}}^{(3)}$  combining step scaling in  $\bar{g}_{\text{GF}}^2$  in the lower-scale region  $\mu_{\text{had}} \leq \mu \leq \mu_0$ , and step scaling in  $\bar{g}_{\text{SF}}^2$  for higher scales  $\mu_0 \leq \mu \leq \mu_{\text{PT}}$ . Both schemes are defined with SF boundary conditions. For  $\bar{g}_{\text{GF}}^2$  a projection to the sector of zero topological charge is included, Eq. (319) is restricted to the magnetic components, and  $c = 0.3$ . The scales  $\mu_{\text{had}}$ ,  $\mu_0$ , and  $\mu_{\text{PT}}$  are defined by  $\bar{g}_{\text{GF}}^2(\mu_{\text{had}}) = 11.3$ ,  $\bar{g}_{\text{SF}}^2(\mu_0) = 2.012$ , and  $\mu_{\text{PT}} = 16\mu_0$  which are roughly estimated as

$$1/L_{\text{max}} \equiv \mu_{\text{had}} \approx 0.2 \text{ GeV}, \quad \mu_0 \approx 4 \text{ GeV}, \quad \mu_{\text{PT}} \approx 70 \text{ GeV}. \quad (322)$$

Step scaling is carried out with an  $\mathcal{O}(a)$ -improved Wilson quark action [112] and Lüscher-Weisz gauge action [113] in the low-scale region and an  $\mathcal{O}(a)$ -improved Wilson quark action [114] and Wilson gauge action in the high-energy part. For the step scaling using steps of  $L/a \rightarrow 2L/a$ , three lattice sizes  $L/a = 8, 12, 16$  were simulated for  $\bar{g}_{\text{GF}}^2$  and four lattice sizes  $L/a = (4,) 6, 8, 12$  for  $\bar{g}_{\text{SF}}^2$ . The final results do not use the small lattices given in parenthesis. The parameter  $\Lambda_{\overline{\text{MS}}}^{(3)}$  is then obtained via

$$\Lambda_{\overline{\text{MS}}}^{(3)} = \underbrace{\frac{\Lambda_{\overline{\text{MS}}}^{(3)}}{\mu_{\text{PT}}}}_{\text{perturbation theory}} \times \underbrace{\frac{\mu_{\text{PT}}}{\mu_{\text{had}}}}_{\text{stepscaling}} \times \underbrace{\frac{\mu_{\text{had}}}{f_{\pi K}}}_{\text{large volume simulation}} \times \underbrace{f_{\pi K}}_{\text{experimental data}}, \quad (323)$$

ically [102].

<sup>4</sup>With 2-loop  $\mathcal{O}(a)$  improvement we here mean  $c_t$  including the  $g_0^4$  term and  $\tilde{c}_t$  with the  $g_0^2$  term. For gluonic observables such as the running coupling this is sufficient for cutoff effects being suppressed to  $\mathcal{O}(g^6 a)$ .

where the hadronic scale  $f_{\pi K}$  is  $f_{\pi K} = \frac{1}{3}(2f_K + f_\pi) = 147.6(5)$  MeV. The first factor on the right-hand side of Eq. (323) is obtained from  $\alpha_{\text{SF}}(\mu_{\text{PT}})$  which is the output from SF step scaling using Eq. (285) with  $\alpha_{\text{SF}}(\mu_{\text{PT}}) \approx 0.1$  and the 3-loop  $\beta$ -function and the exact conversion to the  $\overline{\text{MS}}$ -scheme. The second factor is essentially obtained from step scaling in the GF scheme and the measurement of  $\bar{g}_{\text{SF}}^2(\mu_0)$  (except for the trivial scaling factor of 16 in the SF running). The third factor is obtained from a measurement of the hadronic quantity at large volume.

A large-volume simulation is done for three lattice spacings with sufficiently large volume and reasonable control over the chiral extrapolation so that the scale determination is precise enough. The step scaling results in both schemes satisfy renormalization criteria, perturbation theory criteria, and continuum-limit criteria just as previous studies using step scaling. So we assign green stars for these criteria.

The dependence of  $\Lambda$ , Eq. (285) with 3-loop  $\beta$ -function, on  $\alpha_s$  and on the chosen scheme is discussed in [66]. This investigation provides a warning on estimating the truncation error of perturbative series. Details are explained in Sec. 9.2.3.

The result for the  $\Lambda$ -parameter is  $\Lambda_{\overline{\text{MS}}}^{(3)} = 341(12)$  MeV, where the dominant error comes from the error of  $\alpha_{\text{SF}}(\mu_{\text{PT}})$  after step scaling in the SF scheme. Using 4-loop matching at the charm and bottom thresholds and 5-loop running one finally obtains

$$\alpha_{\overline{\text{MS}}}^{(5)}(M_Z) = 0.11852(84). \quad (324)$$

Several other results do not have a sufficient number of quark flavours or do not yet contain the conversion of the scale to physical units (ALPHA 10A [103], Perez 10 [104]). Thus no value for  $\alpha_{\overline{\text{MS}}}^{(5)}(M_Z)$  is quoted.

The computation of Ishikawa et al. [100] is based on the gradient-flow coupling with twisted boundary conditions [99] (TGF coupling) in the pure gauge theory. Again they use  $c = 0.3$ . Step scaling with a scale factor  $s = 3/2$  is employed, covering a large range of couplings from  $\alpha_s \approx 0.5$  to  $\alpha_s \approx 0.1$  and taking the continuum limit through global fits to the step-scaling function on  $L/a = 12, 16, 18$  lattices with between 6 and 8 parameters. Systematic errors due to variations of the fit functions are estimated. Two physical scales are considered:  $r_0/a$  is taken from [64] and  $\sigma a^2$  from [115] and [116]. As the ratio  $\Lambda_{\text{TGF}}/\Lambda_{\overline{\text{MS}}}$  has not yet been computed analytically, Ref. [100] determines the 1-loop relation between  $\bar{g}_{\text{SF}}$  and  $\bar{g}_{\text{TGF}}$  from MC simulations performed in the weak coupling region and then uses the known  $\Lambda_{\text{SF}}/\Lambda_{\overline{\text{MS}}}$ . Systematic errors due to variations of the fit functions dominate the overall uncertainty.

Two extensive  $N_f = 0$  step-scaling studies have been carried out in Dalla Brida 19 [110] and by Nada and Ramos [109]. They use different strategies for the running from mid to high energies, but use the same gauge configurations and share the running at low energies and matching to the hadronic scales. These results are therefore correlated. However, given the comparatively high value for  $r_0\Lambda_{\overline{\text{MS}}}$ , it is re-assuring that these conceptually different approaches yield perfectly compatible results within errors of similar size of around 1.5% for  $\sqrt{8t_0}\Lambda_{\overline{\text{MS}}} = 0.6227(98)$ , or, alternatively  $r_0\Lambda_{\overline{\text{MS}}} = 0.660(11)$ .

In Dalla Brida 19 [110] two GF-coupling definitions with SF-boundary conditions are considered, corresponding to (colour-) magnetic and electric components of the action density respectively. The coupling definitions include the projection to  $Q = 0$ , as was also done in [105]. The flow-time parameter is set to  $c = 0.3$ , and both Zeuthen and Wilson flow are measured. Lattice sizes range from  $L/a = 8$  to  $L/a = 48$ , covering up to a factor of 3 in lattice spacings for the step-scaling function, where both  $L/a$  and  $2L/a$  are needed. Lattice

effects in the step-scaling function are visible but can be extrapolated using global fits with  $\alpha^2$  errors. Some remnant  $\mathcal{O}(a)$  effects from the boundaries are expected, as their perturbative cancellation is incomplete. These  $\mathcal{O}(a)$  contaminations are treated as a systematic error on the data, following [105], and are found to be subdominant. An intermediate reference scale  $\mu_{\text{ref}}$  is defined where  $\alpha = 0.2$ , and the scales above and below are analyzed separately. Again this is similar to [105], except that here GF-coupling data is available also at high energy scales. The GF  $\beta$ -functions are then obtained by fitting to the continuum extrapolated data for the step-scaling functions. In addition, a nonperturbative matching to the standard SF coupling is performed above  $\mu_{\text{ref}}$  for a range of couplings covering a factor of 2. The nonperturbative  $\beta$ -function for the SF scheme can thus be inferred from the GF  $\beta$ -function. It turns out that GF schemes are very slow to reach the perturbative regime. Particularly the  $\Lambda$ -parameter for the magnetic GF coupling shows a large slope in  $\alpha^2$ , which is the parametric uncertainty with known 3-loop  $\beta$ -function. Also, convincing contact with the 3-loop  $\beta$ -function is barely seen down to  $\alpha = 0.08$ . This is likely to be related to the rather large 3-loop  $\beta$ -function coefficients, especially for the magnetic GF scheme [101]. In contrast, once the GF couplings are matched nonperturbatively to the SF scheme the contact to perturbative running can be safely made. It is also re-assuring that in all cases the extrapolations (linear in  $\alpha^2$ ) to  $\alpha = 0$  for the  $\Lambda$ -parameters agree very well, and the authors argue in favour of such extrapolations. Their data confirms that this procedure yields consistent results with the SF scheme for  $\nu = 0$ , where such an extrapolation is not required.

The low-energy regime between  $\mu_{\text{ref}}$  and a hadronic scale  $\mu_{\text{had}}$  is covered again using the nonperturbative step-scaling function and the derived  $\beta$ -function. Finally, contact between  $\mu_{\text{had}}$  and hadronic scales  $t_0$  and  $r_0$  is established using five lattice spacings covering a factor up to 2.7. The multitude of cross checks of both continuum limit and perturbative truncation errors make this a study which passes all current FLAG criteria by some margin. The comparatively high value for  $r_0\Lambda_{\overline{\text{MS}}}$  found in this study must therefore be taken very seriously.

In Nada 20 [109], Nada and Ramos provide further consistency checks of [110] for scales larger than  $\mu_{\text{ref}}$ . The step-scaling function for  $c = 0.2$  is constructed in two steps, by determining first the relation between couplings for  $c = 0.2$  and  $c = 0.4$  at the same  $L$  and then increasing  $L$  to  $2L$  keeping the flow time fixed (in units of the lattice spacing), so that one arrives again at  $c = 0.2$  on the  $2L$  volume. The authors demonstrate that the direct construction of the step-scaling function for  $c = 0.2$  would require much larger lattices in order to control the continuum limit at the same level of precision. The consistency with [110] for the  $\Lambda$ -parameter is therefore a highly nontrivial check on the systematic effects of the continuum extrapolations. The study obtains results for the  $\Lambda$ -parameter (again extrapolating to  $\alpha = 0$ ) with a similar error as in [110] using the low-energy running and matching to the hadronic scale from that reference. For this reason and since gauge configurations are shared between both papers, these results are not independent of [110], so Dalla Brida 19 will be taken as representative for both works.

Since FLAG 21 a new step-scaling result with  $N_f = 0$  has appeared in Bribian 21 [33]. It uses the gradient flow in a volume with twisted periodic boundary conditions for the gauge field. The volume has two shorter directions by a factor of 3; however, a re-interpretation as a symmetric physical volume is possible using internal degrees of freedom of the gauge field. This is a state-of-the-art step-scaling result, the main problem being the poor perturbative behaviour of the gradient-flow coupling. Since the 3-loop  $\beta$ -function is not known, the parametric uncertainty in estimates of the  $\Lambda$ -parameter is of  $\mathcal{O}(\alpha)$  and is quite large. The problem is by-passed by matching nonperturbatively to the SF scheme, which leads to stable

estimates vs.  $\alpha^2$ , and the result is  $\sqrt{8t_0}\Lambda_{\overline{\text{MS}}} = 0.603(17)$ , or, in units of the Sommer scale,  $r_0\Lambda_{\overline{\text{MS}}} = 0.632(20)$ . All FLAG criteria are passed with  $\star$ , and the data-driven criterion for the continuum limit is irrelevant in this case.

**Scale variations.** With a perturbative matching at  $\mu \approx 80$  GeV, we have computed the change in the determination of  $\alpha_{\overline{\text{MS}}}(M_Z)$  under scale variations as explained above. The systematic errors obtained from scale variations are

$$\delta_{(4)}^* = 0.1\%, \quad \delta_{(2)} = 0.2\% \quad \delta_{(2)}^* = 0.2\%. \quad (325)$$

Because the perturbative matching is performed at a high-energy scale, the systematic error obtained from scale variations is negligible.

## 9.4 The decoupling method

The ALPHA collaboration has proposed and pursued a new strategy to compute the  $\Lambda$  parameter in QCD with  $N_f \geq 3$  flavours based on the simultaneous decoupling of  $N_f \geq 3$  heavy quarks with RGI mass  $M$  [30]. We refer to [12] for a pedagogical introduction. Generically, for large quark mass  $M$ , a running coupling in a mass-dependent renormalization scheme

$$\bar{g}^2(\mu, M)^{(N_f)} = \bar{g}^2(\mu)^{(N_f=0)} + \mathcal{O}(1/M^k) \quad (326)$$

can be represented by the corresponding  $N_f = 0$  coupling, up to power corrections in  $1/M$ . The leading power is usually  $k = 2$ , however renormalization schemes in finite volume may have  $k = 1$ , depending on the set-up. For example, this is the case with standard SF or open boundary conditions in combination with a standard mass term. In practice such boundary contributions can be made numerically small by a careful choice of the scheme's parameters. In principle, power corrections can be either  $(\mu/M)^k$  or  $(\Lambda/M)^k$ . Fixing  $\mu = \mu_{\text{dec}}$ , e.g., by prescribing a value for the mass-independent coupling, such that  $\mu_{\text{dec}}/\Lambda = \mathcal{O}(1)$  thus helps to reduce the need for very large  $M$ . Defining  $\bar{g}^2(\mu_{\text{dec}}, M) = u_M$  at fixed  $\bar{g}^2(\mu_{\text{dec}}, M = 0)$ , Eq. (326) translates to a relation between  $\Lambda$ -parameters, which can be cast in the form,

$$\frac{\Lambda_{\overline{\text{MS}}}^{(N_f)}}{\mu_{\text{dec}}} P\left(\frac{M}{\mu_{\text{dec}}} \frac{\mu_{\text{dec}}}{\Lambda_{\overline{\text{MS}}}^{(N_f)}}\right) = \frac{\Lambda_{\overline{\text{MS}}}^{(0)}}{\Lambda_s^{(0)}} \varphi_s^{(N_f=0)}(\sqrt{u_M}) + \mathcal{O}(M^{-k}), \quad (327)$$

with the function  $\varphi_s$  as defined in Eq. (285), for scheme  $s$  and  $N_f = 0$ . A crucial observation is that the function  $P$ , which gives the ratios of  $\Lambda$ -parameters  $\Lambda_{\overline{\text{MS}}}^{(0)}/\Lambda_{\overline{\text{MS}}}^{(N_f)}$ , can be evaluated perturbatively to a very good approximation [29, 117]. Equation (326) also implies a relation between the couplings in mass-independent schemes, in the theories with  $N_f$  and zero flavours, respectively. In the  $\overline{\text{MS}}$  scheme this relation is analogous to Eq. (292),

$$\left[\bar{g}_{\overline{\text{MS}}}^{(N_f=0)}(m_\star)\right]^2 = \left[\bar{g}_{\overline{\text{MS}}}^{(N_f)}(m_\star)\right]^2 \times C\left(\bar{g}_{\overline{\text{MS}}}^{(N_f)}(m_\star)\right), \quad (328)$$

where the evaluation of the coupling is done at the scale  $m_\star = m_{\overline{\text{MS}}}^{(N_f)}(\mu = m_\star)$ . This removes the leading 1-loop correction of  $\mathcal{O}(g^2)$  in the expansion of the function,  $C(g) = 1 + c_2 g^4 +$



$O(g^6)$ , which is known up to 4-loop order [22–25, 118]. The mass scale  $m_\star$  is in one-to-one correspondence with the RGI mass  $M$ , and  $g^\star(y) = \bar{g}_{\overline{\text{MS}}}^{(N_f)}(m_\star)$  can thus be considered a function of  $y \equiv M^{(N_f)}/\Lambda_{\overline{\text{MS}}}^{(N_f)}$ . The function  $P(y)$  can be evaluated perturbatively in the  $\overline{\text{MS}}$  scheme, as the ratio,

$$P(y) = \frac{\varphi_{\overline{\text{MS}}}^{(N_f=0)} \left( g^\star(y) \sqrt{C(g^\star(y))} \right)}{\varphi_{\overline{\text{MS}}}^{(N_f)}(g^\star(y))}. \quad (329)$$

Note that perturbation theory is only required at the scale set by the heavy-quark mass, which works better the larger  $M$  can be chosen. Given the function  $P(y)$ , the LHS of Eq. (327) can be inferred from a  $N_f = 0$  computation of the RHS in the scheme  $s$ , if the argument  $\sqrt{u_M}$  of  $\varphi_s^{(0)}$  is known (and the ratio  $\Lambda_{\overline{\text{MS}}}/\Lambda_s$  for the scheme  $s$ ). The main challenge then consists in the computation of the mass-dependent coupling  $u_M$  for large masses.

#### 9.4.1 Discussion of computations

To put the decoupling strategy to work, ALPHA 22 [32] uses  $N_f = 3$ , so that information from [105] can be used. Using the massless GF coupling in finite volume from this project,  $\mu_{\text{dec}}$  is defined through  $\bar{g}_{\text{GF}}^2(\mu_{\text{dec}}) = 3.949$ , and thus known in physical units,  $\mu_{\text{dec}} = 789(15)$  MeV. Imposing this condition for lattice sizes between  $L/a = 12$  to  $L/a = 48$ , a corresponding sequence of  $\beta$ -values between 4.302 and 5.174 is obtained (the lattice action is the same as used by CLS, there for much coarser lattice spacings at  $\beta \leq 3.85$ ). Using the available information on nonperturbative mass renormalization [119], six values for the  $O(a)$ -improved RGI quark masses are considered at each of these  $\beta$ -values, such that the ratios  $z = M/\mu_{\text{dec}}$  are close to 2, 4, 6, 8, 10, and 12. While great care is taken to implement nonperturbative  $O(a)$  improvement, there is only perturbative 1-loop information on  $b_g$ , which parameterizes a mass-dependent rescaling of the bare coupling,

$$\tilde{g}_0^2 = g_0^2(1 + b_g(g_0)am_q), \quad b_g(g_0) = 0.012 \times N_f g_0^2 + O(g_0^4).$$

Here,  $m_q$  denotes the subtracted bare quark mass, related to  $M$  by a renormalization factor of  $O(1)$  at the relevant lattice spacings. Consistent  $O(a)$  improvement requires that  $\tilde{\beta} = 6/\tilde{g}_0^2$  be kept fixed as the quark mass is varied. The authors of ALPHA 22 here assume a 100% uncertainty of the perturbative  $b_g$ -estimate, which is treated as a systematic error (cf. below). At the chosen quark-mass parameters, the GF coupling with doubled time extent,  $T = 2L$ , is measured. This GFT coupling is used in order to minimize effects from the time boundaries, which introduce linear effects in  $1/M$  in the decoupling relation, and also residual lattice effects linear in  $a$ . Both of these effects are monitored and found to be negligible. The continuum limit is then taken, either separately for each  $z$ -value, or using a global fit to all  $z$ -values  $z > 2$ , which turns out too small to be useful in the large- $M$  limit (cf. Fig. 9.4.1). The lattice effects are fitted to  $O(a^2)$ , including an  $[\alpha_{\overline{\text{MS}}}(1/a)]^{\hat{\Gamma}}$  term, as expected from Symanzik's effective theory with RG improvement [120–124]. The global fit uses the combined arguments from heavy-quark and Symanzik effective theories to separate the leading  $(aM)^2$  effects with yet another logarithmic correction term. Cuts in the data are considered for  $(aM)^2 < 0.25$  and  $(aM)^2 < 0.16$ . The continuum-extrapolated values include a systematic error due to the uncertainty in  $b_g$ . The fits are repeated for different choices of  $\hat{\Gamma}$  and  $\hat{\Gamma}'$  in intervals constrained by the effective heavy-quark and Symanzik theories, and the variation is used as an estimate of systematic effects due to the possible presence of such non-power-like cutoff



effects. The continuum extrapolated GFT coupling defines the starting point for the  $N_f = 0$  running. Before the GF running can be used, a matching from the GFT to GF scheme is done to high precision in the  $N_f = 0$  theory. The running in  $N_f = 0$  is taken from Dalla Brida 19 [110] and the results are then inserted into the Eq. (327), for each of the available  $M$ -values. This defines “effective”  $\Lambda$ -parameters, equal to the asymptotic value up to  $1/M^2$  effects. Taking the  $z \rightarrow \infty$  limit (again allowing for a logarithmic correction with exponent  $\Gamma_m$ ) then yields the final result, with the scale set using  $\sqrt{t_0}$  from Ref. [125],

$$\Lambda_{\overline{\text{MS}}}^{(3)} = 336(10)(6)_{b_g(3)\Gamma_m} \text{ MeV} = 336(12) \text{ MeV} \quad (330)$$

which translates to  $\alpha_s(m_Z) = 0.11823(84)$ . Despite some common elements with ALPHA 17,

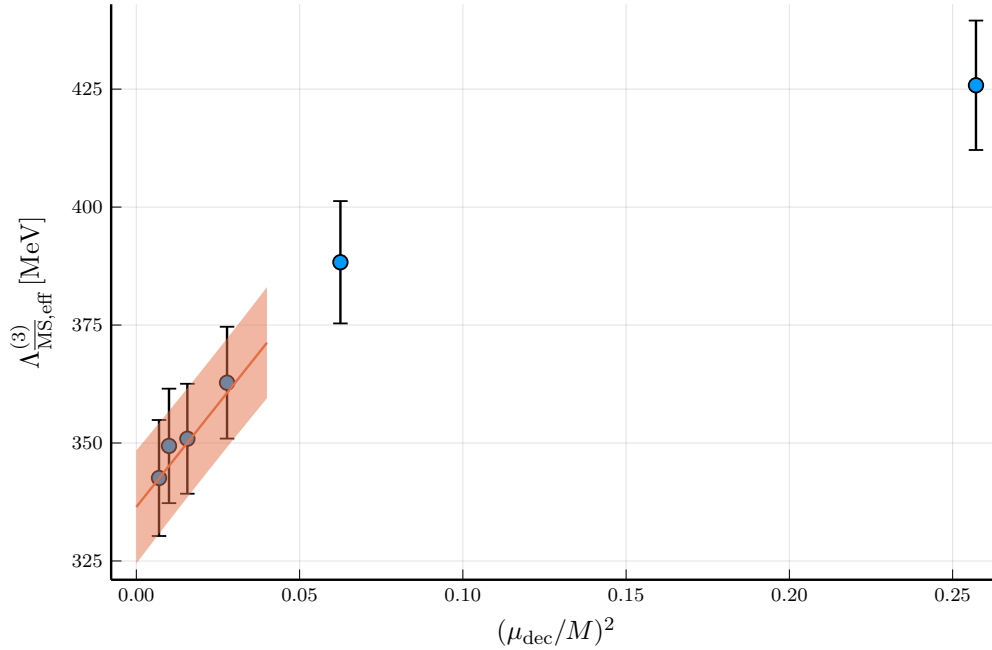


Figure 37: The decoupling limit  $M \rightarrow \infty$  in ALPHA 22, Ref. [32].

the authors emphasize that the decoupling method is largely independent, with the overlap in squared error amounting to 28 percent. This is due to the fact that the error in ALPHA 17 is dominated by the  $N_f = 3$  step-scaling procedure at *high* energy, and this part is completely replaced by the  $N_f = 0$  result by Dalla Brida 19 [110]. ALPHA 22 also give the covariance matrix between both results which allows for combining both results with correlations taken into account.

The FLAG criteria are only indirectly applicable; decoupling relies on the step-scaling analysis with  $N_f = 0$  in Dalla Brida 19 [110], which passes all FLAG criteria (cf. Sect. 9.3). Except for the (well-established, cf. Refs. [29, 117]) perturbative evaluation of the function  $P(y)$ , perturbation theory is only applied in the  $N_f = 0$  theory at very high energy, which yields a ★ for perturbative behaviour and renormalization scale. Using the FLAG criterion for continuum extrapolations (the constraint on values of  $\alpha_{\text{eff}}$  is not applicable here) the relevant scale is  $M$ , and the continuum extrapolations are based on data cut at  $aM < 0.5$  or  $aM < 0.4$ , which leaves 3–4 values satisfying this cut even at the largest mass of  $\mathcal{O}(10 \text{ GeV})$ . A

remaining uncertainty of  $O(aM)$  due to a perturbative estimate of  $b_g$  is treated as a systematic uncertainty, so that full  $O(a)$  improvement is expected to be realized within the errors. This is confirmed by—now available—nonperturbative data on  $b_g$  [126], and we use ★ for continuum extrapolations. With these errors the distance of the extrapolated result is less than one sigma away from the last data point, i.e.,  $\delta(\min) \approx 1$  for the data-driven criterion.

Final remark: The decoupling method offers scope for a further error reduction, by using the result for  $b_g$  and both, improved scale setting and improved  $N_f = 0$  step-scaling results.

In Tab. 57 we list the result.

Collaboration	Ref.	$N_f$	publication status	renormalization scale	perturbative behaviour	continuum extrapolation	scale	$\Lambda_{\overline{\text{MS}}}[\text{MeV}]$	$r_0\Lambda_{\overline{\text{MS}}}$
ALPHA 22	[32]	2+1	A	★	★	★	$\sqrt{t_0}$ [125]	336(12) *	0.804(29) *

\*  $\alpha_{\overline{\text{MS}}}^{(5)}(M_Z) = 0.11823(84)$ ;  $r_0\Lambda_{\overline{\text{MS}}}$  determined using  $r_0 = 0.472 \text{ fm}$

Table 57: Decoupling result.

## 9.5 $\alpha_s$ from the potential at short distances

### 9.5.1 General considerations

The basic method was introduced in Ref. [127] and developed in Ref. [128]. The force or potential between an infinitely massive quark and antiquark pair defines an effective coupling constant via

$$F(r) = \frac{dV(r)}{dr} = C_F \frac{\alpha_{\text{qq}}(r)}{r^2}. \quad (331)$$

The coupling can be evaluated nonperturbatively from the potential through a numerical differentiation, see below. In perturbation theory one also defines couplings in different schemes  $\alpha_{\bar{V}}$ ,  $\alpha_V$  via

$$V(r) = -C_F \frac{\alpha_{\bar{V}}(r)}{r}, \quad \text{or} \quad \tilde{V}(Q) = -C_F \frac{\alpha_V(Q)}{Q^2}, \quad (332)$$

where one fixes the unphysical constant in the potential by  $\lim_{r \rightarrow \infty} V(r) = 0$ , which is compatible with fixed-order perturbation theory.  $\tilde{V}(Q)$  is the Fourier transform of  $V(r)$ . Nonperturbatively, the subtraction of a constant in the potential introduces an additional renormalization constant, the value of  $V(r_{\text{ref}})$  at some distance  $r_{\text{ref}}$ . Perturbatively, it is believed to entail a renormalon ambiguity. In perturbation theory, the different definitions are all simply related to each other, and their perturbative expansions are known including the  $\alpha_s^4$ ,  $\alpha_s^4 \log \alpha_s$  and  $\alpha_s^5 \log \alpha_s$ ,  $\alpha_s^5 (\log \alpha_s)^2$  terms [71, 73, 74, 129–135].

The potential  $V(r)$  is determined from ratios of Wilson loops,  $W(r, t)$ , which behave as

$$\langle W(r, t) \rangle = |c_0|^2 e^{-V(r)t} + \sum_{n \neq 0} |c_n|^2 e^{-V_n(r)t}, \quad (333)$$

where  $t$  is taken as the temporal extension of the loop,  $r$  is the spatial one and  $V_n$  are excited-state potentials. To improve the overlap with the ground state, and to suppress the effects of excited states,  $t$  is taken large. Also various additional techniques are used, such as a variational basis of operators (spatial paths) to help in projecting out the ground state. Furthermore some lattice-discretization effects can be reduced by averaging over Wilson loops related by rotational symmetry in the continuum.

In order to reduce discretization errors it is of advantage to define the numerical derivative giving the force as

$$F(r_I) = \frac{V(r) - V(r - a)}{a}, \quad (334)$$

where  $r_I$  is chosen so that at tree level the force is the continuum force.  $F(r_I)$  is then a ‘tree-level improved’ quantity and similarly the tree-level improved potential can be defined [136].

Lattice potential results are in position space, while perturbation theory is naturally computed in momentum space at large momentum. Usually, the Fourier transform of the perturbative expansion is then matched to lattice data.

Finally, as was noted in Sec. 9.2.1, a determination of the force can also be used to determine the scales  $r_0, r_1$ , by defining them from the static force by

$$r_0^2 F(r_0) = 1.65, \quad r_1^2 F(r_1) = 1. \quad (335)$$

### 9.5.2 Discussion of computations

In Tab. 58, we list results of determinations of  $r_0 \Lambda_{\overline{\text{MS}}}$  (together with  $\Lambda_{\overline{\text{MS}}}$  using the scale determination of the authors).

The first determinations in the three-colour Yang Mills theory are by UKQCD 92 [128] and Bali 92 [149] who used  $\alpha_{\text{qq}}$ , Eq. (331), as explained above, but not in the tree-level improved form. Rather a phenomenologically determined lattice-artifact correction was subtracted from the lattice potentials. The comparison with perturbation theory was on a more qualitative level on the basis of a 2-loop  $\beta$ -function ( $n_l = 1$ ) and a continuum extrapolation could not be performed as yet. A much more precise computation of  $\alpha_{\text{qq}}$  with continuum extrapolation was performed in Refs. [64, 136]. Satisfactory agreement with perturbation theory was found [136] but the stability of the perturbative prediction was not considered sufficient to be able to extract a  $\Lambda$  parameter.

In Brambilla 10 [148] the same quenched lattice results of Ref. [136] were used and a fit was performed to the continuum potential, instead of the force. Perturbation theory to  $n_l = 3$  loop was used including a resummation of terms  $\alpha_s^3 (\alpha_s \ln \alpha_s)^n$  and  $\alpha_s^4 (\alpha_s \ln \alpha_s)^n$ . Close agreement with perturbation theory was found when a renormalon subtraction was performed. Note that the renormalon subtraction introduces a second scale into the perturbative formula which is absent when the force is considered.

Bazavov 14 [141] updates Bazavov 12 [142] and modifies this procedure somewhat. They consider the perturbative expansion for the force. They set  $\mu = 1/r$  to eliminate logarithms

Collaboration	Ref.	$N_f$		publication status	renormalization scale	perturbative behaviour	continuum extrapolation	scale	$\Lambda_{\overline{\text{MS}}}[\text{MeV}]$	$r_0\Lambda_{\overline{\text{MS}}}$
Ayala 20	[137]	2+1	A	○	★	○		$r_1 = 0.3106(17) \text{ fm}^c$	338(13)	0.802(31)
TUMQCD 19	[138]	2+1	A	○	★	○		$r_1 = 0.3106(17) \text{ fm}^c$	$314 \left( {}^{+16}_{-8} \right)$	$0.745 \left( {}^{+38}_{-19} \right)$
Takaura 18	[139, 140]	2+1	A	■	○	○		$\sqrt{t_0} = 0.1465(25) \text{ fm}^a$	$334(10) \left( {}^{+20}_{-18} \right)^b$	$0.799(51)^+$
Bazavov 14	[141]	2+1	A	○	★	○		$r_1 = 0.3106(17) \text{ fm}^c$	$315 \left( {}^{+18}_{-12} \right)^d$	$0.746 \left( {}^{+42}_{-27} \right)$
Bazavov 12	[142]	2+1	A	○ <sup>†</sup>	○	○ <sup>#</sup>		$r_0 = 0.468 \text{ fm}$	$295(30)^*$	$0.70(7)^{**}$
Karbstein 18	[143]	2	A	○	○	○		$r_0 = 0.420(14) \text{ fm}^e$	302(16)	0.643(34)
Karbstein 14	[144]	2	A	○	○	○		$r_0 = 0.42 \text{ fm}$	331(21)	0.692(31)
ETM 11C	[145]	2	A	○	○	○		$r_0 = 0.42 \text{ fm}$	$315(30)^\S$	0.658(55)
Brambilla 23	[37]	0	A	○	○	★		$\sqrt{8t_0} = 0.9569(66)r_0$	$275 \left( {}^{+9}_{-12} \right)^+$	$0.657^{+23}_{-28}$
Husung 20	[146]	0	C	○	★	★		no quoted value for $\Lambda_{\overline{\text{MS}}}$		
Husung 17	[147]	0	C	○	★	★		$r_0 = 0.50 \text{ fm}$	232(6)	0.590(16)
Brambilla 10	[148]	0	A	○	★	○ <sup>††</sup>			$266(13)^+$	$0.637 \left( {}^{+32}_{-30} \right)^{\dagger\dagger}$
UKQCD 92	[128]	0	A	★	○ <sup>++</sup>	■		$\sqrt{\sigma} = 0.44 \text{ GeV}$	256(20)	0.686(54)
Bali 92	[149]	0	A	★	○ <sup>++</sup>	■		$\sqrt{\sigma} = 0.44 \text{ GeV}$	247(10)	0.661(27)

<sup>a</sup> Scale determined from  $t_0$  in Ref. [39].

<sup>b</sup>  $\alpha_{\overline{\text{MS}}}^{(5)}(M_Z) = 0.1179(7) \left( {}^{+13}_{-12} \right)$ .

<sup>c</sup> Determination on lattices with  $m_\pi L = 2.2 - 2.6$ . Scale from  $r_1$  [54] as determined from  $f_\pi$  in Ref. [62].

<sup>d</sup>  $\alpha_{\overline{\text{MS}}}^{(3)}(1.5 \text{ GeV}) = 0.336 \left( {}^{+12}_{-8} \right)$ ,  $\alpha_{\overline{\text{MS}}}^{(5)}(M_Z) = 0.1166 \left( {}^{+12}_{-8} \right)$ .

<sup>e</sup> Scale determined from  $f_\pi$ , see [57].

<sup>†</sup> Since values of  $\alpha_{\text{eff}}$  within our designated range are used, we assign a ○ despite values of  $\alpha_{\text{eff}}$  up to  $\alpha_{\text{eff}} = 0.5$  being used.

<sup>#</sup> Since values of  $2a/r$  within our designated range are used, we assign a ○ although only values of  $2a/r \geq 1.14$  are used at  $\alpha_{\text{eff}} = 0.3$ .

<sup>\*</sup> Using results from Ref. [63].

<sup>\*\*</sup>  $\alpha_{\overline{\text{MS}}}^{(3)}(1.5 \text{ GeV}) = 0.326(19)$ ,  $\alpha_{\overline{\text{MS}}}^{(5)}(M_Z) = 0.1156 \left( {}^{+21}_{-22} \right)$ .

<sup>§</sup> Both potential and  $r_0/a$  are determined on a small ( $L = 3.2r_0$ ) lattice.

<sup>††</sup> Uses lattice results of Ref. [64], some of which have very small lattice spacings where according to more recent investigations a bias due to the freezing of topology may be present.

<sup>+</sup> Our conversion using  $r_0 = 0.472 \text{ fm}$ .

<sup>++</sup> We give a ○ because only a NLO formula is used and the error bars are very large; our criterion does not apply well to these very early calculations.

Table 58: Short-distance potential results.

and then integrate the force to obtain an expression for the potential. The resulting integration constant is fixed by requiring the perturbative potential to be equal to the nonperturbative one exactly at a reference distance  $r_{\text{ref}}$  and the two are then compared at other values of  $r$ . As a further check, the force is also used directly.

For the quenched calculation of Brambilla 10 [148] very small lattice spacings,  $a \sim$

0.025 fm, were available from Ref. [136]. For ETM 11C [145], Bazavov 12 [142], Karbstein 14 [144] and Bazavov 14 [141] using dynamical fermions such small lattice spacings are not yet realized (Bazavov 14 reaches down to  $a \sim 0.041$  fm). They all use the tree-level improved potential as described above. We note that the value of  $\Lambda_{\overline{\text{MS}}}$  in physical units by ETM 11C [145] is based on a value of  $r_0 = 0.42$  fm. This is at least 10% smaller than the large majority of other values of  $r_0$ . Also the values of  $r_0/a$  on the finest lattices in ETM 11C [145] and  $r_1/a$  for Bazavov 14 [141] come from rather small lattices with  $m_\pi L \approx 2.4, 2.2$  respectively.

Instead of the procedure discussed previously, Karbstein 14 [144] reanalyzes the data of ETM 11C [145] by first estimating the Fourier transform  $\tilde{V}(p)$  of  $V(r)$  and then fitting the perturbative expansion of  $\tilde{V}(p)$  in terms of  $\alpha_{\overline{\text{MS}}}(p)$ . Of course, the Fourier transform requires some modelling of the  $r$ -dependence of  $V(r)$  at short and at large distances. The authors fit a linearly rising potential at large distances together with string-like corrections of order  $r^{-n}$  and define the potential at large distances by this fit.<sup>5</sup> Recall that for observables in momentum space we take the renormalization scale entering our criteria as  $\mu = q$ , Eq. (304). The analysis (as in ETM 11C [145]) is dominated by the data at the smallest lattice spacing, where a controlled determination of the overall scale is difficult due to possible finite-size effects. Karbstein 18 [143] is a reanalysis of Karbstein 14 and supersedes it. Some data with a different discretization of the static quark is added (on the same configurations) and the discrete lattice results for the static potential in position space are first parameterized by a continuous function, which then allows for an analytical Fourier transformation to momentum space.

Similarly also for Takaura 18 [139, 140] the momentum space potential  $\tilde{V}(Q)$  is the central object. Namely, they assume that renormalon/power-law effects are absent in  $\tilde{V}(Q)$  and only come in through the Fourier transformation. They provide evidence that renormalon effects (both  $u = 1/2$  and  $u = 3/2$ ) can be subtracted and arrive at a nonperturbative term  $k \Lambda_{\overline{\text{MS}}}^3 r^2$ . Two different analyses are carried out with the final result taken from “Analysis II”. Our numbers including the evaluation of the criteria refer to it. Together with the perturbative 3-loop (including the  $\alpha_s^4 \log \alpha_s$  term) expression, this term is fitted to the nonperturbative results for the potential in the region  $0.04 \text{ fm} \leq r \leq 0.35 \text{ fm}$ , where  $0.04 \text{ fm}$  is  $r = a$  on the finest lattice. The nonperturbative potential data originates from JLQCD ensembles (Symanzik-improved gauge action and Möbius domain-wall quarks) at three lattice spacings with a pion mass around 300 MeV. Since at the maximal distance in the analysis we find  $\alpha_{\overline{\text{MS}}}(2/r) = 0.43$ , the renormalization-scale criterion yields a ■. The perturbative behaviour is ○ because of the high orders in perturbation theory known. The continuum-limit criterion yields a ○.

One of the main issues for all these computations is whether the perturbative running of the coupling constant has been reached. While for  $N_f = 0$  fermions Brambilla 10 [148] reports agreement with perturbative behaviour at the smallest distances, Husung 17 (which goes to shorter distances) finds relatively large corrections beyond the 3-loop  $\alpha_{\text{qq}}$ . For dynamical fermions, Bazavov 12 [142] and Bazavov 14 [141] report good agreement with perturbation theory after the renormalon is subtracted or eliminated.

A second issue is the coverage of configuration space in some of the simulations, which use very small lattice spacings with periodic boundary conditions. Affected are the smallest two lattice spacings of Bazavov 14 [141] where very few tunnelings of the topological charge occur

<sup>5</sup>Note that at large distances, where string breaking is known to occur, this is not any more the ground-state potential defined by Eq. (333).

[54]. With present knowledge, it also seems possible that the older data by Refs. [64, 136] used by Brambilla 10 [148] are partially obtained with (close to) frozen topology.

The computation in Husung 17 [147], for  $N_f = 0$  flavours, first determines the coupling  $\bar{g}_{\text{qq}}^2(r, a)$  from the force and then performs a continuum extrapolation on lattices down to  $a \approx 0.015$  fm, using a step-scaling method at short distances,  $r/r_0 \lesssim 0.5$ . Using the 4-loop  $\beta_{\text{qq}}$  function this allows  $r_0\Lambda_{\text{qq}}$  to be estimated, which is then converted to the  $\overline{\text{MS}}$  scheme.  $\alpha_{\text{eff}} = \alpha_{\text{qq}}$  ranges from  $\sim 0.17$  to large values; we give  $\circ$  for renormalization scale and  $\star$  for perturbative behaviour. The range  $a\mu = 2a/r \approx 0.37\text{--}0.14$  leads to a  $\star$  in the continuum extrapolation. Recently these calculations have been extended in Husung 20 [146]. A finer lattice spacing of  $a = 0.01$  fm (scale from  $r_0 = 0.5$  fm) is reached and lattice volumes up to  $L/a = 192$  are simulated (in Ref. [147] the smallest lattice spacing is 0.015 fm). The Wilson action is used despite its significantly larger cutoff effects compared to Symanzik-improved actions; this avoids unitarity violations, thus allowing for a clean ground-state extraction via a generalized eigenvalue problem. Open boundary conditions are used to avoid the topology-freezing problem. Furthermore, new results for the continuum approach are employed, which determine the cutoff dependence at  $\mathcal{O}(a^2)$  including the exact coupling-dependent terms, in the asymptotic region where the Symanzik effective theory is applicable [122]. An ansatz for the remaining higher-order cutoff effects at  $\mathcal{O}(a^4)$  is propagated as a systematic error to the data, which effectively discards data for  $r/a < 3.5$ . The large-volume step-scaling function with step factor  $3/4$  is computed and compared to perturbation theory. For  $\alpha_{\text{qq}} > 0.2$  there is a noticeable difference between the 2-loop and 3-loop results. Furthermore, the ultra-soft contributions at 4-loop level give a significant contribution to the static  $Q\bar{Q}$  force. While this study is for  $N_f = 0$  flavours it does raise the question whether the weak-coupling expansion for the range of  $r$ -values used in present analyses of  $\alpha_s$  is sufficiently reliable. Around  $\alpha_{\text{qq}} \approx 0.21$  the differences get smaller but the error increases significantly, mainly due to the propagated lattice artifacts. The dependence of  $\Lambda_{\overline{\text{MS}}}^{(N_f=0)}\sqrt{8t_0}$  on  $\alpha_{\text{qq}}^3$  is very similar to the one observed in the previous study but no value for its  $\alpha_{\text{qq}} \rightarrow 0$  limit is quoted. Husung 20 [146] is more pessimistic about the error on the  $\Lambda$  parameter stating the relative error has to be 5% or larger, while Husung 17 quotes a relative error of 3%.

In 2+1-flavour QCD two new papers appeared on the determination of the strong coupling constant from the static quark anti-quark potential after the FLAG 19 report [137, 138]. In TUMQCD 19 [138]<sup>6</sup> the 2014 analysis of Bazavov 14 [141] has been extended by including three finer lattices with lattice spacing  $a = 0.035, 0.030$  and  $0.025$  fm as well as lattice results on the free energy of static quark anti-quark pair at nonzero temperature. On the new fine lattices the effect of freezing topology has been observed, however, it was verified that this does not affect the potential within the estimated errors [150, 151]. The comparison of the lattice result on the static potential has been performed in the interval  $[r_{\text{min}}, r_{\text{max}}]$ , with  $r_{\text{max}} = 0.131, 0.121, 0.098, 0.073$  and  $0.055$  fm. The main result quoted in the paper is based on the analysis with  $r_{\text{max}} = 0.073$  fm [138]. Since the new study employs a much wider range in  $r$  than the previous one [141] we give it a  $\star$  for the perturbative behaviour. Since  $\alpha_{\text{eff}} = \alpha_{\text{qq}}$  varies in the range  $0.2\text{--}0.4$  for the  $r$  values used in the main analysis we give  $\circ$  for the renormalization scale. Several values of  $r_{\text{min}}$  have been used in the analysis, the largest being  $r_{\text{min}}/a = \sqrt{8} \simeq 2.82$ , which corresponds to  $a\mu \simeq 0.71$ . Therefore, we give a  $\circ$  for continuum extrapolation in this case. An important difference compared to the previous study [141] is the variation of the renormalization scale. In Ref. [141] the renormalization scale was varied

<sup>6</sup>The majority of authors are the same as in [141].

by a factor of  $\sqrt{2}$  around the nominal value of  $\mu = 1/r$ , in order to exclude very low scales, for which the running of the strong coupling constant is no longer perturbative. In the new analysis the renormalization scale was varied by a factor of two. As the result, despite the extended data set and shorter distances used in the new study the perturbative error did not decrease [138]. We also note that the scale dependence turned out to be nonmonotonic in the range  $\mu = 1/(2r) - 2/r$  [138]. The final result reads (“us” stands for “ultra-soft”),

$$\begin{aligned}\Lambda_{\overline{\text{MS}}}^{(N_f=3)} &= 314.0 \pm 5.8(\text{stat}) \pm 3.0(\text{lat}) \pm 1.7(\text{scale}) \left( {}^{+13.4}_{-1.8} \right) (\text{pert}) \pm 4.0(\text{pert. us}) \text{ MeV} \\ &= 314 \left( {}^{+16}_{-08} \right) \text{ MeV},\end{aligned}\quad (336)$$

where all errors were combined in quadrature. This is in very good agreement with the previous determination [141].

The analysis was also applied to the singlet static quark anti-quark free energy at short distances. At short distances the free energy is expected to be the same as the static potential. This is verified numerically in the lattice calculations TUMQCD 19 [138] for  $rT < 1/4$  with  $T$  being the temperature. Furthermore, this is confirmed by the perturbative calculations at  $T > 0$  at NLO [152]. The advantage of using the free energy is that it gives access to much shorter distances. On the other hand, one has fewer data points because the condition  $rT < 1/4$  has to be satisfied. The analysis based on the free energy gives

$$\begin{aligned}\Lambda_{\overline{\text{MS}}}^{(N_f=3)} &= 310.9 \pm 11.3(\text{stat}) \pm 3.0(\text{lat}) \pm 1.7(\text{scale}) \left( {}^{+5.6}_{-0.8} \right) (\text{pert}) \pm 2.1(\text{pert. us}) \text{ MeV} \\ &= 311(13) \text{ MeV},\end{aligned}\quad (337)$$

in good agreement with the above result and thus, providing additional confirmation of it.

The analysis of Ayala 20 [137] uses a subset of data presented in TUMQCD 19 [138] with the same correction of the lattice effects. For this reason the continuum extrapolation gets ○, too. They match to perturbation theory for  $1/r > 2 \text{ GeV}$ , which corresponds to  $\alpha_{\text{eff}} = \alpha_{qq} = 0.2\text{--}0.4$ . Therefore, we give ○ for the renormalization scale. They verify the perturbative behaviour in the region  $1 \text{ GeV} < 1/r < 2.9 \text{ GeV}$ , which corresponds to variation of  $\alpha_{\text{eff}}^3$  by a factor of 3.34. However, the relative error on the final result has  $\delta\Lambda/\Lambda \simeq 0.035$  which is larger than  $\alpha_{\text{eff}}^3 = 0.011$ . Therefore, we give a ★ for the perturbative behaviour in this case. The final result for the  $\Lambda$ -parameter reads:

$$\Lambda_{\overline{\text{MS}}}^{(N_f=3)} = 338 \pm 2(\text{stat}) \pm 8(\text{matching}) \pm 10(\text{pert}) \text{ MeV} = 338(13) \text{ MeV}. \quad (338)$$

This is quite different from the above result. This difference is mostly due to the organization of the perturbative series. The authors use ultra-soft (log) resummation, i.e., they resum the terms  $\alpha_s^{3+n} \ln^n \alpha_s$  to all orders instead of using fixed-order perturbation theory. They also include what is called the terminant of the perturbative series associated to the leading renormalon of the force [137]. When they use fixed-order perturbation theory they obtain very similar results to Refs. [138, 141]. It has been argued that log resummation cannot be justified since for the distance range available in the lattice studies  $\alpha_s$  is not small enough and the logarithmic and nonlogarithmic higher-order terms are of a similar size [141]. On the other hand, the resummation of ultra-soft logs does not lead to any anomalous behaviour of the perturbative expansion like large scale dependence or bad convergence [137].

To obtain the value of  $\Lambda_{\overline{\text{MS}}}^{(N_f=3)}$  from the static potential we combine the results in Eqs. (336) and (338) using the weighted average with the weight given by the perturbative error and



using the difference in the central value as the error estimate. This leads to

$$\Lambda_{\overline{\text{MS}}}^{(N_f=3)} = 330(24) \text{ MeV}, \quad (339)$$

from the static potential determination. In the case of TUMQCD 19, where the perturbative error is very asymmetric we used the larger upper error for the calculation of the corresponding weight.

A new analysis with  $N_f = 0$  has been presented in Brambilla 23 [37] where gradient flow is used to study the static force. The use of gradient flow allows an improved determination of the static force while adding to the problem a new scale, the gradient-flow time  $\tau_F$ . The lattice volumes used are  $40 \times 20^3$ ,  $52 \times 26^3$ ,  $60 \times 30^2$  and  $80 \times 40^3$ , with corresponding lattice spacings ranging from 0.06 to 0.03 fm, using the Wilson action. On the finest lattice an increase in the autocorrelation of the topological charge is observed and taken into account by increasing the Monte Carlo time in-between measurements. The reference scale  $t_0$ , used throughout the analysis, is obtained from a measurement of the action density by imposing

$$\tau_F \left\langle \frac{1}{4} G_{\mu\nu} G^{\mu\nu} \right\rangle \Big|_{\tau_F=t_0} = 0.3. \quad (340)$$

The static force is computed from the insertion of the chromoelectric field in the expectation value of the Wilson loop,

$$F(r) = -i \lim_{T \rightarrow \infty} \frac{\langle \text{Tr} [W_{r \times T} \hat{\mathbf{r}} \cdot \mathbf{gE}(\mathbf{r}, \mathbf{t})] \rangle}{\langle \text{Tr} W_{r \times T} \rangle}, \quad (341)$$

and tree-level improvement is used to improve the extrapolation to the continuum limit. The dimensionless product  $r^2 F(r)$  yields the observable used for the extraction of  $\alpha_s$ .

Results extrapolated to  $\tau_F = 0$  are used for a conventional analysis along the lines of previous publications using the static force. The fit uses the perturbative expansion of the force including 3-loop contributions and leading ultrasoft logarithms. Data points with  $r/\sqrt{t_0} \in [0.80, 1.15]$  are included in the fit, which yields

$$\sqrt{8t_0} \Lambda_{\overline{\text{MS}}}^{(N_f=0)} = 0.6353 \pm 0.0032(\text{stat}) \pm 0.0013(\text{AIC}), \quad (342)$$

where the label AIC refers to the Bayesian procedure for combining results from different fit ranges based on Akaike's information criterion, as proposed in Ref. [153]. Note that the error on this result is still dominated by statistics rather than the systematics related to the choice of fitting range. The matching scale in these fits is the usual scale  $\mu = 1/r$ .

Measurements at  $\tau_F \neq 0$  allow an alternative way to extract the strong coupling constant by fitting to the perturbative expression for the force at finite flow time. The latter perturbative expansion is only known at 1-loop, which is used as a correction of the higher-order result at  $\tau_F = 0$ . The best result is obtained by fitting the  $r$ -dependence at fixed values of  $\tau_F$ , which yields

$$\sqrt{8t_0} \Lambda_{\overline{\text{MS}}}^{(N_f=0)} = 0.629_{-26}^{+22}. \quad (343)$$

The scale of perturbative matching is defined as

$$\mu = \frac{1}{\sqrt{sr^2 + 8b\tau_F}}. \quad (344)$$

The uncertainty related to the truncation of the perturbative expansion is estimated by scale variations, where  $b = 0$  and  $s$  is varied by a factor  $\sqrt{2}$  in the zero-flow-time part of the perturbative expansion, while  $s = 1$  and  $b = 0, 1, -0.5$  in the finite-flow-time part. The central value corresponds to  $s = 1, b = 0$ . The error on the result above is dominated by the  $s$ -scale variation. The ratio  $\sqrt{t_0}/r_0$  is computed in Brambilla 23 and allows to quote a final result in units of  $r_0$ ,

$$r_0 \Lambda_{\overline{\text{MS}}}^{(N_f=0)} = 0.657 \left( {}^{+23}_{-28} \right). \quad (345)$$

The continuum extrapolation is based on four lattice spacings. From the data reported in the figures, we see that for  $r = 0.7323\sqrt{t_0}$ , the effective coupling is below the requested threshold of 0.03, while the lattice spacing is such that  $0.2321 \leq \mu a \leq 0.4916$ . Therefore, we can give a ★ for the continuum extrapolation. Fits to the perturbative behaviour are performed for  $0.27 \leq \alpha_{\text{eff}} \leq 0.36$  and  $n_\ell = 3$  in the perturbative expansion. Hence,  $\alpha_{\text{eff}}^{n_\ell}$  changes by a factor of 2.37, which is 5% above the threshold of  $(3/2)^2$ . We feel in this case we can award a ○ for the perturbative behaviour. Finally, given the range of values for  $\alpha_{\text{eff}}$  quoted above, we give a ○ for the renormalization scale.

**Scale variations.** The perturbative matching for the static potential is done at lower scales,  $\mu = 1.5, 2.5, 5.0$  GeV. We have computed the change in the determination of  $\alpha_{\overline{\text{MS}}}(M_Z)$  as explained in Sec. 9.1. The systematic errors depend on the value of the perturbative matching scale. We obtain

$Q = 1.5$  GeV

$$\delta_{(2)} = 2.6\% \quad \delta_{(2)}^* = 2.7\%. \quad (346)$$

The value of  $\delta_{(4)}^*$  cannot be computed in this case, because the matching scale is low, already at the boundary of the region where the perturbative expansion can be trusted.

$Q = 2.5$  GeV

$$\delta_{(4)}^* = 0.9\%, \quad \delta_{(2)} = 1.5\% \quad \delta_{(2)}^* = 1.5\%. \quad (347)$$

$Q = 5.0$  GeV

$$\delta_{(4)}^* = 0.4\%, \quad \delta_{(2)} = 0.8\% \quad \delta_{(2)}^* = 0.8\%. \quad (348)$$

Note that in the last two cases it was possible to compute  $\delta_{(4)}^*$ .

For the larger values of  $Q$ , the error obtained from scale variations is very similar to the error quoted in previous editions of FLAG, where scale variations were not performed systematically. For  $Q = 1.5$  GeV the error is larger, as expected since the matching of perturbation theory happens at lower energy.

## 9.6 $\alpha_s$ from the light-quark vacuum polarization in momentum/position space

### 9.6.1 General considerations

Except for the calculation Cali 20 [48], where position space is used (see below), the light-flavour-current two-point function is usually evaluated in momentum space, in terms of the

vacuum-polarization function. Assuming  $N_f = 3$  flavours in the isospin limit, with flavour nonsinglet currents consisting of up and down quarks,  $J_\mu^a$  ( $a = 1, \dots, 3$ ), the momentum representation takes the form

$$\langle J_\mu^a J_\nu^b \rangle = \delta^{ab} [(\delta_{\mu\nu} Q^2 - Q_\mu Q_\nu) \Pi_J^{(1)}(Q) - Q_\mu Q_\nu \Pi_J^{(0)}(Q)], \quad (349)$$

where  $Q_\mu$  is a space-like momentum and  $J_\mu \equiv V_\mu$  for a vector current and  $J_\mu \equiv A_\mu$  for an axial-vector current.<sup>7</sup> Defining  $\Pi_J(Q) \equiv \Pi_J^{(0)}(Q) + \Pi_J^{(1)}(Q)$ , the operator product expansion (OPE) of  $\Pi_{V/A}(Q)$  is given by

$$\begin{aligned} \Pi_{V/A}|_{\text{OPE}}(Q^2, \alpha_s) &= c + C_1^{V/A}(Q^2) + C_m^{V/A}(Q^2) \frac{\bar{m}^2(Q)}{Q^2} + \sum_{q=u,d,s} C_{\bar{q}q}^{V/A}(Q^2) \frac{\langle m_q \bar{q}q \rangle}{Q^4} \\ &\quad + C_{GG}^{V/A}(Q^2) \frac{\langle \alpha_s GG \rangle}{Q^4} + \mathcal{O}(Q^{-6}), \end{aligned} \quad (350)$$

for large  $Q^2$ . The perturbative coefficient functions  $C_X^{V/A}(Q^2)$  for the operators  $X$  ( $X = 1, \bar{q}q, GG$ ) are given as  $C_X^{V/A}(Q^2) = \sum_{i \geq 0} \left( C_X^{V/A} \right)^{(i)} \alpha_s^i(Q^2)$  and  $\bar{m}$  is the running mass of the mass-degenerate up and down quarks.  $C_1^{V/A}$  is known including  $\alpha_s^4$  in a continuum renormalization scheme such as the  $\overline{\text{MS}}$  scheme [155–158]. Nonperturbatively, there are terms in  $C_X^{V/A}$  that do not have a series expansion in  $\alpha_s$ . For an example for the unit operator see Ref. [159]. The term  $c$  is  $Q$ -independent and divergent in the limit of infinite ultraviolet cutoff. However the Adler function defined as

$$D(Q^2) \equiv -Q^2 \frac{d\Pi(Q^2)}{dQ^2}, \quad (351)$$

is a scheme-independent finite quantity, which gives rise to an effective coupling. Therefore, one can determine the running coupling constant in the  $\overline{\text{MS}}$  scheme from the vacuum-polarization function computed by a lattice-QCD simulation. Of course, there is the choice whether to use the vector or the axial-vector channel, or both, the canonical choice being  $\Pi_{V+A} = \Pi_V + \Pi_A$ . While perturbation theory does not distinguish between these channels, the nonperturbative contributions are different, and the quality of lattice data may differ, too. For a given choice, the lattice data of the vacuum polarization is fitted with the perturbative formula Eq. (350) with fit parameter  $\Lambda_{\overline{\text{MS}}}$  parameterizing the running coupling  $\alpha_{\overline{\text{MS}}}(Q^2)$ .

While there is no problem in discussing the OPE at the nonperturbative level, the ‘condensates’ such as  $\langle \alpha_s GG \rangle$  are ambiguous, since they mix with lower-dimensional operators including the unity operator. Therefore, one should work in the high- $Q^2$  regime where power corrections are negligible within the given accuracy. Thus setting the renormalization scale as  $\mu \equiv \sqrt{Q^2}$ , one should seek, as always, the window  $\Lambda_{\text{QCD}} \ll \mu \ll a^{-1}$ .

### 9.6.2 Definitions in position space

The two-point current correlation functions in position space contain the same physical information as in momentum space, but the technical details are sufficiently different to warrant

<sup>7</sup>For the general mass-nondegenerate case with SU(3) flavour nonsinglet currents see, for example, Ref. [154].

a separate discussion. The (Euclidean) current-current correlation function for  $J_{ff'}^\mu$  (with flavour indices  $f, f'$ ) is taken to be either the flavour nondiagonal vector or axial-vector current, with the Lorentz indices contracted,

$$C_{A,V}(x) = - \sum_{\mu} \left\langle J_{ff'A,V}^\mu(x) J_{ff'A,V}^\mu(0) \right\rangle = \frac{6}{\pi^4(x^2)^3} \left( 1 + \frac{\alpha_s}{\pi} + \mathcal{O}(\alpha^2) \right). \quad (352)$$

In the chiral limit, the perturbative expansion is known to  $\alpha_s^4$  [160], and is identical for vector and axial-vector correlators. The only scale is set by the Euclidean distance  $\mu = 1/|x|$  and the effective coupling can thus be defined as

$$\alpha_{\text{eff}}(\mu = 1/|x|) = \pi \left[ (x^2)^3 (\pi^4/6) C_{A,V}(x) - 1 \right]. \quad (353)$$

As communicated to us by the authors of [48], there is a typo in Eq. (35) of [160]. For future reference, the numerical coefficients for the 3-loop conversion

$$\alpha_{\text{eff}}(\mu) = \alpha_{\overline{\text{MS}}}(\mu) + c_1 \alpha_{\overline{\text{MS}}}^2(\mu) + c_2 \alpha_{\overline{\text{MS}}}^3(\mu) + c_3 \alpha_{\overline{\text{MS}}}^4(\mu), \quad (354)$$

should read

$$c_1 = -1.4346, \quad c_2 = 0.16979, \quad c_3 = 3.21120. \quad (355)$$

### 9.6.3 Discussion of computations

Results using this method in momentum space are, to date, only available using overlap fermions or domain-wall fermions. Cal 20 [48] consider vacuum polarization in position space using  $\mathcal{O}(a)$ -improved Wilson fermions. The results are collected in Tab. 59 for  $N_f = 2$ , JLQCD/TWQCD 08C [161] and for  $N_f = 2 + 1$ , JLQCD 10 [76], Hudspith 18 [77] and Cal 20 [48].

We first discuss the results of JLQCD/TWQCD 08C [161] and JLQCD 10 [76]. The fit to Eq. (350) is done with the 4-loop relation between the running coupling and  $\Lambda_{\overline{\text{MS}}}$ . It is found that without introducing fit parameters for condensate contributions, the momentum scale where the perturbative formula gives good agreement with the lattice results is very narrow,  $aQ \simeq 0.8\text{--}1.0$ . When fit parameters for condensate contributions are included the perturbative formula gives good agreement with the lattice results for the extended range  $aQ \simeq 0.6\text{--}1.0$ . Since there is only a single lattice spacing  $a \approx 0.11$  fm there is a ■ for the continuum limit. The renormalization scale  $\mu$  is in the range of  $Q = 1.6\text{--}2$  GeV. Approximating  $\alpha_{\text{eff}} \approx \alpha_{\overline{\text{MS}}}(Q)$ , we estimate that  $\alpha_{\text{eff}} = 0.25\text{--}0.30$  for  $N_f = 2$  and  $\alpha_{\text{eff}} = 0.29\text{--}0.33$  for  $N_f = 2 + 1$ . Thus we give a ○ and ■ for  $N_f = 2$  and  $N_f = 2 + 1$ , respectively, for the renormalization scale and a ■ for the perturbative behaviour.

A further investigation of this method was initiated in Hudspith 15 [162] and completed by Hudspith 18 [77] (see also [164]) based on domain-wall fermion configurations at three lattice spacings,  $a^{-1} = 1.78, 2.38, 3.15$  GeV, with three different light-quark masses on the two coarser lattices and one on the fine lattice. An extensive discussion of condensates, using continuum finite-energy sum rules was employed to estimate where their contributions might be negligible. It was found that even up to terms of  $O((1/Q^2)^8)$  (a higher order than depicted in Eq. (350) but with constant coefficients) no single condensate dominates and apparent convergence was poor for low  $Q^2$  due to cancellations between contributions of similar size with alternating signs. (See, e.g., the list given by Hudspith 15 [162].) Choosing  $Q^2$  to be

Collaboration	Ref.	$N_f$	publication status	renormalization scale	perturbative behaviour	continuum extrapolation	scale	$\Lambda_{\overline{\text{MS}}}[\text{MeV}]$	$r_0\Lambda_{\overline{\text{MS}}}$
Cali 20	[48]	2+1	A	○	★	★	$m_\Upsilon^\S$	342(17)	0.818(41) <sup>a</sup>
Hudspith 18	[77]	2+1	P	○	○	■	$m_\Omega^*$	337(40)	0.806(96) <sup>b</sup>
Hudspith 15	[162]	2+1	C	○	○	■	$m_\Omega^*$	300(24) <sup>+</sup>	0.717(58)
JLQCD 10	[76]	2+1	A	■	■	■	$r_0 = 0.472 \text{ fm}$	247(5) <sup>†</sup>	0.591(12)
JLQCD/TWQCD 08C [161]		2	A	○	■	■	$r_0 = 0.49 \text{ fm}$	234(9)( <sup>+16</sup> <sub>-0</sub> )	0.581(22)( <sup>+40</sup> <sub>-0</sub> )

<sup>§</sup> via  $t_0/a^2$ , still unpublished. We use  $r_0 = 0.472 \text{ fm}$

<sup>\*</sup> Determined in [163].

<sup>a</sup> Evaluates to  $\alpha_{\overline{\text{MS}}}^{(5)}(M_Z) = 0.11864(114)$

In conversion to  $r_0\Lambda$  we used  $r_0 = 0.472 \text{ fm}$ .

<sup>b</sup>  $\alpha_{\overline{\text{MS}}}^{(5)}(M_Z) = 0.1181(27)(^{+8}_{-22})$ .  $\Lambda_{\overline{\text{MS}}}$  determined by us from  $\alpha_{\overline{\text{MS}}}^{(3)}(2 \text{ GeV}) = 0.2961(185)$ . In conversion to  $r_0\Lambda$  we used  $r_0 = 0.472 \text{ fm}$ .

<sup>+</sup> Determined by us from  $\alpha_{\overline{\text{MS}}}^{(3)}(2 \text{ GeV}) = 0.279(11)$ . Evaluates to  $\alpha_{\overline{\text{MS}}}^{(5)}(M_Z) = 0.1155(18)$ .

<sup>†</sup>  $\alpha_{\overline{\text{MS}}}^{(5)}(M_Z) = 0.1118(3)(^{+16}_{-17})$ .

Table 59: Results from the vacuum polarization in both momentum and position space.

at least  $\sim 3.8 \text{ GeV}^2$  mitigated the problem, but then the coarsest lattice had to be discarded, due to large lattice artefacts. So this gives a ■ for continuum extrapolation. With the higher  $Q^2$  the quark-mass dependence of the results was negligible, so ensembles with different quark masses were averaged over. A range of  $Q^2$  from 3.8–16  $\text{GeV}^2$  gives  $\alpha_{\text{eff}} = 0.31\text{--}0.22$ , so there is a ○ for the renormalization scale. The value of  $\alpha_{\text{eff}}^3$  reaches  $\Delta\alpha_{\text{eff}}/(8\pi b_0\alpha_{\text{eff}})$  and thus gives a ○ for perturbative behaviour. In Hudspith 15 [162] (superseded by Hudspith 18 [77]) about a 20% difference in  $\Pi_V(Q^2)$  was seen between the two lattice spacings and a result is quoted only for the smaller  $a$ .

#### 9.6.4 Vacuum polarization in position space

Cali 20 [48] evaluate the light-current two-point function in position space. The two-point functions for the nonperturbatively renormalized (nonsinglet) flavour currents is computed for distances  $|x|$  between 0.1 and 0.25 fm and extrapolated to the chiral limit. The available CLS configurations are used for this work, with lattice spacings between 0.039 and 0.086 fm. Despite fully nonperturbative renormalization and  $\mathcal{O}(a)$  improvement, the remaining  $\mathcal{O}(a^2)$  effects, as measured by  $O(4)$  symmetry violations, are very large, even after subtraction of

tree-level lattice effects. Therefore the authors performed a numerical stochastic perturbation theory (NSPT) simulation in order to determine the lattice artifacts at  $\mathcal{O}(g^2)$ . Only after subtraction of these effects the constrained continuum extrapolations from three different lattice directions to the same continuum limit are characterized by reasonable  $\chi^2$ -values, so the feasibility of the study crucially depends on this step. Interestingly, there is no subtraction performed of nonperturbative effects. For instance, chiral symmetry breaking would manifest itself in a difference between the vector and the axial-vector two-point functions, and is invisible to perturbation theory, where these two-point functions are known to  $\alpha_s^4$  [160]. According to the authors, phenomenological estimates suggest that a difference of 1.5% between the continuum correlators would occur around 0.3 fm and this difference would not be resolvable by their lattice data. Equality within their errors is confirmed for shorter distances. We note, however, that chiral symmetry breaking effects are but one class of nonperturbative effects, and their smallness does not allow for the conclusion that such effects are generally small. In fact, the need for explicit subtractions in momentum space analyses may lead one to suspect that such effects are not negligible at the available distance scales. For the determination of  $\Lambda_{\overline{\text{MS}}}^{(N_f=3)}$  the authors limit the range of distances to 0.13–0.19 fm, where  $\alpha_{\text{eff}} \in [0.2354, 0.3075]$  (private communication by the authors). These effective couplings are converted to  $\overline{\text{MS}}$  couplings at the same scales  $\mu = 1/|x|$  by solving Eq. (354) numerically. Central values for the  $\Lambda$ -parameter thus obtained are in the range 325–370 MeV (using the  $\beta$ -function at 5-loop order) and a weighted average yields the quoted result 342(17) MeV, where the average emphasizes the data around  $|x| = 0.16$  fm, or  $\mu = 1.3$  GeV.

Applying the FLAG criteria the range of lattice spacings yields ★ for the continuum extrapolation. However, the FLAG criterion implicitly assumes that the remaining cutoff effects after nonperturbative  $\mathcal{O}(a)$  improvement are small, which is not the case here. Some hypercubic lattice artefacts are still rather large even after 1-loop subtraction, but these are not used for the analysis. As for the renormalization scale, the lowest effective coupling entering the analysis is  $0.235 < 0.25$ , so we give ○. As for perturbative behaviour, for the range of couplings in the above interval  $\alpha_{\text{eff}}^3$  changes by  $(0.308/0.235)^3 \approx 2.2$ , marginally reaching  $(3/2)^2 = 2.25$ . The errors  $\Delta\alpha_{\text{eff}}$  after continuum and chiral extrapolations are 4–6% (private communication by the authors) and the induced uncertainty in  $\Lambda$  is comfortably above  $2\alpha_{\text{eff}}^3$ , which gives a ★ according to FLAG criteria.

Although the current FLAG criteria are formally passed by this result, the quoted error of 5% for  $\Lambda$  seems very optimistic. We have performed a simple test, converting to the  $\overline{\text{MS}}$  scheme by inverting Eq. (354) perturbatively (instead of solving the fixed-order equation numerically). The differences between the couplings are of order  $\alpha_s^5$  and thus indicative of the sensitivity to perturbative truncation errors. The resulting  $\Lambda$ -parameter estimates are now in the range 409–468 MeV, i.e., ca. 15–30% larger than before. While the difference between both estimates decreases proportionally to the expected  $\alpha_{\text{eff}}^3$ , an extraction of the  $\Lambda$ -parameter in this energy range is a priori affected by systematic uncertainties corresponding to such differences. The FLAG criterion might fail to capture this, e.g., if the assumption of an  $\mathcal{O}(1)$  coefficient for the asymptotic  $\alpha_{\text{eff}}^3$  behaviour is not correct. Some indication for a problematic behaviour is indeed seen when perturbatively inverting Eq. (354) to order  $\alpha_s^3$ . The resulting  $\overline{\text{MS}}$  couplings are then closer to the values used in CalI 20, although the difference is formally  $\mathcal{O}(\alpha_s^4)$  rather than  $\mathcal{O}(\alpha_s^5)$ .



**Scale variations.** Using scale variations to determine the systematic error due to the truncation of the perturbative series only makes sense when the extrapolation of the observable to the continuum limit is under control. Therefore, we apply our common procedure only to the results in CalI 20 [48]. Using  $\mu \approx 1.3$  GeV as the typical scale set by the inverse of the distance, yields

$$\delta_{(4)}^* = 1.0\%, \quad \delta_{(2)} = 11.6\% \quad \delta_{(2)}^* = 0.6\%. \quad (356)$$

The discrepancy between the variation around  $Q$ ,  $\delta_{(2)} = 11.6\%$ , and the variation around the scale of fastest apparent convergence,  $\delta_{(2)}^* = 0.6\%$ , is due to the large value of the factor  $s_{\text{ref}}^* = 2.72$ . As a consequence the scale of fastest apparent convergence is artificially large compared to the actual scale where the lattice observable is computed. The large value of  $\delta_{(2)}$ , obtained for  $s_{\text{ref}} = 1$ , shows that the scale of the lattice observable is too low to keep the systematic errors under control.

## 9.7 $\alpha_s$ from observables at the lattice spacing scale

### 9.7.1 General considerations

The general method is to evaluate a short-distance quantity  $Q$  at the scale of the lattice spacing  $\sim 1/a$  and then determine its relationship to  $\alpha_{\overline{\text{MS}}}$  via a perturbative expansion.

This is epitomized by the strategy of the HPQCD collaboration [78, 165], discussed here for illustration, which computes and then fits to a variety of short-distance quantities

$$Y = \sum_{n=1}^{n_{\text{max}}} c_n \alpha_{V'}^n(q^*). \quad (357)$$

The quantity  $Y$  is taken as the logarithm of small Wilson loops (including some nonplanar ones), Creutz ratios, ‘tadpole-improved’ Wilson loops and the tadpole-improved or ‘boosted’ bare coupling ( $\mathcal{O}(20)$  quantities in total). The perturbative coefficients  $c_n$  (each depending on the choice of  $Y$ ) are known to  $n = 3$  with additional coefficients up to  $n_{\text{max}}$  being fitted numerically. The running coupling  $\alpha_{V'}$  is related to  $\alpha_V$  from the static-quark potential (see Sec. 9.5).<sup>8</sup>

The coupling constant is fixed at a scale  $q^* = d/a$ . The latter is chosen as the mean value of  $\ln q$  with the one-gluon loop as measure [79, 166]. (Thus a different result for  $d$  is found for every short-distance quantity.) A rough estimate yields  $d \approx \pi$ , and in general the renormalization scale is always found to lie in this region.

For example, for the Wilson loop  $W_{mn} \equiv \langle W(ma, na) \rangle$  we have

$$\ln \left( \frac{W_{mn}}{u_0^{2(m+n)}} \right) = c_1 \alpha_{V'}(q^*) + c_2 \alpha_{V'}^2(q^*) + c_3 \alpha_{V'}^3(q^*) + \dots, \quad (358)$$

for the tadpole-improved version, where  $c_1, c_2, \dots$  are the appropriate perturbative coefficients and  $u_0 = W_{11}^{1/4}$ . Substituting the nonperturbative simulation value in the left hand side, we can determine  $\alpha_{V'}(q^*)$ , at the scale  $q^*$ . Note that one finds empirically that perturbation theory for these tadpole-improved quantities have smaller  $c_n$  coefficients and so the series has a faster apparent convergence compared to the case without tadpole improvement.

<sup>8</sup>  $\alpha_{V'}$  is defined by  $\Lambda_{V'} = \Lambda_V$  and  $b_i^{V'} = b_i^V$  for  $i = 0, 1, 2$  but  $b_i^{V'} = 0$  for  $i \geq 3$ .

Using the  $\beta$ -function in the  $V'$  scheme, results can be run to a reference value, chosen as  $\alpha_0 \equiv \alpha_{V'}(q_0)$ ,  $q_0 = 7.5 \text{ GeV}$ . This is then converted perturbatively to the continuum  $\overline{\text{MS}}$  scheme

$$\alpha_{\overline{\text{MS}}}(q_0) = \alpha_0 + d_1 \alpha_0^2 + d_2 \alpha_0^3 + \cdots, \quad (359)$$

where  $d_1, d_2$  are known 1- and 2-loop coefficients.

Other collaborations have focused more on the bare ‘boosted’ coupling constant and directly determined its relationship to  $\alpha_{\overline{\text{MS}}}$ . Specifically, the boosted coupling is defined by

$$\alpha_P(1/a) = \frac{1}{4\pi} \frac{g_0^2}{u_0^4}, \quad (360)$$

again determined at a scale  $\sim 1/a$ . As discussed previously, since the plaquette expectation value in the boosted coupling contains the tadpole-diagram contributions to all orders, which are dominant contributions in perturbation theory, there is an expectation that the perturbation theory using the boosted coupling has smaller perturbative coefficients [79], and hence smaller perturbative errors.

### 9.7.2 Continuum limit

Lattice results always come along with discretization errors, which one needs to remove by a continuum extrapolation. As mentioned previously, in this respect the present method differs in principle from those in which  $\alpha_s$  is determined from physical observables. In the general case, the numerical results of the lattice simulations at a value of  $\mu$  fixed in physical units can be extrapolated to the continuum limit, and the result can be analyzed as to whether it shows perturbative running as a function of  $\mu$  in the continuum. For observables at the cutoff-scale ( $q^* = d/a$ ), discretization effects cannot easily be separated out from perturbation theory, as the scale for the coupling comes from the lattice spacing. Therefore the restriction  $a\mu \ll 1$  (the ‘continuum-extrapolation’ criterion) is not applicable here. Discretization errors of order  $a^2$  are, however, present. Since  $a \sim \exp(-1/(2b_0 g_0^2)) \sim \exp(-1/(8\pi b_0 \alpha(q^*)))$ , these errors now appear as power corrections to the perturbative running, and have to be taken into account in the study of the perturbative behaviour, which is to be verified by changing  $a$ . One thus usually fits with power corrections in this method.

In order to keep a symmetry with the ‘continuum-extrapolation’ criterion for physical observables and to remember that discretization errors are, of course, relevant, we replace it here by one for the lattice spacings used:

- Lattice spacings
  - ★ 3 or more lattice spacings, at least 2 points below  $a = 0.1 \text{ fm}$
  - 2 lattice spacings, at least 1 point below  $a = 0.1 \text{ fm}$
  - otherwise

### 9.7.3 Discussion of computations

Note that due to  $\mu \sim 1/a$  being relatively large the results easily have a ★ or ○ in the rating on renormalization scale.

Collaboration	Ref.	$N_f$	<div>publication status</div> <div>renormalization scale</div> <div>perturbative behaviour</div> <div>lattice spacings</div>				scale	$\Lambda_{\overline{\text{MS}}}[\text{MeV}]$	$r_0\Lambda_{\overline{\text{MS}}}$
HPQCD 10 <sup>a</sup> §	[167]	2+1	A	○	★	★	$r_1 = 0.3133(23) \text{ fm}$	340(9)	0.812(22)
HPQCD 08A <sup>a</sup>	[78]	2+1	A	○	★	★	$r_1 = 0.321(5) \text{ fm}^{\dagger\dagger}$	338(12) <sup>*</sup>	0.809(29)
Maltman 08 <sup>a</sup>	[168]	2+1	A	○	○	★	$r_1 = 0.318 \text{ fm}$	352(17) <sup>†</sup>	0.841(40)
HPQCD 05A <sup>a</sup>	[165]	2+1	A	○	○	○	$r_1^{\dagger\dagger}$	319(17) <sup>**</sup>	0.763(42)
QCDSF/UKQCD 05	[169]	2	A	★	■	★	$r_0 = 0.467(33) \text{ fm}$	261(17)(26)	0.617(40)(21) <sup>b</sup>
SESAM 99 <sup>c</sup>	[170]	2	A	○	■	■	$c\bar{c}(1\text{S-1P})$		
Wingate 95 <sup>d</sup>	[171]	2	A	★	■	■	$c\bar{c}(1\text{S-1P})$		
Davies 94 <sup>e</sup>	[172]	2	A	★	■	■	$\Upsilon$		
Aoki 94 <sup>f</sup>	[173]	2	A	★	■	■	$c\bar{c}(1\text{S-1P})$		
Kitazawa 16	[174]	0	A	★	★	★	$w_0$	260(5) <sup>j</sup>	0.621(11) <sup>j</sup>
FlowQCD 15	[175]	0	P	★	★	★	$w_{0.4}$ <sup>i</sup>	258(6) <sup>i</sup>	0.618(11) <sup>i</sup>
QCDSF/UKQCD 05	[169]	0	A	★	○	★	$r_0 = 0.467(33) \text{ fm}$	259(1)(20)	0.614(2)(5) <sup>b</sup>
SESAM 99 <sup>c</sup>	[170]	0	A	★	■	■	$c\bar{c}(1\text{S-1P})$		
Wingate 95 <sup>d</sup>	[171]	0	A	★	■	■	$c\bar{c}(1\text{S-1P})$		
Davies 94 <sup>e</sup>	[172]	0	A	★	■	■	$\Upsilon$		
El-Khadra 92 <sup>g</sup>	[176]	0	A	★	■	○	$c\bar{c}(1\text{S-1P})$	234(10)	0.560(24) <sup>h</sup>

<sup>a</sup> The numbers for  $\Lambda$  have been converted from the values for  $\alpha_s^{(5)}(M_Z)$ .

§  $\alpha_{\overline{\text{MS}}}^{(3)}(5 \text{ GeV}) = 0.2034(21)$ ,  $\alpha_{\overline{\text{MS}}}^{(5)}(M_Z) = 0.1184(6)$ , only update of intermediate scale and  $c$ -,  $b$ -quark masses, supersedes HPQCD 08A.

†  $\alpha_{\overline{\text{MS}}}^{(5)}(M_Z) = 0.1192(11)$ .

\*  $\alpha_V^{(3)}(7.5 \text{ GeV}) = 0.2120(28)$ ,  $\alpha_{\overline{\text{MS}}}^{(5)}(M_Z) = 0.1183(8)$ , supersedes HPQCD 05.

†† Scale is originally determined from  $\Upsilon$  mass splitting.  $r_1$  is used as an intermediate scale. In conversion to  $r_0\Lambda_{\overline{\text{MS}}}$ ,  $r_0$  is taken to be 0.472 fm.

\*\*  $\alpha_V^{(3)}(7.5 \text{ GeV}) = 0.2082(40)$ ,  $\alpha_{\overline{\text{MS}}}^{(5)}(M_Z) = 0.1170(12)$ .

<sup>b</sup> This supersedes Refs. [177–179].  $\alpha_{\overline{\text{MS}}}^{(5)}(M_Z) = 0.112(1)(2)$ . The  $N_f = 2$  results were based on values for  $r_0/a$  which have later been found to be too small [59]. The effect will be of the order of 10–15%, presumably an increase in  $\Lambda r_0$ .

<sup>c</sup>  $\alpha_{\overline{\text{MS}}}^{(5)}(M_Z) = 0.1118(17)$ .

<sup>d</sup>  $\alpha_V^{(3)}(6.48 \text{ GeV}) = 0.194(7)$  extrapolated from  $N_f = 0, 2$ .  $\alpha_{\overline{\text{MS}}}^{(5)}(M_Z) = 0.107(5)$ .

<sup>e</sup>  $\alpha_P^{(3)}(8.2 \text{ GeV}) = 0.1959(34)$  extrapolated from  $N_f = 0, 2$ .  $\alpha_{\overline{\text{MS}}}^{(5)}(M_Z) = 0.115(2)$ .

<sup>f</sup> Estimated  $\alpha_{\overline{\text{MS}}}^{(5)}(M_Z) = 0.108(5)(4)$ .

<sup>g</sup> This early computation violates our requirement that scheme conversions are done at the 2-loop level.  $\Lambda_{\overline{\text{MS}}}^{(4)} = 160(^{+47}_{-37}) \text{ MeV}$ ,  $\alpha_{\overline{\text{MS}}}^{(4)}(5 \text{ GeV}) = 0.174(12)$ . We converted this number to give  $\alpha_{\overline{\text{MS}}}^{(5)}(M_Z) = 0.106(4)$ .

<sup>h</sup> We used  $r_0 = 0.472 \text{ fm}$  to convert to  $r_0\Lambda_{\overline{\text{MS}}}$ .

<sup>i</sup> Reference scale  $w_{0.4}$  where  $w_x$  is defined by  $t\partial_t[t^2\langle E(t)\rangle]|_{t=w_x^2} = x$  in terms of the action density  $E(t)$  at positive flow time  $t$  [175]. Our conversion to  $r_0$  scale using [175]  $r_0/w_{0.4} = 2.587(45)$  and  $r_0 = 0.472 \text{ fm}$ .

<sup>j</sup> Our conversion from  $w_0\Lambda_{\overline{\text{MS}}} = 0.2154(12)$  to  $r_0$  scale using  $r_0/w_0 = (r_0/w_{0.4}) \cdot (w_{0.4}/w_0) = 2.885(50)$  with the factors cited by the collaboration [175] and with  $r_0 = 0.472 \text{ fm}$ .

Table 60: Wilson loop results. Some early results for  $N_f = 0, 2$  did not determine  $\Lambda_{\overline{\text{MS}}}$ .

The work of El-Khadra 92 [176] employs a 1-loop formula to relate  $\alpha_{\overline{\text{MS}}}^{(0)}(\pi/a)$  to the boosted coupling for three lattice spacings  $a^{-1} = 1.15, 1.78, 2.43 \text{ GeV}$ . (The lattice spacing is determined from the charmonium 1S-1P splitting.) They obtain  $\Lambda_{\overline{\text{MS}}}^{(0)} = 234 \text{ MeV}$ , corresponding to  $\alpha_{\text{eff}} = \alpha_{\overline{\text{MS}}}^{(0)}(\pi/a) \approx 0.15\text{--}0.2$ . The work of Aoki 94 [173] calculates  $\alpha_V^{(2)}$  and  $\alpha_{\overline{\text{MS}}}^{(2)}$  for a single lattice spacing  $a^{-1} \sim 2 \text{ GeV}$ , again determined from charmonium 1S-1P splitting in two-flavour QCD. Using 1-loop perturbation theory with boosted coupling, they obtain  $\alpha_V^{(2)} = 0.169$  and  $\alpha_{\overline{\text{MS}}}^{(2)} = 0.142$ . Davies 94 [172] gives a determination of  $\alpha_V$  from the expansion

$$-\ln W_{11} \equiv \frac{4\pi}{3} \alpha_V^{(N_f)}(3.41/a) \times [1 - (1.185 + 0.070 N_f) \alpha_V^{(N_f)}], \quad (361)$$

neglecting higher-order terms. They compute the  $\Upsilon$  spectrum in  $N_f = 0, 2$  QCD for single lattice spacings at  $a^{-1} = 2.57, 2.47 \text{ GeV}$  and obtain  $\alpha_V(3.41/a) \simeq 0.15, 0.18$ , respectively. Extrapolating the inverse coupling linearly in  $N_f$ , a value of  $\alpha_V^{(3)}(8.3 \text{ GeV}) = 0.196(3)$  is obtained. SESAM 99 [170] follows a similar strategy, again for a single lattice spacing. They linearly extrapolated results for  $1/\alpha_V^{(0)}, 1/\alpha_V^{(2)}$  at a fixed scale of  $9 \text{ GeV}$  to give  $\alpha_V^{(3)}$ , which is then perturbatively converted to  $\alpha_{\overline{\text{MS}}}^{(3)}$ . This finally gave  $\alpha_{\overline{\text{MS}}}^{(5)}(M_Z) = 0.1118(17)$ . Wingate 95 [171] also follows this method. With the scale determined from the charmonium 1S-1P splitting for single lattice spacings in  $N_f = 0, 2$  giving  $a^{-1} \simeq 1.80 \text{ GeV}$  for  $N_f = 0$  and  $a^{-1} \simeq 1.66 \text{ GeV}$  for  $N_f = 2$ , they obtain  $\alpha_V^{(0)}(3.41/a) \simeq 0.15$  and  $\alpha_V^{(2)} \simeq 0.18$ , respectively. Extrapolating the inverse coupling linearly in  $N_f$ , they obtain  $\alpha_V^{(3)}(6.48 \text{ GeV}) = 0.194(17)$ .

The QCDSF/UKQCD collaboration, QCDSF/UKQCD 05 [169], [177–179], use the 2-loop relation (re-written here in terms of  $\alpha$ )

$$\frac{1}{\alpha_{\overline{\text{MS}}}(\mu)} = \frac{1}{\alpha_P(1/a)} + 4\pi(2b_0 \ln a\mu - t_1^P) + (4\pi)^2(2b_1 \ln a\mu - t_2^P)\alpha_P(1/a), \quad (362)$$

where  $t_1^P$  and  $t_2^P$  are known. (A 2-loop relation corresponds to a 3-loop lattice  $\beta$ -function.) This was used to directly compute  $\alpha_{\overline{\text{MS}}}$ , and the scale was chosen so that the  $\mathcal{O}(\alpha_P^0)$  term vanishes, i.e.,

$$\mu^* = \frac{1}{a} \exp[t_1^P/(2b_0)] \approx \begin{cases} 2.63/a & N_f = 0 \\ 1.4/a & N_f = 2 \end{cases}. \quad (363)$$

The method is to first compute  $\alpha_P(1/a)$  and from this, using Eq. (362) to find  $\alpha_{\overline{\text{MS}}}(\mu^*)$ . The RG equation, Eq. (285), then determines  $\mu^*/\Lambda_{\overline{\text{MS}}}$  and hence using Eq. (363) leads to the result for  $r_0\Lambda_{\overline{\text{MS}}}$ . This avoids giving the scale in MeV until the end. In the  $N_f = 0$  case seven lattice spacings were used [64], giving a range  $\mu^*/\Lambda_{\overline{\text{MS}}} \approx 24\text{--}72$  (or  $a^{-1} \approx 2\text{--}7 \text{ GeV}$ ) and  $\alpha_{\text{eff}} = \alpha_{\overline{\text{MS}}}(\mu^*) \approx 0.15\text{--}0.10$ . Neglecting higher-order perturbative terms (see discussion after Eq. (364) below) in Eq. (362) this is sufficient to allow a continuum extrapolation of  $r_0\Lambda_{\overline{\text{MS}}}$ . A similar computation for  $N_f = 2$  by QCDSF/UKQCD 05 [169] gave  $\mu^*/\Lambda_{\overline{\text{MS}}} \approx 12\text{--}17$  (or roughly  $a^{-1} \approx 2\text{--}3 \text{ GeV}$ ) and  $\alpha_{\text{eff}} = \alpha_{\overline{\text{MS}}}(\mu^*) \approx 0.20\text{--}0.18$ . The  $N_f = 2$  results of QCDSF/UKQCD 05 [169] are affected by an uncertainty which was not known at the time of publication: It has been realized that the values of  $r_0/a$  of Ref. [169] were significantly too low [59]. As this effect is expected to depend on  $a$ , it influences the perturbative behaviour leading us to assign a ■ for that criterion.

Results for the  $N_f = 0$   $\Lambda$ -parameter by FlowQCD 15 [175], later updated and published in Kitazawa 16 [174], are obtained following the same strategy, cf. Eqs. (362), (363), except that

the scale  $r_0$  is replaced by the gradient-flow scale  $w_0$ , leading to a determination of  $w_0\Lambda_{\overline{\text{MS}}}$ . The continuum limit is estimated by extrapolating the data at six lattice spacings linearly in  $a^2$ . The data range used is  $\mu^*/\Lambda_{\overline{\text{MS}}} \approx 50\text{--}120$  (or  $a^{-1} \approx 5\text{--}11$  GeV) and  $\alpha_{\overline{\text{MS}}}(\mu^*) \approx 0.12\text{--}0.095$ . Since a very small value of  $\alpha_{\overline{\text{MS}}}$  is reached, there is a ★ in the perturbative behaviour. Note that our conversion to the common  $r_0$  scale unfortunately leads to a significant increase of the error of the  $\Lambda$  parameter compared to using  $w_0$  directly [180]. Again we note that the results of QCDSF/UKQCD 05 [169] ( $N_f = 0$ ) and Kitazawa 16 [174] may be affected by frozen topology as they have lattice spacings significantly below  $a = 0.05$  fm. Kitazawa 16 [174] investigate this by evaluating  $w_0/a$  in a fixed topology and estimate any effect at about  $\sim 1\%$ .

The work of HPQCD 05A [165] (which supersedes the original work [181]) uses three lattice spacings  $a^{-1} \approx 1.2, 1.6, 2.3$  GeV for  $2 + 1$  flavour QCD. Typically the renormalization scale  $q \approx \pi/a \approx 3.50\text{--}7.10$  GeV, corresponding to  $\alpha_{V'} \approx 0.22\text{--}0.28$ .

In the later update HPQCD 08A [78] twelve data sets (with six lattice spacings) are now used reaching up to  $a^{-1} \approx 4.4$  GeV, corresponding to  $\alpha_{V'} \approx 0.18$ . The values used for the scale  $r_1$  were further updated in HPQCD 10 [167]. Maltman 08 [168] uses most of the same lattice ensembles as HPQCD 08A [78], but not the one at the smallest lattice spacing,  $a \approx 0.045$  fm. Maltman 08 [168] also considers a much smaller set of quantities (three versus 22) that are less sensitive to condensates. They also use different strategies for evaluating the condensates and for the perturbative expansion, and a slightly different value for the scale  $r_1$ . The central values of the final results from Maltman 08 [168] and HPQCD 08A [78] differ by 0.0009 (which would be decreased to 0.0007 taking into account a reduction of 0.0002 in the value of the  $r_1$  scale used by Maltman 08 [168]).

As mentioned before, the perturbative coefficients are computed through 3-loop order [182], while the higher-order perturbative coefficients  $c_n$  with  $n_{\text{max}} \geq n > 3$  (with  $n_{\text{max}} = 10$ ) are numerically fitted using the lattice-simulation data for the lattice spacings with the help of Bayesian methods. It turns out that corrections in Eq. (358) are of order  $|c_i/c_1|\alpha^i = 5\text{--}15\%$  and  $3\text{--}10\%$  for  $i = 2, 3$ , respectively. The inclusion of a fourth-order term is necessary to obtain a good fit to the data, and leads to a shift of the result by 1–2 sigma. For all but one of the 22 quantities, central values of  $|c_4/c_1| \approx 2\text{--}4$  were found, with errors from the fits of  $\approx 2$ . It should be pointed out that the description of lattice results for the short-distance quantities does not require Bayesian priors, once the term proportional to  $c_4$  is included [168]. We also stress that different short-distance quantities have quite different nonperturbative contributions [183]. Hence the fact that different observables lead to consistent  $\alpha_s$  values is a nontrivial check of the approach.

An important source of uncertainty is the truncation of perturbation theory. In HPQCD 08A [78], HPQCD 10 [167] it is estimated to be about 0.4% of  $\alpha_{\overline{\text{MS}}}(M_Z)$ . In FLAG 13 we included a rather detailed discussion of the issue with the result that we prefer for the time being a more conservative error based on the above estimate  $|c_4/c_1| = 2$ . From Eq. (357) this gives an estimate of the uncertainty in  $\alpha_{\text{eff}}$  of

$$\Delta\alpha_{\text{eff}}(\mu_1) = \left| \frac{c_4}{c_1} \right| \alpha_{\text{eff}}^4(\mu_1), \quad (364)$$

at the scale  $\mu_1$  where  $\alpha_{\text{eff}}$  is computed from the Wilson loops. This can be used with a variation in  $\Lambda$  at lowest order of perturbation theory and also applied to  $\alpha_s$  evolved to a

different scale  $\mu_2$ ,<sup>9</sup>

$$\frac{\Delta\Lambda}{\Lambda} = \frac{1}{8\pi b_0\alpha_s} \frac{\Delta\alpha_s}{\alpha_s}, \quad \frac{\Delta\alpha_s(\mu_2)}{\Delta\alpha_s(\mu_1)} = \frac{\alpha_s^2(\mu_2)}{\alpha_s^2(\mu_1)}. \quad (365)$$

With  $\mu_2 = M_Z$  and  $\alpha_s(\mu_1) = 0.2$  (a typical value extracted from Wilson loops in HPQCD 10 [167], HPQCD 08A [78] at  $\mu = 5 \text{ GeV}$ ) we have

$$\Delta\alpha_{\overline{\text{MS}}}(m_Z) = 0.0012, \quad (366)$$

which we shall later use as the typical perturbative uncertainty of the method with  $2 + 1$  fermions.

Table 60 summarizes the results. Within the errors of 3–5%  $N_f = 3$  determinations of  $r_0\Lambda$  nicely agree.

**Scale variations.** As discussed above, the short-distance observables are fitted to a perturbative expansion where the higher-order coefficients are actual parameters in the fit. Here instead we follow the exact same procedure introduced for all the observables, and we describe the observables using only the known perturbative coefficients. For illustration, we report the result of the scale variations for two observables, namely the simple  $1 \times 1$  plaquette and the  $2 \times 1$  Wilson loop. The perturbative coefficients are reported in Tab. 55 and the typical scale is  $\mu \approx 2.4/a \approx 4.4 \text{ GeV}$ . With these values we obtain the following results.

$-\log W_{11}$

$$\delta_{(4)}^* = 2.8\%, \quad \delta_{(2)} = 3.3\% \quad \delta_{(2)}^* = 2.5\%. \quad (367)$$

$-\log W_{112}/u_0^6$

$$\delta_{(4)}^* = 3.5\%, \quad \delta_{(2)} = 3.2\% \quad \delta_{(2)}^* = 3.1\%. \quad (368)$$

This analysis suggests a systematic error around 3% for these kind of analyses on the available ensembles.

## 9.8 $\alpha_s$ from heavy-quark current two-point functions

### 9.8.1 General considerations

The method has been introduced in HPQCD 08, Ref. [184], and updated in HPQCD 10, Ref. [167], see also Ref. [185]. In addition there is a 2+1+1-flavour result, HPQCD 14A [186].

The basic observable is constructed from a current,

$$J(x) = iam_c \bar{\psi}_c(x) \gamma_5 \psi_{c'}(x), \quad (369)$$

of two mass-degenerate heavy-valence quarks,  $c, c'$ , usually taken to be at or around the charm-quark mass. The pre-factor  $m_c$  denotes the bare mass of the quark. When the lattice discretization respects chiral symmetry,  $J(x)$  is a renormalization group invariant local field,

<sup>9</sup>From Eq. (292) we see that at low order in PT the coupling  $\alpha_s$  is continuous and differentiable across the mass thresholds (at the same scale). Therefore to leading order  $\alpha_s$  and  $\Delta\alpha_s$  are independent of  $N_f$ .



i.e., it requires no renormalization. Staggered fermions and twisted-mass fermions have such a residual chiral symmetry. The (Euclidean) time-slice correlation function

$$G(x_0) = a^6 \sum_{\vec{x}} \langle J^\dagger(x) J(0) \rangle, \quad (370)$$

$(J^\dagger(x) = iam_c \bar{\psi}_c(x) \gamma_5 \psi_c(x))$  has a  $\sim x_0^{-3}$  singularity at short distances and moments

$$G_n = a \sum_{x_0=-(T/2-a)}^{T/2-a} x_0^n G(x_0) \quad (371)$$

are nonvanishing for even  $n$  and furthermore finite for  $n \geq 4$  in the  $a \rightarrow 0$  limit. Here  $T$  is the time extent of the lattice. The moments are dominated by contributions at  $x_0$  of order  $1/m_c$ . For large mass  $m_c$  these are short distances and the moments become increasingly perturbative for decreasing  $n$ . Denoting the lowest-order perturbation theory moments by  $G_n^{(0)}$ , one defines the normalized moments

$$R_n = \begin{cases} G_4/G_4^{(0)} & \text{for } n = 4, \\ \frac{am_{\eta_c}}{2am_c} \left( \frac{G_n}{G_n^{(0)}} \right)^{1/(n-4)} & \text{for } n \geq 6, \end{cases} \quad (372)$$

of even order  $n$ . Note that Eq. (369) contains the variable (bare) heavy-quark mass  $m_c$ . The normalization  $G_n^{(0)}$  is introduced to help in reducing lattice artifacts. In addition, one can also define moments with different normalizations,

$$\tilde{R}_n = 2R_n/m_{\eta_c} \quad \text{for } n \geq 6. \quad (373)$$

While  $\tilde{R}_n$  also remains renormalization-group invariant, it now also has a scale which might introduce an additional ambiguity [187].

The normalized moments can then be parameterized in terms of functions

$$R_n \equiv \begin{cases} r_4(\alpha_s(\mu)) & \text{for } n = 4, \\ \frac{m_{\eta_c}}{2\bar{m}_c(\mu_m)} r_n(\alpha_s(\mu)) & \text{for } n \geq 6, \end{cases} \quad (374)$$

with  $\bar{m}_c(\mu_m)$  being the renormalized heavy-quark mass. The scale  $\mu_m$  at which the heavy-quark mass is defined could be different from the scale  $\mu$  at which  $\alpha_s$  is defined [188]. The HPQCD collaboration, however, used the choice  $\mu = \mu_m = 3m_c(\mu)$ . This ensures that the renormalization scale is never too small. The reduced moments  $r_n$  have a perturbative expansion

$$r_n = 1 + r_{n,1}\alpha_s + r_{n,2}\alpha_s^2 + r_{n,3}\alpha_s^3 + \dots, \quad (375)$$

where the written terms  $r_{n,i}(\mu/\bar{m}_c(\mu))$ ,  $i \leq 3$  are known for low  $n$  from Refs. [80, 189–192]. In practice, the expansion is performed in the  $\overline{\text{MS}}$  scheme. Matching nonperturbative lattice results for the moments to the perturbative expansion, one determines an approximation to  $\alpha_{\overline{\text{MS}}}(\mu)$  as well as  $\bar{m}_c(\mu)$ . With the lattice spacing (scale) determined from some extra physical input, this calibrates  $\mu$ . As usual suitable pseudoscalar masses determine the bare-quark masses, here in particular the charm-quark mass, and then through Eq. (374) the renormalized charm-quark mass.

A difficulty with this approach is that large masses are needed to enter the perturbative domain. Lattice artifacts can then be sizeable and have a complicated form. The ratios in Eq. (372) use the tree-level lattice results in the usual way for normalization. This results in unity as the leading term in Eq. (375), suppressing some of the kinematical lattice artifacts. We note that in contrast to, e.g., the definition of  $\alpha_{\text{qq}}$ , here the cutoff effects are of order  $a^k \alpha_s$ , while there the tree-level term defines  $\alpha_s$  and therefore the cutoff effects after tree-level improvement are of order  $a^k \alpha_s^2$ . To obtain the continuum results for the moments it is important to perform fits with high powers of  $a$ . This implies many fit parameters. To deal with this problem the HPQCD collaboration used Bayesian fits of their lattice results. More recent analyses of the moments, however, did not rely on Bayesian fits [31, 187, 193, 194].

Finite-size effects (FSE) due to the omission of  $|x_0| > T/2$  in Eq. (371) grow with  $n$  as  $(m_{\eta_c} T/2)^n \exp(-m_{\eta_c} T/2)$ . In practice, however, since the (lower) moments are short-distance dominated, the FSE are expected to be small at the present level of precision. Possible exception could be the ratio  $R_8/R_{10}$ , where the finite-volume effects could be significant as discussed below.

Moments of correlation functions of the quark's electromagnetic current can also be obtained from experimental data for  $e^+e^-$  annihilation [195, 196]. This enables a nonlattice determination of  $\alpha_s$  using a similar analysis method. In particular, the same continuum perturbation-theory computation enters both the lattice and the phenomenological determinations.

### 9.8.2 Discussion of computations

The determination of the strong coupling constant from the moments of quarkonium correlators by HPQCD collaboration have been discussed in detail in the FLAG 16 and 19 reports. Therefore, we only give the summary of these determinations in Tab. 61. There were no new determinations of the strong coupling constant in 2+1 flavour QCD by other groups since the FLAG 21 report. The only new development was that Petreczky 20 [31] is now published and therefore this determination enters the FLAG average. The determinations of  $\alpha_s$  by Maezawa 16, JLQCD16, Petreczky 19 and Boito 20 have been discussed in detail in the FLAG 21 report, so we do not discuss them here again and only give the summary of these determinations in Tab. 61. We will only discuss the results of Petreczky 20 [31] here.

Petreczky 20 is based on the same lattice data as Petreczky 19 [194]. Here the pseudo-scalar correlation functions have been computed using HISQ ensembles from HotQCD Collaboration [54] for physical strange-quark mass and light-quark masses corresponding to the pion mass of 160 MeV in the continuum limit, and lattice spacings  $a^{-1} = 1.81, 2.07, 2.39, 2.67, 3.01, 3.28, 4.00$  and 4.89 GeV. Additional calculations have been performed for light-quark mass corresponding to the pion mass of 300 MeV and lattice spacings  $a^{-1} = 2.39, 4.89, 5.58, 6.62$  and 7.85 GeV using the gauge configurations from the study of QCD equation of state at high temperatures [150]. No significant light-quark-mass dependence of heavy pseudo-scalar correlators have been observed [194]. Therefore, the results for the two light-quark masses have been combined into a single analysis. Calculations have been performed at four values of the heavy-quark mass equal to the physical charm-quark mass, one and half times the charm-quark mass, two times the charm-quark mass and three times the charm-quark mass. In this study random-colour wall sources which greatly reduced the statistical errors were used. In fact, the statistical errors on the moments were completely negligible compared to other sources of errors. The strong coupling constant was extracted from  $R_4$  [31]. To obtain the

Collaboration	Ref.	$N_f$	publication status renormalization scale perturbative behaviour continuum extrapolation				scale	$\Lambda_{\overline{\text{MS}}}[\text{MeV}]$	$r_0\Lambda_{\overline{\text{MS}}}$
HPQCD 14A	[186]	2+1+1	A	○	★	○	$w_0 = 0.1715(9) \text{ fm}^a$	$294(11)^{bc}$	$0.703(26)$
Petreczky 20	[31]	2+1	A	○	○	★	$r_1 = 0.3106(18) \text{ fm}$	$332(17)^h$	$0.792(41)^g$
Boito 20	[197]	2+1	A	■	■	○	$m_c(m_c) = 1.28(2) \text{ GeV}$	$328(30)^h$	$0.785(72)$
Petreczky 19, $m_h=m_c$	[194]	2+1	A	■	■	★	$r_1 = 0.3106(18) \text{ fm}^g$	$314(10)$	$0.751(24)^g$
Petreczky 19, $\frac{m_h}{m_c}=1.5$	[194]	2+1	A	■	■	○	$r_1 = 0.3106(18) \text{ fm}^g$	$310(10)$	$0.742(24)^g$
Maezawa 16	[193]	2+1	A	■	■	○	$r_1 = 0.3106(18) \text{ fm}^d$	$309(10)^e$	$0.739(24)^e$
JLQCD 16	[187]	2+1	A	■	○	○	$\sqrt{t_0} = 0.1465(25) \text{ fm}$	$331(38)^f$	$0.792(89)^f$
HPQCD 10	[167]	2+1	A	○	★	○	$r_1 = 0.3133(23) \text{ fm}^\dagger$	$338(10)^*$	$0.809(25)$
HPQCD 08B	[184]	2+1	A	■	■	■	$r_1 = 0.321(5) \text{ fm}^\dagger$	$325(18)^+$	$0.777(42)$

<sup>a</sup> Scale determined in [198] using  $f_\pi$ .

<sup>b</sup>  $\alpha_{\overline{\text{MS}}}^{(4)}(5 \text{ GeV}) = 0.2128(25)$ ,  $\alpha_{\overline{\text{MS}}}^{(5)}(M_Z) = 0.11822(74)$ .

<sup>c</sup> We evaluated  $\Lambda_{\overline{\text{MS}}}^{(4)}$  from  $\alpha_{\overline{\text{MS}}}^{(4)}$ . We also used  $r_0 = 0.472 \text{ fm}$ .

<sup>d</sup> Scale is determined from  $f_\pi$ .

<sup>e</sup>  $\alpha_{\overline{\text{MS}}}^{(3)}(m_c = 1.267 \text{ GeV}) = 0.3697(85)$ ,  $\alpha_{\overline{\text{MS}}}^{(5)}(M_Z) = 0.11622(84)$ . Our conversion with  $r_0 = 0.472 \text{ fm}$ .

<sup>f</sup> We evaluated  $\Lambda_{\overline{\text{MS}}}^{(3)}$  from the given  $\alpha_{\overline{\text{MS}}}^{(4)}(3 \text{ GeV}) = 0.2528(127)$ .  $\alpha_{\overline{\text{MS}}}^{(5)}(M_Z) = 0.1177(26)$ . We also used  $r_0 = 0.472 \text{ fm}$  to convert.

<sup>g</sup> We used  $r_0 = 0.472 \text{ fm}$  to convert.

<sup>h</sup> We back-engineered from  $\alpha_{\overline{\text{MS}}}^{(5)}(M_Z) = 0.1177(20)$ . We used  $r_0 = 0.472 \text{ fm}$  to convert.

<sup>\*</sup>  $\alpha_{\overline{\text{MS}}}^{(3)}(5 \text{ GeV}) = 0.2034(21)$ ,  $\alpha_{\overline{\text{MS}}}^{(5)}(M_Z) = 0.1183(7)$ .

<sup>†</sup> Scale is determined from  $\Upsilon$  mass splitting.

<sup>+</sup> We evaluated  $\Lambda_{\overline{\text{MS}}}^{(3)}$  from the given  $\alpha_{\overline{\text{MS}}}^{(4)}(3 \text{ GeV}) = 0.251(6)$ .  $\alpha_{\overline{\text{MS}}}^{(5)}(M_Z) = 0.1174(12)$ .

Table 61: Heavy-quark current two-point function results. Note that all analysis using  $2+1$  flavour simulations perturbatively add a dynamical charm quark. Partially they then quote results in four-flavour QCD, which we converted back to  $N_f = 3$ , corresponding to the non-perturbative sea quark content.

continuum limit the lattice-spacing dependence of the results of  $R_4$  at different quark masses was fitted simultaneously in a similar manner as in the HPQCD 10 and HPQCD 14 analyses, but without using Bayesian priors. In extracting  $\alpha_s$  several choices of the renormalization scale  $\mu$  in the range  $2/3m_h-3m_h$  have been considered. The perturbative truncation error was estimated by varying the coefficient of the unknown 4-loop term in Eq. (375) between  $-1.6r_3$  and  $+1.6r_3$ . However, the uncertainty of the results due to the scale variation was larger than the estimated perturbative truncation error. The final error of the result  $\Lambda_{\overline{\text{MS}}}^{N_f=3} = 331(17) \text{ MeV}$  comes mostly from the scale variation [31]. Since there are three lattice spacing available with  $a\mu < 0.5$  we give ★ for continuum extrapolation. Because  $\alpha_{\text{eff}} = 0.22 - 0.38$  we give ○ for the renormalization scale. Finally, since  $(\Delta\Lambda/\Lambda)_{\Delta\alpha} > \alpha_{\text{eff}}^2$  for the smallest  $\alpha_{\text{eff}}$  value we give ○ for the perturbative behaviour. In addition to  $R_4$  Petreczky 20 also considered using  $R_6/R_8$  and  $R_8/R_{10}$  for the  $\alpha_s$  determination. It was pointed out that the lattice spac-

ing dependence of  $R_6/R_8$  is quite subtle and therefore reliable continuum extrapolations for this ratio are not possible for  $m_h \geq 2m_c$  [31]. For  $m_h = m_c$  and  $1.5m_c$  the ratio  $R_6/R_8$  leads to  $\alpha_s$  values that are consistent with the ones from  $R_4$ . Furthermore, it was argued that finite-volume effects in the case of  $R_8/R_{10}$  are large for  $m_h = m_c$  and therefore the corresponding data are not suitable for extracting  $\alpha_s$ . This observation may explain why the central values of  $\alpha_s$  extracted from  $R_8/R_{10}$  in some previous studies were systematically lower [184, 193, 194]. On the other hand for  $m_h \geq 1.5m_c$  the finite-volume effects are sufficiently small in the continuum extrapolated results if some small-volume lattice data are excluded from the analysis [31]. The  $\alpha_s$  obtained from  $R_8/R_{10}$  with  $m_h \geq 1.5m_c$  were consistent with the ones obtained from  $R_4$ .

Aside from the final results for  $\alpha_s(m_Z)$  obtained by matching with perturbation theory, it is interesting to make a comparison of the short distance quantities in the continuum limit  $R_n$  which are available from HPQCD 08 [184], JLQCD 16 [187], Maezawa 16 [193], Petreczky 19 [194] and Petreczky 20 [31] (all using 2 + 1 flavours). This comparison is shown in Tab. 62. The results are in quite good agreement with each other. For future studies it is

	HPQCD 08	HPQCD 10	Maezawa 16	JLQCD 16	Petreczky 19	Petreczky 20
$R_4$	1.272(5)	1.282(4)	1.265(7)	-	1.279(4)	1.278(2)
$R_6$	1.528(11)	1.527(4)	1.520(4)	1.509(7)	1.521(3)	1.522(2)
$R_8$	1.370(10)	1.373(3)	1.367(8)	1.359(4)	1.369(3)	1.368(3)
$R_{10}$	1.304(9)	1.304(2)	1.302(8)	1.297(4)	1.311(7)	1.301(3)
$R_6/R_8$	1.113(2)	-	1.114(2)	1.111(2)	1.1092(6)	1.10895(32)
$R_8/R_{10}$	1.049(2)	-	1.0495(7)	1.0481(9)	1.0485(8)	-

Table 62: Moments and the ratios of the moments from  $N_f = 3$  simulations at the charm-quark mass.

of course interesting to check agreement of these numbers before turning to the more involved determination of  $\alpha_s$ .

While there have been no new determinations of  $\alpha_s$  from the moments of the heavy-quark current two-point functions in 2+1+1 flavour or 2+1 flavour QCD since the FLAG 21 report, this method has been scrutinized in quenched QCD ( $N_f = 0$ ) in three conference proceedings [36, 199, 200]. In these works the Wilson gauge action was used for several values of the lattices spacings, down to lattice spacing of  $a = 0.01$  fm, which is 2.5 times smaller than the smallest lattice spacing used in 2+1 flavour QCD. The box size was sufficiently large for the heavy-quark current two-point functions, namely  $L = 2$  fm was used. In the temporal direction open boundary conditions have been used, and the extent in the time direction was 6 fm. For heavy-quark twisted-mass fermion formulation was used at the maximal twist. Five different heavy-quark masses have been used in these studies, namely  $0.77M_c$ ,  $1.16M_c$ ,  $1.55M_c$ ,  $2.32M_c$  and  $3.48M_c$ , with  $M_c$  being the physical charm-quark RGI mass [36, 199, 200]. The continuum extrapolation of  $R_4$  has been performed and from it the value of  $\Lambda_{\overline{MS}}^{(N_f=0)}$  was obtained for different heavy-quark masses and different choices of  $\mu$ . It turned out, however, that the results obtained for different heavy-quark masses and values of  $\mu$  are not consistent with each other and often are not compatible with the value determined from step scaling [110]. It was argued that this is due to the log-enhanced discretization errors in  $R_4$ , i.e., discretization errors that are proportional to  $a^2 \log(am_c)$  [200], and that reliable continuum extrapolation

of  $R_4$  is not possible for this lattice setup. A practical way to circumvent this problem was also proposed in Ref. [200] and relies on considering a special combination of  $R_4$  evaluated at two heavy-quark masses. The ratios  $R_6/R_8$  and  $R_8/R_{10}$  do not have log-enhanced discretization effects [36, 200] and therefore, can be used to obtain  $\Lambda_{\overline{\text{MS}}}^{(N_f=0)}$ . Such an analysis was performed in Ref. [36]. Here to deal with perturbative error it was assumed that  $\Lambda_{\overline{\text{MS}}}^{(N_f=0)}\sqrt{8t_0}$  obtained at different renormalization scales  $\mu$  is linear in  $\alpha_s^2(\mu)$  as expected from 3-loop perturbative calculations. Performing linear extrapolations in  $\alpha_s^2(\mu)$  the final values of  $\Lambda_{\overline{\text{MS}}}^{(N_f=0)}\sqrt{8t_0}$  have been obtained. The corresponding results for the  $\Lambda$ -parameter agree with the result of the step-scaling analysis but have much larger errors, and thus are not competitive [36].

**Scale variations.** Moments of heavy-quark correlators are computed at scales that are set by the mass of the charm quark. We compute scale variations for the moments  $r_4$ ,  $r_6$  and  $r_8$  at different values of the matching scale.

**HQ**  $r_4$ ,  $\mu = m_c$

$$\delta_{(2)} = 2.7\% \quad \delta_{(2)}^* = 2.8\% . \quad (376)$$

**HQ**  $r_4$ ,  $\mu = 2m_c$

$$\delta_{(4)}^* = 1.2\% , \quad \delta_{(2)} = 1.5\% \quad \delta_{(2)}^* = 1.6\% . \quad (377)$$

**HQ**  $r_6$ ,  $\mu = 2m_c$

$$\delta_{(2)} = 2.3\% \quad \delta_{(2)}^* = 1.2\% . \quad (378)$$

**HQ**  $r_8$ ,  $\mu = 2m_c$

$$\delta_{(2)} = 2.8\% \quad \delta_{(2)}^* = 4.8\% . \quad (379)$$

We note here that the errors from the scale variations are in the same ballpark as previous estimates published in FLAG reviews. The moment  $r_4$  computed at the scale  $Q = 2m_c$  happens to have a systematic error in the range 1 – 2%.

## 9.9 Gradient-flow schemes

### 9.9.1 General considerations

The gradient flow [38, 96] (cf. the paragraph around Eq. (317) for the basic equations) allows for the definition of many new observables, both in pure gauge theory and QCD, which are gauge invariant and automatically renormalized after the standard QCD renormalizations of parameters and composite fields have been carried out. This has been established perturbatively to all orders in Ref. [201] and confirmed up to 2-loop level in practical calculations [83]. It is generally assumed to be valid beyond perturbation theory and many simulation results corroborate this assumption.

The gradient flow comes with the flow-time parameter,  $t$ , which has dimensions of length squared and thus introduces a new energy scale which is, by analogy with the diffusion

equation, naturally identified as  $\mu = 1/\sqrt{8t}$  (in four dimensions). The most widely used observable is the action density at finite flow time,

$$E(t, x) = -\frac{1}{2} \text{tr}\{G_{\mu\nu}(t, x)G_{\mu\nu}(x)\}. \quad (380)$$

Its expectation value has a perturbative expansion starting at  $O(\alpha)$ , which gives rise to the definition of the coupling in the GF scheme,

$$\alpha_{\text{GF}}(\mu) \equiv \frac{\bar{g}_{\text{GF}}^2(\mu)}{4\pi} = \frac{4\pi t^2}{3} \langle E(t, x) \rangle \quad (381)$$

and is known to 3-loop order,

$$\alpha_{\text{GF}}(\mu = 1/\sqrt{8t}) = \alpha_{\overline{\text{MS}}}(\mu) + k_1 \alpha_{\overline{\text{MS}}}(\mu)^2 + k_2 \alpha_{\overline{\text{MS}}}(\mu)^3 + \dots \quad (382)$$

with  $k_1$  and  $k_2$  computed in Refs. [38] and [83], respectively (cf. Tab. 55). Note that the GF coupling directly relates to the scale  $t_0$ ; its definition is equivalent to  $\bar{g}_{\text{GF}}^2(1/\sqrt{8t_0}) = 15.8$ . With the flow time setting the renormalization scale, the  $\beta$ -function is readily obtained during the numerical integration of the flow equation, by also tracking the flow-time derivative of  $\langle E(t, x) \rangle$ ,

$$\beta_{\text{GF}}(\bar{g}_{\text{GF}}) = -2t \frac{d}{dt} \bar{g}_{\text{GF}}(1/\sqrt{8t}), \quad (383)$$

and the 3-loop  $\beta$ -function coefficient  $b_2$  is known. In the pure gauge theory is is given by

$$b_2^{\text{GF}} = -1.90395(4)/(4\pi)^3, \quad (N_f = 0). \quad (384)$$

This is almost three times larger in magnitude than in the  $\overline{\text{MS}}$  scheme and of opposite sign. One naturally worries about higher-order corrections being large, too. As a result, making contact with perturbation theory requires very small couplings. To quantify the problem, we have done the following exercises (all for  $N_f = 0$ ): First one may evaluate the difference in  $\sqrt{8t}\Lambda_{\text{GF}}$  obtained by integrating the perturbative  $\beta$ -function at 2- vs. 3-loop order from zero coupling to a reference value  $\bar{g}_{\text{GF}}^2(1/\sqrt{8t}) = 1.2$ , which corresponds to the smallest coupling reached in the works discussed below. We find that this difference is about 11 percent, again about three times larger than with the  $\overline{\text{MS}}$  scheme. In order to vary the scale we convert to the  $\overline{\text{MS}}$  scheme,

$$\alpha_{\text{GF}}(\mu) = \alpha_{\overline{\text{MS}}}(s\mu) + k_1(s) \alpha_{\overline{\text{MS}}}^2(s\mu) + k_2(s) \alpha_{\overline{\text{MS}}}^3(s\mu) + O(\alpha_{\overline{\text{MS}}}^4), \quad (385)$$

where the  $s$ -dependence of the coefficients is given as

$$k_1(s) - k_1(1) = 8\pi b_0 \ln(s), \quad k_2(s) - k_2(1) = 32\pi^2 b_1 \ln(s) + k_1^2(s) - k_1^2(1). \quad (386)$$

In order to obtain the  $\overline{\text{MS}}$  coupling in terms of the reference coupling one needs to invert Eq. (385), which we do either perturbatively or numerically for the truncated equation. We then compute,

$$\sqrt{8t}\Lambda_{\overline{\text{MS}}} = s \times \varphi_{\overline{\text{MS}}}(\bar{g}_{\overline{\text{MS}}}(s/\sqrt{8t})), \quad (387)$$

for scale factors  $s = 1/2, 1, 2$ , using the 5-loop  $\beta$ -function in the  $\overline{\text{MS}}$  scheme. We find that the resulting variation in the  $\Lambda$ -parameter depends on how the  $\overline{\text{MS}}$ -coupling is obtained: With perturbative inversion, the variation is plus 7.5 and minus 4 percent, with numerical inversion,



one obtains plus 2.5 and plus 3.3 percent, i.e., even monotony is lost. The central values for  $s = 1$  differ by 5 percent. As an alternative, we consider the scale factor  $s^* = 0.534$  which implies  $k_1(s^*) = 0$ . Varying by a factor two around  $s^*$  one finds that the difference in central values reduces to 1.3 percent, and the  $\Lambda$ -parameter changes by minus 6 percent and plus 4 percent for perturbative inversion, and by plus 9.7% and minus 2.7% for numerical inversion.

We conclude that at this reference coupling a determination of the  $\Lambda$ -parameter to better than five percent seems impossible.

### 9.9.2 Discussion of computations

A determination of the  $\beta$ -function directly from the flow-time dependence of the GF coupling requires a controlled infinite-volume extrapolation. This was first suggested in Ref. [202], where the strategy was applied to a BSM model. Since then, two works have applied this scheme to the pure gauge theory (QCD with  $N_f = 0$ ), namely Hasenfratz 23 [34] and Wong 23 [35], in a proceedings contribution. We mainly discuss Hasenfratz 23 who provide more details: the data produced for the GF coupling ranges from 15.8 down to 1.2, lattice sizes vary between  $L/a = 20$  and  $L/a = 48$ , depending on the  $\beta$ -value, and periodic boundary conditions are imposed on the gauge field. Wong 23 do have data for larger lattices up to  $L/a = 64$  and even  $L/a = 80, 96$  at selected bare couplings. The data for both  $\bar{g}_{\text{GF}}^2$  and  $\beta_{\text{GF}}$  are extrapolated to the infinite-volume limit at fixed lattice spacing, assuming corrections  $\propto (a/L)^4$ , with Wong 23 also allowing for a subleading  $(a/L)^6$  term. Then the continuum limit is taken for  $a^2/t$ -values in the range 0.25–0.5, corresponding to  $a\mu$ -values in the range 0.177–0.25, and a somewhat wider range in Wong 23. The continuum extrapolation data for the  $\beta$ -function at fixed GF coupling are shown in plots. For Hasenfratz 23 these extrapolations look fine and would pass any reasonable data-driven criterion. Wong 23 only show the extrapolation at the largest GF coupling which looks fine, too. Hence we give ★ for the continuum extrapolation and also for renormalization scale, given that  $\alpha_{\text{eff}}$  reaches down to below 0.1. Regarding the formal FLAG criterion for perturbative behaviour, Hasenfratz 23 give an overall error of 0.6% for  $\alpha_{\text{GF}}$ . Using this error we have, at the smallest couplings reached,  $\alpha_{\text{eff}}^{n_1} = (0.1)^2 < 0.006 \times 2.85 = 0.017$ , which satisfies the criterion comfortably. This warrants a ★ for Hasenfratz 23. For Wong 23 the accuracy of  $\alpha_{\text{GF}}$  is not given but they quote a per-mille accuracy for the beta function at  $\bar{g}_{\text{GF}}^2 = 15.8$ ; we assign a ○, which assumes their coupling data is perhaps a factor 2 but still less than a factor 3–4 more accurate relative to the 0.6% of Hasenfratz 23.

Unfortunately, the formal FLAG criteria do not capture the anomalously bad behaviour of the GF scheme. As discussed above, even at  $\alpha_{\text{eff}} = 0.1$  the estimate of the  $\Lambda$ -parameter is ambiguous at the level of about 5 percent.

Contact to perturbation theory is not really established, as the obtained  $\beta$ -function seems to show a slope that is different from the perturbative expectation. Imposing perturbative asymptotics and evaluating the integral over the beta function numerically leads to the estimate  $\sqrt{8t_0}\Lambda_{\overline{\text{MS}}} = 0.622(10)$ . Wong 23 obtain an even smaller error,  $\sqrt{8t_0}\Lambda_{\overline{\text{MS}}} = 0.632(7)$ .<sup>10</sup> Note that both values are in agreement with each other and with Dalla Brida 19 (who obtained 0.623(10)) and would lend support to the high central value compared to older results in the literature. Despite this consistency, the claimed high accuracy seems at odds with the bad perturbative behaviour of this scheme.

Regarding the infinite-volume limit, the main problem is the lack of guidance from theory regarding the fit ansatz. With  $N_f = 0$  and in the hadronic regime, one may expect an

<sup>10</sup>Wong 23 write  $t_0\Lambda_{\overline{\text{MS}}}$ , instead of  $\sqrt{8t_0}\Lambda_{\overline{\text{MS}}}$ , which we interpret as a typo.

exponential approach to the infinite-volume limit  $\propto \exp(-m_G L)$ , with  $m_G$  the  $0^{++}$  glueball mass. At high energies one is necessarily in small volumes where hadrons cannot form, and leading effects  $\propto (a/L)^4$  are used as a plausible ansatz by both groups of authors. However, there is an intermediate regime where the situation is quite unclear, and even at high energies, once the volume is large enough to contain hadrons, the large-volume asymptotics should be expected to change. The situation may be even more complicated in full QCD, where massless pions are expected at low energies. Chiral perturbation theory may help but only as long as pions are relevant degrees of freedom.

Note that boundary conditions should not matter in the infinite-volume limit, so that any of the GF finite-volume couplings that have been used in step-scaling studies (cf. Sec. 9.3) could be used to improve our understanding of it. In fact, the first discussion can be found in Ref. [95], there with open-SF boundary conditions. In Dalla Brida 19, two different finite-volume schemes are considered which should both converge to the infinite-volume GF scheme.

In step-scaling studies, the gradient-flow scale is fixed in units of  $L$  to a constant  $c = \sqrt{8t}/L$ , with typical values around  $c = 0.3$ . This means that the  $\beta$ -function cannot be obtained directly and a detour via the step-scaling function is used in practice [110]. Since the schemes are defined in a finite volume,  $c$  becomes an integral part of the scheme definition as do the boundary conditions (SF, twisted periodic, etc.). In particular, the perturbative 2-loop result in Eq. (382) cannot be used. For  $N_f = 0$  and twisted periodic boundary conditions there is a 1-loop computation [102] while for  $N_f = 0$  and SF boundary conditions there is a 2-loop result obtained using a stochastic perturbative approach [101]. As in infinite volume, the perturbative behaviour of the finite-volume gradient-flow schemes is quite bad [110]. This problem was circumvented in Refs. [33, 100, 110] by matching nonperturbatively to the SF scheme, in order to benefit from its good perturbative behaviour. The option of such a matching is also mentioned in Hasenfratz 23 where it is left to future work.

In Tab. 63 we list these results.

Collaboration	Ref.	$N_f$	publication status	renormalization scale	perturbative behaviour	continuum extrapolation	scale	$\sqrt{8t_0}\Lambda_{\overline{\text{MS}}}$	$r_0\Lambda_{\overline{\text{MS}}}^*$
Hasenfratz 23	[34]	0	A	★	★	★	$\sqrt{t_0}$	0.622(10)	0.659(11)
Wong 23	[35]	0	C	★	○	★	$\sqrt{t_0}$	0.632(7)	0.670(8)

\*  $r_0\Lambda_{\overline{\text{MS}}}$  determined by us using  $\sqrt{8t_0}/r_0 = 0.9435(97)$  from Dalla Brida 19 [110] without propagating the error.

Table 63: Results for the GF scheme in infinite volume.

**Scale variations.** As discussed in the general considerations of the previous subsection, the matching with perturbation theory is performed for  $\bar{g}_{\text{GF}}^2(1/\sqrt{8t}) = 1.2$ . The corresponding

energy scale  $\mu = 1/\sqrt{8t}$  is not given in the publications, preventing us from using the generic procedure that we used for the majority of the observables. Instead, we defined an alternative procedure to estimate the effect of scale variations directly on the ratio of  $\Lambda$ -parameters, as discussed in Sec. 9.9.1.

## 9.10 Summary

Having reviewed the individual computations, we are now in a position to discuss the overall result. We first look at the current results of the  $\Lambda$ -parameter for QCD with  $N_f = 0, 2, 3, 4$  flavours in units of the scale  $r_0$  (and  $\sqrt{8t_0}$  for  $N_f = 0$ ). These results are directly obtained from lattice simulations of QCD with given  $N_f$ . For the  $\Lambda$ -parameter with  $N_f = 0$  we present a more in depth discussion. As emphasized in our last report, even though  $N_f = 0$  is unphysical, the  $\Lambda$ -parameter enters into the decoupling result, which is one of the most accurate lattice determinations of  $\alpha_{\overline{\text{MS}}}^{(5)}(m_Z)$ . Fortunately, this has motivated several collaborations to help clarify the situation, which is characterized by many historical results, with a large spread of central values, that are mutually incompatible due to the smallness of some error estimates. We have decided to estimate ranges for different methods and give a corresponding FLAG estimate.

Then we discuss the central  $\alpha_{\overline{\text{MS}}}(m_Z)$  results in five-flavour QCD. We give ranges for each sub-group discussed previously, and give a final FLAG average as well as an overall average together with the current PDG nonlattice numbers. In the end, we return to the  $\Lambda$ -parameter; for  $N_f = 3, 4, 5$  we derive their values from the FLAG estimate of  $\alpha_{\overline{\text{MS}}}(m_Z)$ .

We end with an outlook and some concluding remarks.

### 9.10.1 Ranges for $[r_0\Lambda_{\overline{\text{MS}}}]^{(N_f)}$ and $\Lambda_{\overline{\text{MS}}}^{(N_f)}$

In the present situation, we give ranges for  $[r_0\Lambda_{\overline{\text{MS}}}]^{(N_f)}$  and  $\Lambda_{\overline{\text{MS}}}$ , discussing their determination case by case. We include results with  $N_f < 3$  because it is interesting to see the  $N_f$ -dependence of the connection of low- and high-energy QCD. This aids our understanding of the field theory and helps in finding possible ways to tackle it beyond the lattice approach. It is also of interest in providing an impression on the size of the vacuum-polarization effects of quarks, in particular with an eye on the still difficult-to-treat heavier charm and bottom quarks. Most importantly, however, the decoupling strategy described in subsection 9.4 means that  $\Lambda$ -parameters at different  $N_f$  can be connected by a nonperturbative matching computation. Thus, even results at unphysical flavour numbers, in particular  $N_f = 0$ , may enter results for the physically interesting case. Rather than phasing out results for “unphysical flavour numbers”, continued scrutiny by FLAG will be necessary. Having said this, we emphasize that results for  $[r_0\Lambda_{\overline{\text{MS}}}]^{(0)}$  and  $[r_0\Lambda_{\overline{\text{MS}}}]^{(2)}$  are *not* meant to be used directly for phenomenology.

For the ranges we obtain:

$$[r_0\Lambda_{\overline{\text{MS}}}]^{(4)} = 0.70(3), \quad (388)$$

$$[r_0\Lambda_{\overline{\text{MS}}}]^{(3)} = 0.809(23), \quad (389)$$

$$[r_0\Lambda_{\overline{\text{MS}}}]^{(2)} = 0.79^{(+5)}_{(-15)}, \quad (390)$$

$$[r_0\Lambda_{\overline{\text{MS}}}]^{(0)} = 0.647(11). \quad (391)$$

No change has occurred since FLAG 21 for  $N_f = 2, 4$ , so we refer to the respective discussions in earlier FLAG reports.

For  $N_f = 2 + 1$ , we take as a central value the weighted average of ALPHA 22 [32], Petreczky 20 [31], CalI 20 [48], Ayala 20 [137], TUMQCD 19 [138], ALPHA 17 [105], HPQCD 10 [167], PACS-CS 09A [106] and Maltman 08 [168], and arrive at our range,

$$[r_0\Lambda_{\overline{\text{MS}}}]^{(3)} = 0.809(23), \quad (392)$$

where the error is the one from the weighted average of those results, which are statistics-dominated, namely PACS-CS 09A, ALPHA 17 and ALPHA 22, and the known correlation between the latter two is taken into account. This is to be compared with the much smaller error of 0.010, as obtained from the weighted average. There is good agreement with all 2+1 results without red tags. In physical units, using  $r_0 = 0.472$  fm and neglecting its error, we get

$$\Lambda_{\overline{\text{MS}}}^{(3)} = 338(10) \text{ MeV}, \quad (393)$$

whereas the error of the straight weighted average is around 4 MeV.

For  $N_f = 0$  there are now 12 results which pass the FLAG criteria, four of which are new since FLAG 21. Instead of averaging individual results we will group them by method, produce pre-ranges and a final estimate for the range from combining the pre-ranges. There are four different methods used:

- Step scaling: Combining Dalla Brida 19 with Bribian 21, Ishikawa 17 (with symmetrized larger error) and ALPHA 98 in a weighted average, we obtain

$$[r_0\Lambda_{\overline{\text{MS}}}]^{(0)} = 0.648(11). \quad (394)$$

Leaving out Ishikawa 17 with its asymmetric error, this would change to 0.651(11). For the error we take the statistics-dominated one from Dalla Brida 19.

- Static potential/force: We combine Brambilla 10 with Brambilla 23 (both with symmetrized error, using the larger ones) in a weighted average,

$$[r_0\Lambda_{\overline{\text{MS}}}]^{(0)} = 0.648(28), \quad (395)$$

where we use the error of the newer result for our estimate of the range.

- There are two new determinations with the GF scheme in infinite volume and continuous  $\beta$ -function, by Wong 23 and Hasenfratz 23. We use the central value of the published paper by Hasenfratz 23 and include a perturbative uncertainty of five percent as discussed in Sec. 9.9, and obtain,

$$[r_0\Lambda_{\overline{\text{MS}}}]^{(0)} = 0.659(33). \quad (396)$$

- Wilson loops: There are two results which are, due to their tiny errors, causing the tension noticed in our previous FLAG report. We performed a scale-variation analysis, similar to the one explained in Sec. 9.9 for the GF scheme. Variations around the scale of fastest apparent convergence (cf. Sec. 9.2.3) result in changes of up to 13 percent even at the finest available lattice spacings. Another way to look at the data is to

note that both works perform continuum extrapolations of the  $\Lambda$ -parameter assuming an  $a^2$ -behaviour. On the other hand, there is a parametric uncertainty of  $O(\alpha_P^2(1/a))$  which is neglected. If included as a second term in a fit, the error gets much larger, and central values tend to increase. Stopping short of changing central values, we take the (unweighted) average central value and include a symmetric range of  $\pm 7$  percent as perturbative uncertainty,

$$[r_0\Lambda_{\overline{\text{MS}}}]^{(0)} = 0.618(43). \quad (397)$$

With these pre-ranges we perform a weighted average to obtain the central value, and then take the statistics-dominated Dalla Brida 19 step-scaling error as our estimate of the range,

$$[r_0\Lambda_{\overline{\text{MS}}}]^{(0)} = 0.647(11) \quad \Rightarrow \quad [\sqrt{8t_0}\Lambda_{\overline{\text{MS}}}]^{(0)} = 0.610(10). \quad (398)$$

All results are shown in Fig. 38 and the  $N_f = 0$  results, with our pre-range by method are shown in Fig. 39.

### 9.10.2 Our range for $\alpha_{\overline{\text{MS}}}^{(5)}$

We now turn to the status of the essential result for phenomenology,  $\alpha_{\overline{\text{MS}}}^{(5)}(M_Z)$ . We only consider lattice results with  $N_f = 3$  or  $N_f = 4$  sea quarks. Converting a  $\Lambda$ -parameter to  $\alpha_{\overline{\text{MS}}}^{(5)}(M_Z)$  involves the perturbative matching of the coupling across the charm- and bottom-quark thresholds, which is available up to 4-loop order [22, 23]. Note that perturbative matching at 4-loops is consistent with using the  $\beta$ -function at 5-loop order, which is also available in the  $\overline{\text{MS}}$  scheme [19, 210]. One then needs the  $Z$ -boson mass and the charm- and bottom-quark masses as additional input. For definiteness, we use  $m_Z = 91.1876$  GeV, and, for the  $\overline{\text{MS}}$  quark masses at their own scale,  $m_c = 1.275(13)$  GeV and  $m_b = 4.203(11)$  GeV [205]. Fortunately, the exact choices are almost irrelevant at the current accuracy: A change in the charm-quark mass by one percent shifts the value of  $\alpha_s(m_Z)$  by  $3 \times 10^{-5}$ , and the effect for the bottom-quark mass is even smaller. This is down by over a factor of 20 compared to the current best total errors on  $\alpha_s$ . The combined perturbative uncertainty of decoupling across both the charm- and the bottom-quark threshold is around  $25 \times 10^{-5}$ , if one takes the difference between 3-loop and 5-loop order as estimate, as was done, for example, in ALPHA 17 [105]. Even this generous estimate is still a factor 2–3 below the best total errors. Incidentally we also note that perturbative decoupling has been tested nonperturbatively [29]. It was found that the decoupling of a heavy quark in gluonic observables (such as the ones used to define  $\alpha_{\text{eff}}$ ), is well described by perturbation theory. Even for the charm quark the nonperturbative effects are expected to be at the few per-mille level. This result justifies the use of  $N_f = 3$  QCD to obtain  $\alpha_{\overline{\text{MS}}}^{(5)}(M_Z)$ , and it motivated the development of the decoupling method used in ALPHA 22 [32].

As can be seen from the tables and figures, several computations satisfy the FLAG criteria for inclusion in the FLAG average. Since FLAG 21 the contribution by Petreczky 20 [31] has been published and is now included in the average and there is the first result from the decoupling method by the ALPHA collaboration, ALPHA 22 [32].

We now explain the determination of our range. We only include those results without a red tag and that are published in a refereed journal.

A general issue with most determinations of  $\alpha_{\overline{\text{MS}}}$ , both lattice and nonlattice, is that they are dominated by perturbative truncation errors, which are difficult to estimate. Further, all

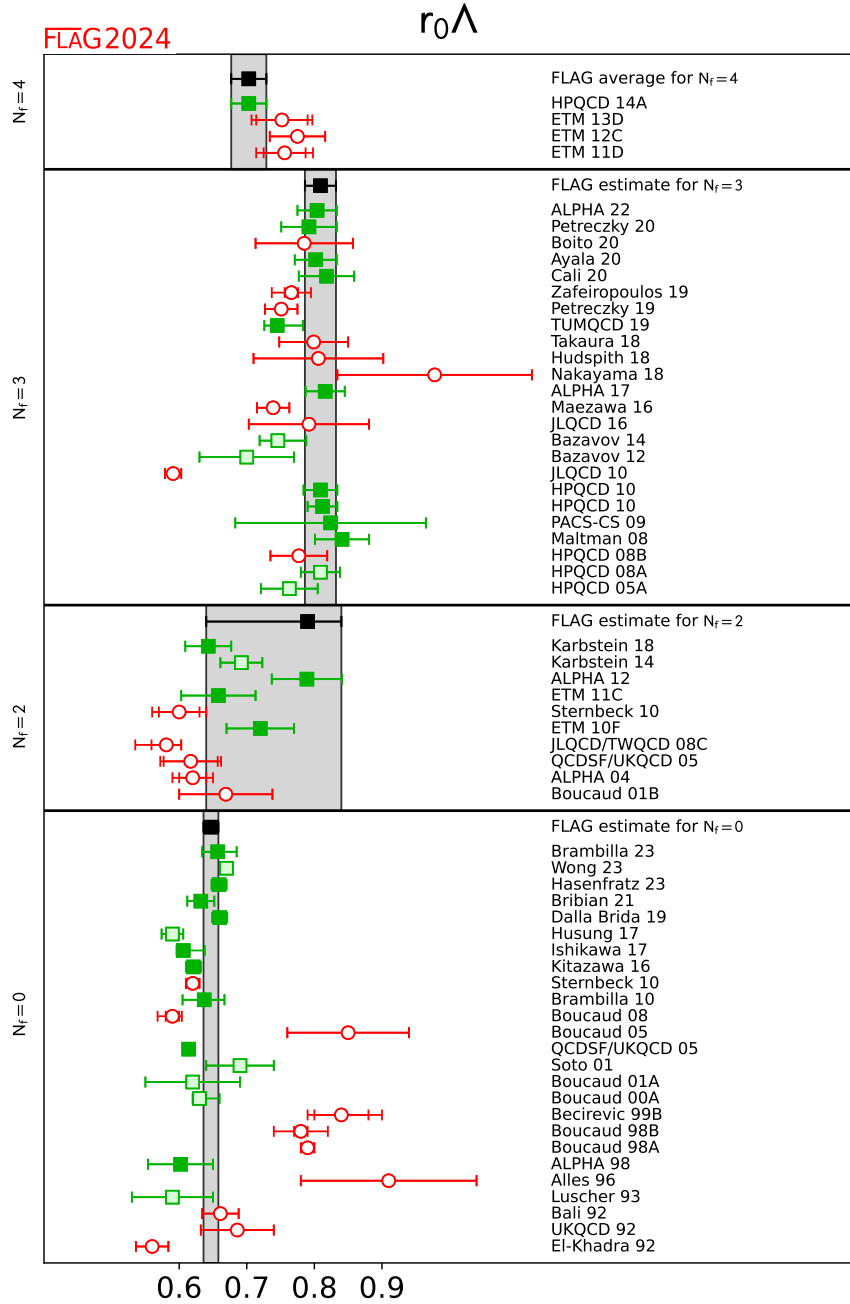


Figure 38:  $r_0\Lambda_{\overline{\text{MS}}}$  estimates for  $N_f = 0, 2, 3, 4$  flavours. Full green squares are used in our final ranges, pale green squares also indicate that there are no red squares in the colour coding but the computations were superseded by later more complete ones or not published, while red open circles mean that there is at least one red square in the colour coding.

results discussed here except for those of Secs. 9.3, 9.7, 9.4 are based on extractions of  $\alpha_{\overline{\text{MS}}}$  that are largely influenced by data with  $\alpha_{\text{eff}} \geq 0.3$ . At smaller  $\alpha_s$  the momentum scale  $\mu$  quickly gets at or above  $a^{-1}$ . We have included computations using  $a\mu$  up to 1.5 and  $\alpha_{\text{eff}}$



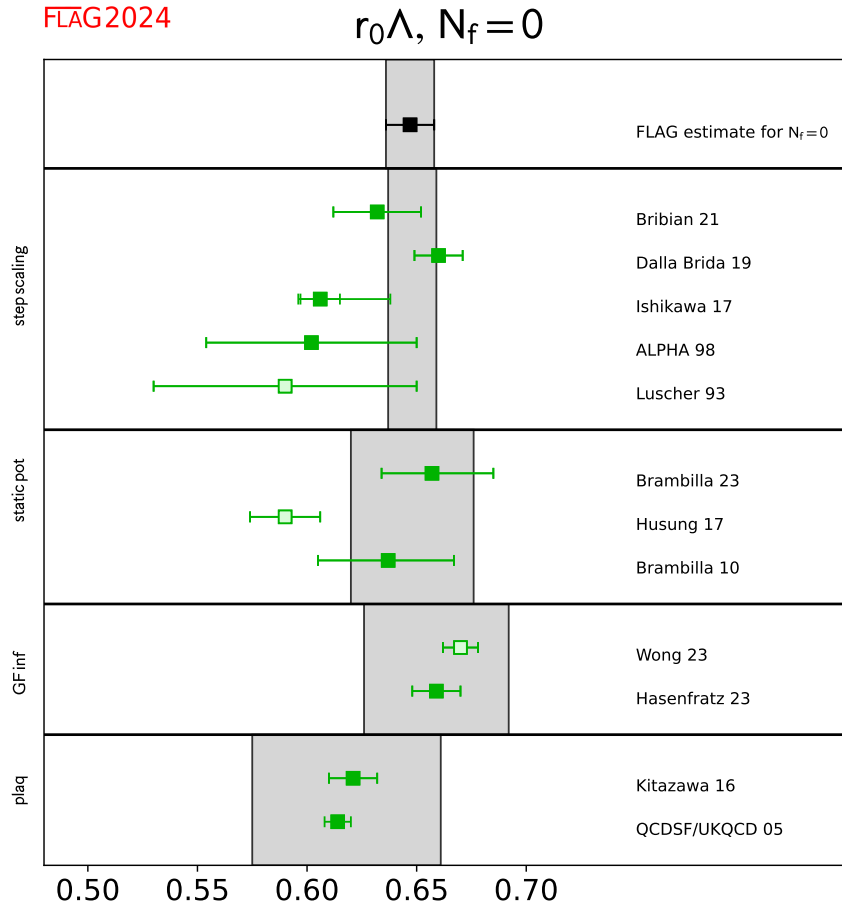


Figure 39:  $r_0\Lambda_{\overline{\text{MS}}}$  estimates for  $N_f = 0$  flavours. As discussed in the text, we group the results by method and estimate pre-ranges. Only full green squares are used in our final ranges, pale green squares indicate that the computations were not published or superseded by later more complete ones.

up to 0.4, but one would ideally like to be significantly below that. Accordingly, we choose to not simply perform weighted averages with the individual errors estimated by each group. Rather, we use our own more conservative estimates of the perturbative truncation errors in the weighted average. In order to improve our assessment we have also performed scale variations as is commonly done in phenomenology. In Tab. 65, we provide a summary of the variations in  $\alpha_{\overline{\text{MS}}}^{(5)}(M_Z)$  obtained from the procedure explained in Sec. 9.1 and suggested in Ref. [11].

In the following we first obtain separate estimates for  $\alpha_s$  from each of the six methods with results that pass the FLAG criteria: step scaling, decoupling, the heavy-quark potential, Wilson loops, heavy-quark current two-point functions and vacuum polarization. In a second step we combine them to obtain the overall FLAG estimate. All results are collected in Tab. 64.

Collaboration	Ref.	$N_f$	publication status	renormalization scale	perturbative behaviour	continuum extrapolation	$\alpha_{\overline{\text{MS}}}(M_Z)$	Remark	Tab.
ALPHA 17	[105]	2+1	A	★	★	★	0.11852( 84)	step scaling	56
PACS-CS 09A	[106]	2+1	A	★	★	○	0.11800(300)	step scaling	56
pre-range (average)							0.11848( 81)		
AIPHA 22	[32]	2+1	A	★	★	★	0.11823(84)	decoupling $N_f = 3$ to $N_f = 0$ & step scaling	57
pre-range (average)							0.11823(84)		
Ayala 20	[137]	2+1	A	○	★	○	0.11836(88)	$Q\text{-}\bar{Q}$ potential	58
TUMQCD 19	[138]	2+1	A	○	★	○	0.11671( $^{+110}_{-57}$ )	$Q\text{-}\bar{Q}$ potential (and free energy)	58
Takaura 18	[139, 140]	2+1	A	■	○	○	0.11790(70)( $^{+130}_{-120}$ )	$Q\text{-}\bar{Q}$ potential	58
Bazavov 14	[141]	2+1	A	○	★	○	0.11660(100)	$Q\text{-}\bar{Q}$ potential	58
Bazavov 12	[142]	2+1	A	○	○	○	0.11560( $^{+210}_{-220}$ )	$Q\text{-}\bar{Q}$ potential	58
pre-range with estimated pert. error							0.11782(165)		
Cali 20	[48]	2+1	A	○	★	★	0.11863(114)	vacuum pol. (position space)	59
Hudspith 18	[77]	2+1	P	○	★	■	0.11810(270)( $^{+80}_{-220}$ )	vacuum polarization	59
JLQCD 10	[76]	2+1	A	■	○	■	0.11180(30)( $^{+160}_{-170}$ )	vacuum polarization	59
pre-range with estimated pert. error							0.11863(360)		
HPQCD 10	[167]	2+1	A	○	★	★	0.11840( 60)	Wilson loops	60
Maltman 08	[168]	2+1	A	○	○	★	0.11920(110)	Wilson loops	60
pre-range with estimated pert. error							0.11871(128)		
Petreczky 20	[31]	2+1	A	○	○	★	0.11773(119)	heavy current two points	61
Boito 20	[197, 203]	2+1	A	■	■	○	0.1177(20)	use published lattice data	61
Petreczky 19	[194]	2+1	A	■	■	★	0.1159(12)	heavy current two points	61
JLQCD 16	[187]	2+1	A	■	○	○	0.11770(260)	heavy current two points	61
Maezawa 16	[193]	2+1	A	■	■	○	0.11622( 84)	heavy current two points	61
HPQCD 14A	[186]	2+1+1	A	○	★	○	0.11822( 74)	heavy current two points	61
HPQCD 10	[167]	2+1	A	○	★	○	0.11830( 70)	heavy current two points	61
HPQCD 08B	[184]	2+1	A	■	■	■	0.11740(120)	heavy current two points	61
pre-range with estimated pert. error							0.11818(119)		
Zafeiropoulos 19	[204]	2+1	A	■	■	■	0.1172(11)	gluon-ghost vertex	66 in [205]
ETM 13D	[206]	2+1+1	A	○	○	■	0.11960(40)(80)(60)	gluon-ghost vertex	66 in [205]
ETM 12C	[207]	2+1+1	A	○	○	■	0.12000(140)	gluon-ghost vertex	66 in [205]
ETM 11D	[208]	2+1+1	A	○	○	■	0.11980(90)(50)( $^{+0}_{-50}$ )	gluon-ghost vertex	66 in [205]
Nakayama 18	[209]	2+1	A	★	○	■	0.12260(360)	Dirac eigenvalues	67 in [205]

Table 64: Results for  $\alpha_{\overline{\text{MS}}}(M_Z)$ . Different methods are listed separately and they are combined to a pre-range when computations are available without any ■. The FLAG estimate is given by 0.11833(67), where the error is the statistics-dominated error of the combined decoupling and step-scaling results.

- *Step scaling*

The step-scaling computations of PACS-CS 09A [106] and ALPHA 17 [105] reach energies around the  $Z$ -mass where perturbative uncertainties in the three-flavour theory are negligible. We form a weighted average of the two results and obtain  $\alpha_{\overline{\text{MS}}} = 0.11848(81)$ , where the error is dominated by the statistical error from the simulations.

- *Decoupling*

There is a single result which has been discussed in Sec. 9.4. The result is  $\alpha_{\overline{\text{MS}}} = 0.11823(84)$  with a statistics-dominated error.

Observable	loops	$Q$ [GeV]	$\delta_{(4)}^*$ [%]	$\delta_{(2)}$ [%]	$\delta_{(2)}^*$ [%]	Refs.
Step scaling	2	80	0.1	0.2	0.2	[69, 70]
	3	1.5		2.6	2.7	[71–75]
Potential		2.5	0.9	1.5	1.5	
		5.0	0.4	0.8	0.8	
Vacuum polarization	3	1.3	1.0	11.6	0.6	[48]
$-\log W_{11}$	2	4.4	2.8	3.3	2.5	[78, 79]
$-\log W_{12}/u_0^6$		4.4	3.5	3.2	3.1	
HQ $r_4$	2	$m_c$		2.7	2.8	[80–82]
HQ $r_4$		$2m_c$	1.2	1.5	1.6	
HQ $r_6$		$2m_c$		2.3	1.2	
HQ $r_8$		$2m_c$		2.8	4.8	

Table 65: Summary of the results of scale variations. We report results for those observables for which we could use the common procedure introduced earlier.

- *Static-quark potential computations*

Brambilla 10 [148], ETM 11C [145] and Bazavov 12 [142] give evidence that they have reached distances where perturbation theory can be used. However, in addition to  $\Lambda$ , a scale is introduced into the perturbative prediction by the process of subtracting the renormalon contribution. This subtraction is avoided in Bazavov 14 [141] by using the force and again agreement with perturbative running is reported. Husung 17 [147] (unpublished) studied the reliability of perturbation theory in the pure gauge theory with lattice spacings down to 0.015 fm and found that at weak coupling there is a downwards trend in the  $\Lambda$ -parameter with a slope  $\Delta\Lambda/\Lambda \approx 9\alpha_s^3$ . The downward trend is broadly confirmed in Husung 20 [146] albeit with larger errors.

Bazavov 14 [141] satisfies all of the criteria to enter the FLAG average for  $\alpha_s$  but has been superseded by TUMQCD 19 [138]. Moreover, there is another study, Ayala 20 [137] who use the very same data as TUMQCD 19, but treat perturbation theory differently, resulting in a rather different central value. This shows that perturbative truncation errors are the main source of errors. We combine the results for  $\Lambda_{\overline{\text{MS}}}^{N_f=3}$  from both groups as a weighted average (with the larger upward error of TUMQCD 19) and take the difference of the central values as the uncertainty of the average. We obtain  $\Lambda_{\overline{\text{MS}}}^{N_f=3} = 330(24)$  MeV, which translates to  $\alpha_s(m_Z) = 0.11782(165)$ . This uncertainty of 1.4 percent is in line with estimates from scale variations.

- *Small Wilson loops*

Here the situation is unchanged since FLAG 16. In the determination of  $\alpha_s$  from observables at the lattice spacing scale, there is an interplay of higher-order perturbative terms and lattice artifacts. In HPQCD 05A [165], HPQCD 08A [78] and Maltman 08 [168] both lattice artifacts (which are power corrections in this approach) and higher-order perturbative terms are fitted. We note that Maltman 08 [168] and HPQCD 08A [78] analyze largely the same data set but use different versions of the perturbative expansion and treatments of nonperturbative terms. After adjusting for the slightly different lattice scales used, the values of  $\alpha_{\overline{\text{MS}}}(M_Z)$  differ by 0.0004 to 0.0008 for the three quantities considered. In fact the largest of these differences (0.0008) comes from a tadpole-improved loop, which is expected to be best behaved perturbatively. We therefore replace the perturbative-truncation errors from [168] and [167] with our estimate

of the perturbative uncertainty Eq. (366). Taking the perturbative errors to be 100% correlated between the results, we obtain for the weighted average  $\alpha_{\overline{\text{MS}}} = 0.11871(128)$ . We note that this assessment, taken over from FLAG 21, seems optimistic in the light of the uncertainty induced by scale variations, which are at the level of three percent for the plaquette and rectangle Wilson loops. One may expect that simultaneous consideration of many quantities stabilizes the estimates as do terms of higher order in  $\alpha$ . It would be interesting to see a new study of this kind, possibly with a different action. We may have to revise our range in the future.

- *Heavy-quark current two-point functions*

Further computations with small errors are HPQCD 10 [167] and HPQCD 14A [186], where correlation functions of heavy valence quarks are used to construct short-distance quantities. Due to the large quark masses needed to reach the region of small coupling, considerable discretization errors are present, see Fig. 30 of FLAG 16. These are treated by fits to the perturbative running (a 5-loop running  $\alpha_{\overline{\text{MS}}}$  with a fitted 5-loop coefficient in the  $\beta$ -function is used) with high-order terms in a double expansion in  $a^2\Lambda^2$  and  $a^2m_c^2$  supplemented by priors which limit the size of the coefficients. The priors play an especially important role in these fits given the much larger number of fit parameters than data points. We note, however, that the size of the coefficients does not prevent high-order terms from contributing significantly, since the data includes values of  $am_c$  that are rather close to one.

From a physics perspective it seems natural to use the renormalization scale set by the charm-quark mass; however, this implies  $\alpha_{\text{eff}} \simeq 0.38$ , which is the reason why JLQCD 16, Petreczky 19 [194] and Boito 20 [197] do not pass the FLAG criteria. Still some valuable insight can be gained from these works. While Petreczky 19/Petreczky 20 share the same lattice data for heavy quark masses in the range  $m_h = m_c - 4m_c$  they use a different strategy for continuum extrapolations and a different treatment of perturbative uncertainties. Petreczky 19 [194] perform continuum extrapolation separately for each value of the valence-quark mass, while Petreczky 20 rely on joint continuum extrapolations of the lattice data at different heavy-quark masses, similar to the analysis of HPQCD, but without Bayesian priors. It is concluded that reliable continuum extrapolations for  $m_h \geq 2m_c$  require a joint fit to the data. This limits the eligible  $\alpha_s$  determinations in Petreczky 19 [194] to  $m_h = m_c$  and  $1.5m_c$ , for which, however, the FLAG criteria are not satisfied. There is also a difference in the choice of renormalization scale between both analyses: Petreczky 19 [194] uses  $\mu = m_h$ , while Petreczky 20 [31] considers several choices of  $\mu$  in the range  $\mu = 2/3m_h - 3m_h$ , which leads to larger perturbative uncertainties in the determination of  $\alpha_s$  [31]. Boito 20 [197] use published continuum extrapolated lattice results for  $m_h = m_c$  and performs their own extraction of  $\alpha_s$ . Limiting the choice of  $m_h$  to the charm-quark mass means that the FLAG criteria are not met ( $\alpha_{\text{eff}} \simeq 0.38$ ). However, their analysis gives valuable insight into the perturbative error. In addition to the renormalization scale  $\mu$ , Boito 20 also vary the renormalization scale  $\mu_m$  at which the charm-quark mass is defined. The corresponding result  $\alpha_s(M_Z) = 0.1177(20)$  agrees well with previous lattice determination but has a larger error, which is dominated by the perturbative uncertainty due to the variation of both scales.

Since the FLAG 21 report the results of Petreczky 20 have been published and pass

all FLAG criteria. There are now three determinations of  $\alpha_s$  from the heavy-quark current two-point functions that satisfy all the FLAG criteria and enter the FLAG average:  $\alpha_{\overline{MS}}(M_Z) = 0.11773(119)$  from Petreczky 20 [31],  $\alpha_{\overline{MS}}(M_Z) = 0.11822(74)$  from HPQCD 14 [186] and  $\alpha_{\overline{MS}}(M_Z) = 0.11830(70)$  from HPQCD 10 [167]. All three determinations agree well with each other within errors. Since these determinations are uncorrelated we take the weighted average of these results as an estimate for the strong coupling constants from the heavy-quark current two-point functions. The analysis in Petreczky 20 does not use Bayesian priors and considers five different choices of the renormalization scale, while HPQCD 10 and HPQCD 14 analyses use  $\mu = 3m_c$ . Therefore, the error of Petreczky 20 can be considered to be more conservative and we take it as the range for  $\alpha_{\overline{MS}}(m_Z)$ . With this we arrive at  $\alpha_{\overline{MS}}(M_Z) = 0.11818(119)$  from the method of the heavy-quark current two-point functions. Comparing with the scale variations, the perturbative uncertainty is estimated to be 1-2 percent so a one percent range is roughly in line.

- *Light-quark vacuum polarization*

Cali 20 [48] use the light-quark current two-point functions in position space, evaluated on a subset of CLS configurations for lattice spacings in the range 0.038–0.076 fm, and for Euclidean distances 0.13–0.19 fm, corresponding to renormalization scales  $\mu = 1$ –1.5 GeV. Both flavour-nonsinglet vector and axial-vector currents are considered and their difference is shown to vanish within errors. After continuum and chiral limits are taken, the effective coupling from the axial-vector two-point function is converted at 3-loop order to  $\alpha_{\overline{MS}}(\mu)$ . The authors do this by numerical solution for  $\alpha_{\overline{MS}}$  and then perform a weighted average of the  $\Lambda$ -parameter estimates for the available energy range, which yields  $\Lambda_{\overline{MS}}^{N_f=3} = 342(17)$  MeV. Note that this is the first calculation in the vacuum polarization category that passes the current FLAG criteria. Yet the renormalization scales are rather low and one might suspect that nonperturbative effects that do not break chiral symmetry may still be sizeable. Our main issue is a rather optimistic estimate of perturbative truncation errors, based only on the variation of the  $\Lambda$ -parameter from the range of effective couplings considered. If the solution for the  $\overline{MS}$  coupling is done by series expansion in  $\alpha_{\text{eff}}$ , the differences in  $\alpha_{\overline{MS}}$ , formally of order  $\alpha_{\text{eff}}^5$ , are still large at the scales considered. Hence, as a measure of the systematic uncertainty we take the difference 409 – 355 MeV between  $\Lambda_{\overline{MS}}^{N_f=3}$  estimates at  $\mu = 1.5$  GeV as a proxy for the total error, i.e.,  $\Lambda_{\overline{MS}}^{N_f=3} = 342(54)$  MeV, which translates to our pre-range,  $\alpha_s(m_Z) = 0.11863(360)$ , from vacuum polarization. Looking at scale variation it appears that these are of  $\mathcal{O}(10)$  percent if the scale is identified as done by the authors. The scale is simply too low for perturbation theory. It is an interesting observation that a variation around the scale of fastest apparent convergence, cf. Sec. 9.2.3, yields much smaller ambiguities of the order of one percent. A reanalysis of the data might be warranted.

- *Other methods*

Computations using other methods do not qualify for an average yet, predominantly due to a lacking  $\odot$  in the continuum extrapolation.

We form the average in two steps, due to the known correlation between ALPHA 17 and ALPHA 22. We thus first combine these two results by combining the respective  $\Lambda$ -parameters and then obtain  $\alpha_s(m_Z) = 0.11836(69)$ . Next we combine with the step-scaling

result by PACS CS-09A, and get  $\alpha_{\overline{\text{MS}}}^{(5)}(m_Z) = 0.11834(67)$ . This average is interesting as it combines the three results where the error is dominated by statistics. A weighted average with the remaining pre-ranges yields the central value, we quote as the new FLAG estimate,

$$\alpha_{\overline{\text{MS}}}^{(5)}(M_Z) = 0.11833(67) = 0.1183(7). \quad (399)$$

where we have used the above statistics-dominated error as our range, rather than the 25 percent smaller error from the weighted average. All central values are remarkably consistent, as can also be seen in Figure 40.

### 9.10.3 Conclusions

With the present results our range for the strong coupling is (repeating Eq. (399))

$$\alpha_{\overline{\text{MS}}}^{(5)}(M_Z) = 0.1183(7) \quad \text{Refs. [31, 32, 48, 105, 106, 137, 138, 167, 168, 186],}$$

and the associated  $\Lambda$ -parameters

$$\Lambda_{\overline{\text{MS}}}^{(5)} = 213(8) \text{ MeV} \quad \text{Refs. [31, 32, 48, 105, 106, 137, 138, 167, 168, 186],} \quad (400)$$

$$\Lambda_{\overline{\text{MS}}}^{(4)} = 295(10) \text{ MeV} \quad \text{Refs. [31, 32, 48, 105, 106, 137, 138, 167, 168, 186],} \quad (401)$$

$$\Lambda_{\overline{\text{MS}}}^{(3)} = 338(10) \text{ MeV} \quad \text{Refs. [31, 32, 48, 105, 106, 137, 138, 167, 168, 186],} \quad (402)$$

Compared with FLAG 21, the central values have only moved slightly and the errors have been reduced by ca. 15-20 percent. Overall we find excellent agreement between all published results that pass the FLAG criteria. The error for the reference value  $\alpha_{\overline{\text{MS}}}^{(5)}(M_Z)$  has reached the level of 0.6 percent, and, as we emphasize again, is dominated by the statistical errors originating from the stochastic process inherent in lattice simulations. The same cannot be said about nonlattice determinations, for which PDG 24 quote the value  $\alpha_{\overline{\text{MS}}}^{(5)}(M_Z) = 0.1175(10)$ . Combining FLAG and PDG nonlattice estimates, we obtain

$$\alpha_{\overline{\text{MS}}}^{(5)}(M_Z) = 0.1181(7), \quad \text{FLAG 24 + PDG 24,} \quad (403)$$

where we assign the error of the FLAG estimate as our range. In Fig. 40, we have collected and summarized the results that go into the FLAG estimate and the PDG 24 average. The agreement with nonlattice results is very good. Despite our conservative error estimate the FLAG lattice estimate has an error that is 30% smaller than the PDG 24 nonlattice result. Compared to high-energy experiments, lattice QCD has the advantage that the complicated transition between hadronic and quark and gluon degrees of freedom never needs to be dealt with explicitly. All hadronic input quantities are very well measured properties of hadrons, such as their masses and decay widths. We would like to encourage experimentalists and phenomenologists at collider experiments to make use of the FLAG lattice estimate. The higher accuracy and precision, with improvements still possible and expected in the near future, may help our understanding of other important physics aspects at the LHC and in other experiments. Currently, many experiments attempt their own determination of  $\alpha_s$ , and the spread of the results is then taken as indication of the size of systematic effects. While this provides valuable information, one may ask whether one can learn more from the data about the origin of the systematic uncertainties, by using the precise lattice result for  $\alpha_s$  as

input for the analysis. This may clarify where tensions or inconsistencies arise and help our understanding of nonperturbative effects, e.g., in hadronization processes, or in some corners of parameter space. There is also the theoretical possibility that QCD does not provide the full picture of the strong interactions. While experimental data would be affected by any new physics, lattice QCD, by design, excludes such effects. Hence, any inconsistencies encountered in the analysis might also point to such new effects.

We finish by commenting on perspectives for the future. This edition of the FLAG report has seen the first result from the decoupling strategy, which complements the step-scaling result. In fact, the decoupling result also relies on the step-scaling technique, however, here it is applied in the  $N_f = 0$  theory and therefore technically simpler, and with different systematics. The nice agreement between  $N_f = 3$  step-scaling and decoupling results is therefore a very strong consistency check. Of course, further results with different schemes and systematics would be very welcome. For step scaling with  $N_f = 0$ , Dalla Brida 19 have used two different finite-volume schemes with SF boundary conditions, and there is now a new result by Bribian 21 with twisted periodic b.c.'s. There are also results with the GF scheme in infinite volume, where the  $\beta$ -function can be measured directly, by Hasenfratz 23 and Wong 23. In some sense, the case of  $N_f = 0$  flavours is more difficult than full QCD, in that the asymptotic regime is often harder to reach. Of course, part of the problem lies in the smallness of statistical errors, which means that even moderate systematic errors easily stand out. In particular, in GF schemes, both in finite and infinite volume, the parametric uncertainties in the  $\Lambda$ -parameter of order  $\alpha^{n_1}$ , Eq. (291), can be still quite large at the largest scales reached while showing the expected asymptotic behaviour  $\propto \alpha^{n_1}$  over a wide range. Rather than assigning a large systematic uncertainty at the highest scale reached, one might be inclined to allow for an extrapolation in  $\alpha^{n_1}$ , together with a data-driven criterion to assess its quality. We will reconsider this issue in the next edition of the FLAG report.

Finally we emphasize the importance that errors remain dominated by statistics. Only in this case a probabilistic interpretation is obvious. This is currently not the case for the majority of lattice calculations, the exception being the step-scaling and decoupling approaches. For those determinations, further improvements will require access to higher energy scales, for instance, by implementing some elements of the step-scaling approach.

## References

- [1] LHC HIGGS CROSS SECTION WORKING GROUP collaboration, *Handbook of LHC Higgs Cross Sections: 4. Deciphering the Nature of the Higgs Sector*, [1610.07922](#).
- [2] G.P. Salam, *The strong coupling: a theoretical perspective*, in *From My Vast Repertoire ...: Guido Altarelli's Legacy*, A. Levy, S. Forte and G. Ridolfi, eds., pp. 101–121 (2019), DOI [[1712.05165](#)].
- [3] S. Dittmaier et al., *Handbook of LHC Higgs Cross Sections: 2. Differential Distributions*, [1201.3084](#).
- [4] LHC HIGGS CROSS SECTION WORKING GROUP collaboration, *Handbook of LHC Higgs Cross Sections: 3. Higgs Properties*, [1307.1347](#).
- [5] LBNE collaboration, *Scientific Opportunities with the Long-Baseline Neutrino Experiment*, [1307.7335](#).



- [6] S. Dawson, A. Gritsan, H. Logan, J. Qian, C. Tully et al., *Higgs Working Group Report of the Snowmass 2013 Community Planning Study*, [1310.8361](#).
- [7] A. Accardi et al., *A critical appraisal and evaluation of modern PDFs*, *Eur. Phys. J. C* **76** (2016) 471 [[1603.08906](#)].
- [8] G.P. Lepage, P.B. Mackenzie and M.E. Peskin, *Expected Precision of Higgs Boson Partial Widths within the Standard Model*, [1404.0319](#).
- [9] D. Buttazzo, G. Degrandi, P.P. Giardinò, G.F. Giudice, F. Sala, A. Salvio et al., *Investigating the near-criticality of the Higgs boson*, *JHEP* **12** (2013) 089 [[1307.3536](#)].
- [10] J.R. Espinosa, *Vacuum Stability and the Higgs Boson*, *PoS LATTICE2013* (2014) 010 [[1311.1970](#)].
- [11] L. Del Debbio and A. Ramos, *Lattice determinations of the strong coupling*, *Physics Reports* **920** (2021) 1 [[2101.04762](#)].
- [12] M. Dalla Brida, *Past, present, and future of precision determinations of the QCD parameters from lattice QCD*, *Eur. Phys. J. A* **57** (2021) 66 [[2012.01232](#)].
- [13] S. Forte and Z. Kassabov, *Why  $\alpha_s$  cannot be determined from hadronic processes without simultaneously determining the parton distributions*, *Eur. Phys. J. C* **80** (2020) 182 [[2001.04986](#)].
- [14] PARTICLE DATA GROUP collaboration, *Review of Particle Physics*, *PTEP* **2020** (2020) 083C01.
- [15] PARTICLE DATA GROUP collaboration, *Review of particle physics*, *Phys. Rev. D* **110** (2024) 030001.
- [16] T. van Ritbergen, J. A. M. Vermaseren and S. A. Larin, *The four-loop  $\beta$ -function in Quantum Chromodynamics*, *Phys. Lett. B* **400** (1997) 379 [[hep-ph/9701390](#)].
- [17] M. Czakon, *The Four-loop QCD beta-function and anomalous dimensions*, *Nucl. Phys. B* **710** (2005) 485 [[hep-ph/0411261](#)].
- [18] T. Luthe, A. Maier, P. Marquard and Y. Schröder, *Towards the five-loop Beta function for a general gauge group*, *JHEP* **07** (2016) 127 [[1606.08662](#)].
- [19] F. Herzog, B. Ruijl, T. Ueda, J.A.M. Vermaseren and A. Vogt, *The five-loop beta function of Yang-Mills theory with fermions*, *JHEP* **02** (2017) 090 [[1701.01404](#)].
- [20] P.A. Baikov, K.G. Chetyrkin and J.H. Kuhn, *Five-Loop Running of the QCD coupling constant*, *Phys. Rev. Lett.* **118** (2017) 082002 [[1606.08659](#)].
- [21] W. Bernreuther and W. Wetzel, *Decoupling of heavy quarks in the minimal subtraction scheme*, *Nucl. Phys. B* **197** (1982) 228.
- [22] K. Chetyrkin, J.H. Kuhn and C. Sturm, *QCD decoupling at four loops*, *Nucl. Phys. B* **744** (2006) 121 [[hep-ph/0512060](#)].

- [23] Y. Schröder and M. Steinhauser, *Four-loop decoupling relations for the strong coupling*, *JHEP* **01** (2006) 051 [[hep-ph/0512058](#)].
- [24] B.A. Kniehl, A.V. Kotikov, A.I. Onishchenko and O.L. Veretin, *Strong-coupling constant with flavor thresholds at five loops in the anti-MS scheme*, *Phys. Rev. Lett.* **97** (2006) 042001 [[hep-ph/0607202](#)].
- [25] A.G. Grozin, M. Hoeschele, J. Hoff and M. Steinhauser, *Simultaneous decoupling of bottom and charm quarks*, *JHEP* **09** (2011) 066 [[1107.5970](#)].
- [26] K.G. Chetyrkin, J.H. Kuhn and M. Steinhauser, *RunDec: A Mathematica package for running and decoupling of the strong coupling and quark masses*, *Comput. Phys. Commun.* **133** (2000) 43 [[hep-ph/0004189](#)].
- [27] F. Herren and M. Steinhauser, *Version 3 of RunDec and CRunDec*, *Comput. Phys. Commun.* **224** (2018) 333 [[1703.03751](#)].
- [28] A.H. Hoang, C. Lepenik and V. Mateu, *REvolver: Automated running and matching of couplings and masses in QCD*, *Comput. Phys. Commun.* **270** (2022) 108145 [[2102.01085](#)].
- [29] A. Athenodorou, J. Finkenrath, F. Knechtli, T. Korzec, B. Leder, M.K. Marinkovic et al., *How perturbative are heavy sea quarks?*, *Nucl. Phys.* **B943** (2019) 114612 [[1809.03383](#)].
- [30] [ALPHA 19A] M. Dalla Brida, R. Höllwieser, F. Knechtli, T. Korzec, A. Ramos and R. Sommer, *Non-perturbative renormalization by decoupling*, *Phys. Lett. B* **807** (2020) 135571 [[1912.06001](#)].
- [31] P. Petreczky and J.H. Weber, *Strong coupling constant from moments of quarkonium correlators revisited*, *Eur. Phys. J. C* **82** (2022) 64 [[2012.06193](#)].
- [32] [ALPHA 22] M. Dalla Brida, R. Höllwieser, F. Knechtli, T. Korzec, A. Nada, A. Ramos et al., *Determination of  $\alpha_s(m_Z)$  by the non-perturbative decoupling method*, *Eur. Phys. J. C* **82** (2022) 1092 [[2209.14204](#)].
- [33] E. I. Bribian, J.L.D. Golan, M.G. Perez and A. Ramos, *Memory efficient finite volume schemes with twisted boundary conditions*, *Eur. Phys. J. C* **81** (2021) 951 [[2107.03747](#)].
- [34] A. Hasenfratz, C.T. Peterson, J. van Sickle and O. Witzel,  *$\Lambda$  parameter of the  $SU(3)$  Yang-Mills theory from the continuous  $\beta$  function*, *Phys. Rev. D* **108** (2023) 014502 [[2303.00704](#)].
- [35] C.H. Wong, S. Borsanyi, Z. Fodor, K. Holland and J. Kuti, *Toward a novel determination of the strong QCD coupling at the Z-pole*, *PoS LATTICE2022* (2023) 043 [[2301.06611](#)].
- [36] L. Chimirri, *A Quenched Exploration of Heavy Quark Moments and their Perturbative Expansion*, *PoS LATTICE2022* (2023) 350 [[2301.09959](#)].
- [37] N. Brambilla, V. Leino, J. Mayer-Steudte and A. Vairo, *Static force from generalized Wilson loops on the lattice using the gradient flow*, *Phys. Rev. D* **109** (2024) 114517 [[2312.17231](#)].

- [38] M. Lüscher, *Properties and uses of the Wilson flow in lattice QCD*, *JHEP* **08** (2010) 071 [[1006.4518](#)], [Erratum: *JHEP* **03** (2014) 092].
- [39] [BMW 12A] S. Borsanyi, S. Dür, Z. Fodor, C. Hoelbling, S.D. Katz et al., *High-precision scale setting in lattice QCD*, *JHEP* **1209** (2012) 010 [[1203.4469](#)].
- [40] R. Sommer, *A new way to set the energy scale in lattice gauge theories and its applications to the static force and  $\alpha_s$  in  $SU(2)$  Yang-Mills theory*, *Nucl. Phys.* **B411** (1994) 839 [[hep-lat/9310022](#)].
- [41] C.W. Bernard et al., *The static quark potential in three flavor QCD*, *Phys. Rev.* **D62** (2000) 034503 [[hep-lat/0002028](#)].
- [42] G. Martinelli and C.T. Sachrajda, *On the difficulty of computing higher twist corrections*, *Nucl.Phys.* **B478** (1996) 660 [[hep-ph/9605336](#)].
- [43] S. Bethke, A.H. Hoang, S. Kluth, J. Schieck, I.W. Stewart et al., *Workshop on Precision Measurements of  $\alpha_s$* , [1110.0016](#).
- [44] A.H. Hoang and C. Regner, *On the Difference between FOPT and CIPT for Hadronic Tau Decays*, vol. 230, 2021, DOI [[2105.11222](#)].
- [45] M.A. Benitez-Rathgeb, D. Boito, A.H. Hoang and M. Jamin, *Reconciling the contour-improved and fixed-order approaches for  $\tau$  hadronic spectral moments. Part II. Renormalon norm and application in  $\alpha_s$  determinations*, *JHEP* **09** (2022) 223 [[2207.01116](#)].
- [46] D. Boito, M. Golterman, K. Maltman, J. Osborne and S. Peris, *Strong coupling from the revised ALEPH data for hadronic  $\tau$  decays*, *Phys. Rev.* **D91** (2015) 034003 [[1410.3528](#)].
- [47] D. Boito, M. Golterman, K. Maltman and S. Peris, *Strong coupling from hadronic  $\tau$  decays: A critical appraisal*, *Phys. Rev.* **D95** (2017) 034024 [[1611.03457](#)].
- [48] S. Cali, K. Cichy, P. Korcyl and J. Simeth, *Running coupling constant from position-space current-current correlation functions in three-flavor lattice QCD*, *Phys. Rev. Lett.* **125** (2020) 242002 [[2003.05781](#)].
- [49] L. Del Debbio, H. Panagopoulos and E. Vicari, *Theta dependence of  $SU(N)$  gauge theories*, *JHEP* **08** (2002) 044 [[hep-th/0204125](#)].
- [50] C. Bernard et al., *Topological susceptibility with the improved Asqtad action*, *Phys. Rev.* **D68** (2003) 114501 [[hep-lat/0308019](#)].
- [51] [ALPHA 10C] S. Schaefer, R. Sommer and F. Virota, *Critical slowing down and error analysis in lattice QCD simulations*, *Nucl.Phys.* **B845** (2011) 93 [[1009.5228](#)].
- [52] A. Chowdhury, A. Harindranath, J. Maiti and P. Majumdar, *Topological susceptibility in lattice Yang-Mills theory with open boundary condition*, *JHEP* **02** (2014) 045 [[1311.6599](#)].
- [53] [LSD 14] R. C. Brower et al., *Maximum-Likelihood Approach to Topological Charge Fluctuations in Lattice Gauge Theory*, *Phys. Rev.* **D90** (2014) 014503 [[1403.2761](#)].

- [54] [HotQCD 14] A. Bazavov et al., *Equation of state in (2+1)-flavor QCD*, *Phys.Rev.* **D90** (2014) 094503 [[1407.6387](#)].
- [55] [JLQCD 15] H. Fukaya, S. Aoki, G. Cossu, S. Hashimoto, T. Kaneko and J. Noaki,  *$\eta'$  meson mass from topological charge density correlator in QCD*, *Phys. Rev.* **D92** (2015) 111501 [[1509.00944](#)].
- [56] M. Lüscher and S. Schaefer, *Lattice QCD without topology barriers*, *JHEP* **1107** (2011) 036 [[1105.4749](#)].
- [57] [ETM 09C] R. Baron et al., *Light meson physics from maximally twisted mass lattice QCD*, *JHEP* **08** (2010) 097 [[0911.5061](#)].
- [58] [ETM 09J] B. Blossier et al., *Pseudoscalar decay constants of kaon and D-mesons from  $N_f = 2$  twisted mass Lattice QCD*, *JHEP* **07** (2009) 043 [[0904.0954](#)].
- [59] [ALPHA 12] P. Fritzsche, F. Knechtli, B. Leder, M. Marinkovic, S. Schaefer et al., *The strange quark mass and the  $\Lambda$  parameter of two flavor QCD*, *Nucl.Phys.* **B865** (2012) 397 [[1205.5380](#)].
- [60] [QCDSF 12] G. Bali, P. Bruns, S. Collins, M. Deka, B. Glasle et al., *Nucleon mass and sigma term from lattice QCD with two light fermion flavors*, *Nucl.Phys.* **B866** (2013) 1 [[1206.7034](#)].
- [61] [HPQCD 09B] C. T. H. Davies, E. Follana, I. Kendall, G.P. Lepage and C. McNeile, *Precise determination of the lattice spacing in full lattice QCD*, *Phys.Rev.* **D81** (2010) 034506 [[0910.1229](#)].
- [62] [MILC 10] A. Bazavov et al., *Results for light pseudoscalar mesons*, *PoS LAT2010* (2010) 074 [[1012.0868](#)].
- [63] [HotQCD 11] A. Bazavov, T. Bhattacharya, M. Cheng, C. DeTar, H. Ding et al., *The chiral and deconfinement aspects of the QCD transition*, *Phys.Rev.* **D85** (2012) 054503 [[1111.1710](#)].
- [64] S. Necco and R. Sommer, *The  $N_f = 0$  heavy quark potential from short to intermediate distances*, *Nucl.Phys.* **B622** (2002) 328 [[hep-lat/0108008](#)].
- [65] M. Lüscher and P. Weisz, *Quark confinement and the bosonic string*, *JHEP* **0207** (2002) 049 [[hep-lat/0207003](#)].
- [66] [ALPHA 16] M. Dalla Brida, P. Fritzsche, T. Korzec, A. Ramos, S. Sint and R. Sommer, *Determination of the QCD  $\Lambda$ -parameter and the accuracy of perturbation theory at high energies*, *Phys. Rev. Lett.* **117** (2016) 182001 [[1604.06193](#)].
- [67] [ALPHA 18] M. Dalla Brida, P. Fritzsche, T. Korzec, A. Ramos, S. Sint and R. Sommer, *A non-perturbative exploration of the high energy regime in  $N_f = 3$  QCD*, *Eur. Phys. J.* **C78** (2018) 372 [[1803.10230](#)].
- [68] M. Cacciari and N. Houdeau, *Meaningful characterisation of perturbative theoretical uncertainties*, *JHEP* **09** (2011) 039 [[1105.5152](#)].

- [69] [ALPHA 98A] A. Bode, U. Wolff and P. Weisz, *Two loop computation of the Schrödinger functional in pure  $SU(3)$  lattice gauge theory*, *Nucl. Phys. B* **540** (1999) 491 [[hep-lat/9809175](#)].
- [70] [ALPHA 99] A. Bode, P. Weisz and U. Wolff, *Two loop computation of the Schrödinger functional in lattice QCD*, *Nucl.Phys.* **B576** (2000) 517 [[hep-lat/9911018](#)].
- [71] W. Fischler, *Quark-antiquark potential in QCD*, *Nucl.Phys.* **B129** (1977) 157.
- [72] M. Peter, *The Static quark - anti-quark potential in QCD to three loops*, *Phys. Rev. Lett.* **78** (1997) 602 [[hep-ph/9610209](#)].
- [73] M. Peter, *The static potential in QCD: a full two loop calculation*, *Nucl.Phys.* **B501** (1997) 471 [[hep-ph/9702245](#)].
- [74] A.V. Smirnov, V.A. Smirnov and M. Steinhauser, *Three-loop static potential*, *Phys.Rev.Lett.* **104** (2010) 112002 [[0911.4742](#)].
- [75] A.V. Smirnov, V.A. Smirnov and M. Steinhauser, *Fermionic contributions to the three-loop static potential*, *Phys. Lett. B* **668** (2008) 293 [[0809.1927](#)].
- [76] [JLQCD 10] E. Shintani, S. Aoki, H. Fukaya, S. Hashimoto, T. Kaneko et al., *Strong coupling constant from vacuum polarization functions in three-flavor lattice QCD with dynamical overlap fermions*, *Phys.Rev.* **D82** (2010) 074505, Erratum [[1002.0371](#)].
- [77] R.J. Hudspith, R. Lewis, K. Maltman and E. Shintani,  $\alpha_s$  from the Lattice Hadronic Vacuum Polarisation, [1804.10286](#).
- [78] [HPQCD 08A] C. T. H. Davies et al., *Update: accurate determinations of  $\alpha_s$  from realistic lattice QCD*, *Phys. Rev.* **D78** (2008) 114507 [[0807.1687](#)].
- [79] G.P. Lepage and P.B. Mackenzie, *On the viability of lattice perturbation theory*, *Phys.Rev.* **D48** (1993) 2250 [[hep-lat/9209022](#)].
- [80] K. Chetyrkin, J.H. Kuhn and C. Sturm, *Four-loop moments of the heavy quark vacuum polarization function in perturbative QCD*, *Eur.Phys.J.* **C48** (2006) 107 [[hep-ph/0604234](#)].
- [81] K.G. Chetyrkin, J.H. Kuhn and M. Steinhauser, *Heavy quark current correlators to  $O(\alpha_s^2)$* , *Nucl. Phys. B* **505** (1997) 40 [[hep-ph/9705254](#)].
- [82] D.J. Broadhurst, *Three loop on-shell charge renormalization without integration: Lambda-MS (QED) to four loops*, *Z. Phys. C* **54** (1992) 599.
- [83] R.V. Harlander and T. Neumann, *The perturbative QCD gradient flow to three loops*, *JHEP* **06** (2016) 161 [[1606.03756](#)].
- [84] M. Lüscher, P. Weisz and U. Wolff, *A numerical method to compute the running coupling in asymptotically free theories*, *Nucl.Phys.* **B359** (1991) 221.
- [85] M. Lüscher, R. Narayanan, P. Weisz and U. Wolff, *The Schrödinger functional: a renormalizable probe for non-abelian gauge theories*, *Nucl. Phys.* **B384** (1992) 168 [[hep-lat/9207009](#)].

- [86] S. Sint, *On the Schrödinger functional in QCD*, *Nucl.Phys.* **B421** (1994) 135 [[hep-lat/9312079](#)].
- [87] A. Coste, A. Gonzalez-Arroyo, J. Jurkiewicz and C. Korthals Altes, *Zero momentum contribution to Wilson loops in periodic boxes*, *Nucl.Phys.* **B262** (1985) 67.
- [88] M. Lüscher, R. Sommer, P. Weisz and U. Wolff, *A precise determination of the running coupling in the  $SU(3)$  Yang-Mills theory*, *Nucl.Phys.* **B413** (1994) 481 [[hep-lat/9309005](#)].
- [89] S. Sint and R. Sommer, *The running coupling from the QCD Schrödinger functional: a one loop analysis*, *Nucl.Phys.* **B465** (1996) 71 [[hep-lat/9508012](#)].
- [90] [CP-PACS 04] S. Takeda, S. Aoki, M. Fukugita, K.-I. Ishikawa, N. Ishizuka et al., *A scaling study of the step scaling function in  $SU(3)$  gauge theory with improved gauge actions*, *Phys.Rev.* **D70** (2004) 074510 [[hep-lat/0408010](#)].
- [91] M. Lüscher, *A Semiclassical Formula for the Topological Susceptibility in a Finite Space-time Volume*, *Nucl. Phys.* **B205** (1982) 483.
- [92] P. Fritzsch, A. Ramos and F. Stollenwerk, *Critical slowing down and the gradient flow coupling in the Schrödinger functional*, *PoS Lattice2013* (2014) 461 [[1311.7304](#)].
- [93] M. Dalla Brida, P. Fritzsch, T. Korzec, A. Ramos, S. Sint and R. Sommer, *Slow running of the Gradient Flow coupling from 200 MeV to 4 GeV in  $N_f = 3$  QCD*, *Phys. Rev.* **D95** (2017) 014507 [[1607.06423](#)].
- [94] C. Bonanno, J.L. Dasilva Golán, M. D’Elia, M. García Pérez and A. Giorgieri, *The  $SU(3)$  twisted gradient flow strong coupling without topology freezing*, *Eur. Phys. J. C* **84** (2024) 916 [[2403.13607](#)].
- [95] M. Lüscher, *Step scaling and the Yang-Mills gradient flow*, *JHEP* **06** (2014) 105 [[1404.5930](#)].
- [96] R. Narayanan and H. Neuberger, *Infinite  $N$  phase transitions in continuum Wilson loop operators*, *JHEP* **03** (2006) 064 [[hep-th/0601210](#)].
- [97] Z. Fodor, K. Holland, J. Kuti, D. Nogradi and C.H. Wong, *The Yang-Mills gradient flow in finite volume*, *JHEP* **1211** (2012) 007 [[1208.1051](#)].
- [98] P. Fritzsch and A. Ramos, *The gradient flow coupling in the Schrödinger functional*, *JHEP* **1310** (2013) 008 [[1301.4388](#)].
- [99] A. Ramos, *The gradient flow running coupling with twisted boundary conditions*, *JHEP* **11** (2014) 101 [[1409.1445](#)].
- [100] K.-I. Ishikawa, I. Kanamori, Y. Murakami, A. Nakamura, M. Okawa and R. Ueno, *Non-perturbative determination of the  $\Lambda$ -parameter in the pure  $SU(3)$  gauge theory from the twisted gradient flow coupling*, *JHEP* **12** (2017) 067 [[1702.06289](#)].
- [101] M. Dalla Brida and M. Lüscher, *SMD-based numerical stochastic perturbation theory*, *Eur. Phys. J. C* **77** (2017) 308 [[1703.04396](#)].



- [102] E.I. Bribian and M. Garcia Perez, *The twisted gradient flow coupling at one loop*, *JHEP* **03** (2019) 200 [[1903.08029](#)].
- [103] [ALPHA 10A] F. Tekin, R. Sommer and U. Wolff, *The running coupling of QCD with four flavors*, *Nucl.Phys.* **B840** (2010) 114 [[1006.0672](#)].
- [104] P. Perez-Rubio and S. Sint, *Non-perturbative running of the coupling from four flavour lattice QCD with staggered quarks*, *PoS LAT2010* (2010) 236 [[1011.6580](#)].
- [105] [ALPHA 17] M. Bruno, M. Dalla Brida, P. Fritzsch, T. Korzec, A. Ramos, S. Schaefer et al., *QCD Coupling from a Nonperturbative Determination of the Three-Flavor  $\Lambda$  Parameter*, *Phys. Rev. Lett.* **119** (2017) 102001 [[1706.03821](#)].
- [106] [PACS-CS 09A] S. Aoki et al., *Precise determination of the strong coupling constant in  $N_f = 2 + 1$  lattice QCD with the Schrödinger functional scheme*, *JHEP* **0910** (2009) 053 [[0906.3906](#)].
- [107] [ALPHA 04] M. Della Morte et al., *Computation of the strong coupling in QCD with two dynamical flavours*, *Nucl. Phys.* **B713** (2005) 378 [[hep-lat/0411025](#)].
- [108] [ALPHA 01A] A. Bode et al., *First results on the running coupling in QCD with two massless flavors*, *Phys.Lett.* **B515** (2001) 49 [[hep-lat/0105003](#)].
- [109] A. Nada and A. Ramos, *An analysis of systematic effects in finite size scaling studies using the gradient flow*, *Eur. Phys. J. C* **81** (2021) 1 [[2007.12862](#)].
- [110] M. Dalla Brida and A. Ramos, *The gradient flow coupling at high-energy and the scale of  $SU(3)$  Yang–Mills theory*, *Eur. Phys. J. C* **79** (2019) 720 [[1905.05147](#)].
- [111] [ALPHA 98] S. Capitani, M. Lüscher, R. Sommer and H. Wittig, *Nonperturbative quark mass renormalization in quenched lattice QCD*, *Nucl.Phys.* **B544** (1999) 669 [[hep-lat/9810063](#)].
- [112] J. Bulava and S. Schaefer, *Improvement of  $N_f = 3$  lattice QCD with Wilson fermions and tree-level improved gauge action*, *Nucl. Phys.* **B874** (2013) 188 [[1304.7093](#)].
- [113] M. Lüscher and P. Weisz, *On-shell improved lattice gauge theories*, *Commun. Math. Phys.* **97** (1985) 59.
- [114] [JLQCD/CP-PACS 04] N. Yamada et al., *Non-perturbative  $O(a)$ -improvement of Wilson quark action in three-flavor QCD with plaquette gauge action*, *Phys.Rev.* **D71** (2005) 054505 [[hep-lat/0406028](#)].
- [115] [RBC/UKQCD 08] C. Allton et al., *Physical results from 2+1 flavor domain wall QCD and  $SU(2)$  chiral perturbation theory*, *Phys. Rev.* **D78** (2008) 114509 [[0804.0473](#)].
- [116] A. Gonzalez-Arroyo and M. Okawa, *The string tension from smeared Wilson loops at large  $N$* , *Phys. Lett.* **B718** (2013) 1524 [[1206.0049](#)].
- [117] [ALPHA 14A] M. Bruno, J. Finkenrath, F. Knechtli, B. Leder and R. Sommer, *Effects of Heavy Sea Quarks at Low Energies*, *Phys. Rev. Lett.* **114** (2015) 102001 [[1410.8374](#)].



- [118] M. Gerlach, F. Herren and M. Steinhauser, *Wilson coefficients for Higgs boson production and decoupling relations to  $\mathcal{O}(\alpha_s^4)$* , *JHEP* **11** (2018) 141 [[1809.06787](#)].
- [119] [ALPHA 18C] I. Campos, P. Fritzsch, C. Pena, D. Preti, A. Ramos and A. Vladikas, *Non-perturbative quark mass renormalisation and running in  $N_f = 3$  QCD*, *Eur. Phys. J. C* **78** (2018) 387 [[1802.05243](#)].
- [120] J. Balog, F. Niedermayer and P. Weisz, *The Puzzle of apparent linear lattice artifacts in the 2d non-linear sigma-model and Symanzik’s solution*, *Nucl. Phys. B* **824** (2010) 563 [[0905.1730](#)].
- [121] J. Balog, F. Niedermayer and P. Weisz, *Logarithmic corrections to  $O(a^{**2})$  lattice artifacts*, *Phys. Lett. B* **676** (2009) 188 [[0901.4033](#)].
- [122] N. Husung, P. Marquard and R. Sommer, *Asymptotic behavior of cutoff effects in Yang–Mills theory and in Wilson’s lattice QCD*, *Eur. Phys. J. C* **80** (2020) 200 [[1912.08498](#)].
- [123] N. Husung, P. Marquard and R. Sommer, *The asymptotic approach to the continuum of lattice QCD spectral observables*, *Phys. Lett. B* **829** (2022) 137069 [[2111.02347](#)].
- [124] N. Husung, *Logarithmic corrections to  $O(a)$  and  $O(a^2)$  effects in lattice QCD with Wilson or Ginsparg–Wilson quarks*, *Eur. Phys. J. C* **83** (2023) 142 [[2206.03536](#)], [Erratum: Eur.Phys.J.C 83, 144 (2023)].
- [125] [CLS 16] M. Bruno, T. Korzec and S. Schaefer, *Setting the scale for the CLS 2+1 flavor ensembles*, *Phys. Rev. D* **95** (2017) 074504 [[1608.08900](#)].
- [126] [ALPHA 24] M. Dalla Brida, R. Höllwieser, F. Knechtli, T. Korzec, S. Sint and R. Sommer, *Heavy Wilson quarks and  $O(a)$  improvement: nonperturbative results for  $b_g$* , *JHEP* **2024** (2024) 188 [[2401.00216](#)].
- [127] C. Michael, *The running coupling from lattice gauge theory*, *Phys.Lett. B* **283** (1992) 103 [[hep-lat/9205010](#)].
- [128] [UKQCD 92] S. P. Booth et al., *The running coupling from  $SU(3)$  lattice gauge theory*, *Phys. Lett. B* **294** (1992) 385 [[hep-lat/9209008](#)].
- [129] A. Billoire, *How heavy must be quarks in order to build coulombic  $q\bar{q}$  bound states*, *Phys.Lett. B* **92** (1980) 343.
- [130] Y. Schröder, *The static potential in QCD to two loops*, *Phys.Lett. B* **447** (1999) 321 [[hep-ph/9812205](#)].
- [131] N. Brambilla, A. Pineda, J. Soto and A. Vairo, *The infrared behavior of the static potential in perturbative QCD*, *Phys.Rev. D* **60** (1999) 091502 [[hep-ph/9903355](#)].
- [132] C. Anzai, Y. Kiyo and Y. Sumino, *Static QCD potential at three-loop order*, *Phys.Rev.Lett. B* **104** (2010) 112003 [[0911.4335](#)].
- [133] N. Brambilla, A. Vairo, X. Garcia i Tormo and J. Soto, *The QCD static energy at NNNLL*, *Phys.Rev. D* **80** (2009) 034016 [[0906.1390](#)].

- [134] A.H. Hoang, A.V. Manohar and I.W. Stewart, *The Running Coulomb potential and Lamb shift in QCD*, *Phys. Rev. D* **64** (2001) 014033 [[hep-ph/0102257](#)].
- [135] A.H. Hoang and I.W. Stewart, *Ultrasoft renormalization in nonrelativistic QCD*, *Phys. Rev. D* **67** (2003) 114020 [[hep-ph/0209340](#)].
- [136] S. Necco and R. Sommer, *Testing perturbation theory on the  $N_f = 0$  static quark potential*, *Phys.Lett.* **B523** (2001) 135 [[hep-ph/0109093](#)].
- [137] C. Ayala, X. Lobregat and A. Pineda, *Determination of  $\alpha(M_z)$  from an hyperasymptotic approximation to the energy of a static quark-antiquark pair*, *JHEP* **09** (2020) 016 [[2005.12301](#)].
- [138] [TUMQCD 19] A. Bazavov, N. Brambilla, X. Garcia i Tormo, P. Petreczky, J. Soto, A. Vairo et al., *Determination of the QCD coupling from the static energy and the free energy*, *Phys. Rev. D* **100** (2019) 114511 [[1907.11747](#)].
- [139] H. Takaura, T. Kaneko, Y. Kiyo and Y. Sumino, *Determination of  $\alpha_s$  from static QCD potential with renormalon subtraction*, *Phys. Lett.* **B789** (2019) 598 [[1808.01632](#)].
- [140] H. Takaura, T. Kaneko, Y. Kiyo and Y. Sumino, *Determination of  $\alpha_s$  from static QCD potential: OPE with renormalon subtraction and Lattice QCD*, *JHEP* **04** (2019) 155 [[1808.01643](#)].
- [141] A. Bazavov, N. Brambilla, X. Garcia i Tormo, P. Petreczky, S. J. and A. Vairo, *Determination of  $\alpha_s$  from the QCD static energy: An update*, *Phys.Rev.* **D90** (2014) 074038 [[1407.8437](#)].
- [142] A. Bazavov, N. Brambilla, X. Garcia i Tormo, P. Petreczky, J. Soto et al., *Determination of  $\alpha_s$  from the QCD static energy*, *Phys.Rev.* **D86** (2012) 114031 [[1205.6155](#)].
- [143] F. Karbstein, M. Wagner and M. Weber, *Determination of  $\Lambda_{\overline{MS}}^{(n_f=2)}$  and analytic parametrization of the static quark-antiquark potential* *Determination of  $\Lambda_{\overline{MS}}^{(n_f=2)}$  and analytic parametrization of the static quark-antiquark potential*, *Phys. Rev.* **D98** (2018) 114506 [[1804.10909](#)].
- [144] F. Karbstein, A. Peters and M. Wagner,  *$\Lambda_{\overline{MS}}^{(n_f=2)}$  from a momentum space analysis of the quark-antiquark static potential*, *JHEP* **1409** (2014) 114 [[1407.7503](#)].
- [145] [ETM 11C] K. Jansen, F. Karbstein, A. Nagy and M. Wagner,  *$\Lambda_{\overline{MS}}$  from the static potential for QCD with  $N_f = 2$  dynamical quark flavors*, *JHEP* **1201** (2012) 025 [[1110.6859](#)].
- [146] N. Husung, A. Nada and R. Sommer, *Yang Mills short distance potential and perturbation theory*, *PoS LATTICE2019* (2020) 263.
- [147] N. Husung, M. Koren, P. Krah and R. Sommer,  *$SU(3)$  Yang Mills theory at small distances and fine lattices*, *EPJ Web Conf.* **175** (2018) 14024 [[1711.01860](#)].
- [148] N. Brambilla, X. Garcia i Tormo, J. Soto and A. Vairo, *Precision determination of  $r_0 \Lambda_{\overline{MS}}$  from the QCD static energy*, *Phys.Rev.Lett.* **105** (2010) 212001 [[1006.2066](#)].

- [149] G. S. Bali and K. Schilling, *Running coupling and the  $\Lambda$ -parameter from  $SU(3)$  lattice simulations*, *Phys.Rev.* **D47** (1993) 661 [[hep-lat/9208028](#)].
- [150] A. Bazavov, P. Petreczky and J. Weber, *Equation of State in 2+1 Flavor QCD at High Temperatures*, *Phys. Rev. D* **97** (2018) 014510 [[1710.05024](#)].
- [151] J.H. Weber, A. Bazavov and P. Petreczky, *Equation of state in (2+1) flavor QCD at high temperatures*, *PoS Confinement2018* (2019) 166 [[1811.12902](#)].
- [152] M. Berwein, N. Brambilla, P. Petreczky and A. Vairo, *Polyakov loop correlator in perturbation theory*, *Phys. Rev. D* **96** (2017) 014025 [[1704.07266](#)], [Addendum: *Phys.Rev.D* 101, 099903 (2020)].
- [153] W.I. Jay and E.T. Neil, *Bayesian model averaging for analysis of lattice field theory results*, *Phys. Rev. D* **103** (2021) 114502 [[2008.01069](#)].
- [154] R. Brüser, A.H. Hoang and M. Stahlhofen, *Three-Loop OPE Wilson Coefficients of Dimension-Four Operators for (Axial-)Vector and (Pseudo-)Scalar Current Correlators*, *JHEP* **12** (2024) 103 [[2408.03989](#)].
- [155] K.G. Chetyrkin, A.L. Kataev and F.V. Tkachov, *Higher Order Corrections to Sigma-t ( $e^+e^- \rightarrow \text{Hadrons}$ ) in Quantum Chromodynamics*, *Phys. Lett.* **85B** (1979) 277.
- [156] L.R. Surguladze and M.A. Samuel, *Total hadronic cross-section in  $e^+e^-$  annihilation at the four loop level of perturbative QCD*, *Phys. Rev. Lett.* **66** (1991) 560 [Erratum: *Phys. Rev. Lett.* 66,2416(1991)].
- [157] S.G. Gorishnii, A.L. Kataev and S.A. Larin, *The  $O(\alpha_s^3)$  corrections to  $\sigma_{tot}(e^+e^- \rightarrow \text{hadrons})$  and  $\Gamma(\tau^- \rightarrow \nu_\tau + \text{hadrons})$  in QCD*, *Phys. Lett.* **B259** (1991) 144.
- [158] P.A. Baikov, K.G. Chetyrkin and J.H. Kuhn, *Order  $\alpha_s^4$  QCD Corrections to Z and tau Decays*, *Phys. Rev. Lett.* **101** (2008) 012002 [[0801.1821](#)].
- [159] I. Balitsky, M. Beneke and V.M. Braun, *Instanton contributions to the  $\tau$  decay widths*, *Phys.Lett.* **B318** (1993) 371 [[hep-ph/9309217](#)].
- [160] K. Chetyrkin and A. Maier, *Massless correlators of vector, scalar and tensor currents in position space at orders  $\alpha_s^3$  and  $\alpha_s^4$ : Explicit analytical results*, *Nucl. Phys. B* **844** (2011) 266 [[1010.1145](#)].
- [161] [JLQCD/TWQCD 08C] E. Shintani et al., *Lattice study of the vacuum polarization function and determination of the strong coupling constant*, *Phys.Rev.* **D79** (2009) 074510 [[0807.0556](#)].
- [162] R.J. Hudspith, R. Lewis, K. Maltman and E. Shintani, *Determining the QCD coupling from lattice vacuum polarization*, in *Proceedings, 33rd International Symposium on Lattice Field Theory (Lattice 2015)*, vol. LATTICE2015, p. 268, 2016, <http://inspirehep.net/record/1398355/files/arXiv:1510.04890.pdf> [[1510.04890](#)].
- [163] [RBC/UKQCD 14B] T. Blum et al., *Domain wall QCD with physical quark masses*, *Phys. Rev.* **D93** (2016) 074505 [[1411.7017](#)].

- [164] R. Hudspith, R. Lewis, K. Maltman and E. Shintani,  $\alpha_s$  from the Hadronic Vacuum Polarisation, *EPJ Web Conf.* **175** (2018) 10006.
- [165] [HPQCD 05A] Q. Mason et al., Accurate determinations of  $\alpha_s$  from realistic lattice QCD, *Phys. Rev. Lett.* **95** (2005) 052002 [[hep-lat/0503005](#)].
- [166] K. Hornbostel, G. Lepage and C. Morningstar, Scale setting for  $\alpha_s$  beyond leading order, *Phys.Rev.* **D67** (2003) 034023 [[hep-ph/0208224](#)].
- [167] [HPQCD 10] C. McNeile, C. T. H. Davies, E. Follana, K. Hornbostel and G. P. Lepage, High-precision  $c$  and  $b$  masses and QCD coupling from current-current correlators in lattice and continuum QCD, *Phys. Rev.* **D82** (2010) 034512 [[1004.4285](#)].
- [168] K. Maltman, D. Leinweber, P. Moran and A. Sternbeck, The realistic lattice determination of  $\alpha_s(M_Z)$  revisited, *Phys. Rev.* **D78** (2008) 114504 [[0807.2020](#)].
- [169] [QCDSF/UKQCD 05] M. Göckeler, R. Horsley, A. Irving, D. Pleiter, P. Rakow, G. Schierholz et al., A determination of the Lambda parameter from full lattice QCD, *Phys.Rev.* **D73** (2006) 014513 [[hep-ph/0502212](#)].
- [170] [SESAM 99] A. Spitz et al.,  $\alpha_s$  from upsiion spectroscopy with dynamical Wilson fermions, *Phys.Rev.* **D60** (1999) 074502 [[hep-lat/9906009](#)].
- [171] M. Wingate, T.A. DeGrand, S. Collins and U.M. Heller, From spectroscopy to the strong coupling constant with heavy Wilson quarks, *Phys.Rev.* **D52** (1995) 307 [[hep-lat/9501034](#)].
- [172] C. T. H. Davies, K. Hornbostel, G. Lepage, A. Lidsey, J. Shigemitsu et al., A precise determination of  $\alpha_s$  from lattice QCD, *Phys.Lett.* **B345** (1995) 42 [[hep-ph/9408328](#)].
- [173] S. Aoki, M. Fukugita, S. Hashimoto, N. Ishizuka, H. Mino et al., Manifestation of sea quark effects in the strong coupling constant in lattice QCD, *Phys.Rev.Lett.* **74** (1995) 22 [[hep-lat/9407015](#)].
- [174] M. Kitazawa, T. Iritani, M. Asakawa, T. Hatsuda and H. Suzuki, Equation of State for  $SU(3)$  Gauge Theory via the Energy-Momentum Tensor under Gradient Flow, *Phys. Rev.* **D94** (2016) 114512 [[1610.07810](#)].
- [175] [FlowQCD 15] M. Asakawa, T. Iritani, M. Kitazawa and H. Suzuki, Determination of Reference Scales for Wilson Gauge Action from Yang–Mills Gradient Flow, [1503.06516](#).
- [176] A. X. El-Khadra, G. Hockney, A.S. Kronfeld and P.B. Mackenzie, A determination of the strong coupling constant from the charmonium spectrum, *Phys.Rev.Lett.* **69** (1992) 729.
- [177] [QCDSF/UKQCD 04A] M. Göckeler, R. Horsley, A. Irving, D. Pleiter, P. Rakow, G. Schierholz et al., Determination of  $\Lambda$  in quenched and full QCD: an update, *Nucl.Phys.Proc.Suppl.* **140** (2005) 228 [[hep-lat/0409166](#)].
- [178] S. Booth, M. Göckeler, R. Horsley, A. Irving, B. Joo, S. Pickles et al., The strong coupling constant from lattice QCD with  $N_f = 2$  dynamical quarks, *Nucl.Phys.Proc.Suppl.* **106** (2002) 308 [[hep-lat/0111006](#)].

- [179] [QCDSF/UKQCD 01] S. Booth, M. Göckeler, R. Horsley, A. Irving, B. Joo, S. Pickles et al., *Determination of  $\Lambda_{\overline{\text{MS}}}$  from quenched and  $N_f = 2$  dynamical QCD*, *Phys.Lett. B* **519** (2001) 229 [[hep-lat/0103023](#)].
- [180] R. Sommer, *Scale setting in lattice QCD*, *PoS LATTICE2013* (2014) 015 [[1401.3270](#)].
- [181] [HPQCD 03A] C. T. H. Davies et al., *High-precision lattice QCD confronts experiment*, *Phys. Rev. Lett.* **92** (2004) 022001 [[hep-lat/0304004](#)].
- [182] Q.J. Mason, *High-precision lattice QCD: Perturbations in a non-perturbative world*, Ph.D. thesis, Cornell U., LNS, 2004.
- [183] K. Maltman, *Two recent high-precision determinations of  $\alpha(s)$* , *AIP Conf. Proc.* **1261** (2010) 159.
- [184] [HPQCD 08B] I. Allison et al., *High-precision charm-quark mass from current-current correlators in lattice and continuum QCD*, *Phys. Rev. D* **78** (2008) 054513 [[0805.2999](#)].
- [185] A. Bochkarev and P. de Forcrand, *Determination of the renormalized heavy quark mass in lattice QCD*, *Nucl.Phys. B* **477** (1996) 489 [[hep-lat/9505025](#)].
- [186] [HPQCD 14A] B. Chakraborty, C.T.H. Davies, G.C. Donald, R.J. Dowdall, B. Galloway, P. Knecht et al., *High-precision quark masses and QCD coupling from  $n_f = 4$  lattice QCD*, *Phys.Rev. D* **91** (2015) 054508 [[1408.4169](#)].
- [187] [JLQCD 16] K. Nakayama, B. Fahy and S. Hashimoto, *Short-distance charmonium correlator on the lattice with Möbius domain-wall fermion and a determination of charm quark mass*, *Phys. Rev. D* **94** (2016) 054507 [[1606.01002](#)].
- [188] B. Dehnadi, A.H. Hoang and V. Mateu, *Bottom and Charm Mass Determinations with a Convergence Test*, *JHEP* **08** (2015) 155 [[1504.07638](#)].
- [189] R. Boughezal, M. Czakon and T. Schutzmeier, *Charm and bottom quark masses from perturbative QCD*, *Phys.Rev. D* **74** (2006) 074006 [[hep-ph/0605023](#)].
- [190] A. Maier, P. Maierhofer and P. Marquard, *The second physical moment of the heavy quark vector correlator at  $O(\alpha_s^3)$* , *Phys.Lett. B* **669** (2008) 88 [[0806.3405](#)].
- [191] A. Maier, P. Maierhofer, P. Marquard and A. Smirnov, *Low energy moments of heavy quark current correlators at four loops*, *Nucl.Phys. B* **824** (2010) 1 [[0907.2117](#)].
- [192] Y. Kiyo, A. Maier, P. Maierhofer and P. Marquard, *Reconstruction of heavy quark current correlators at  $O(\alpha_s^3)$* , *Nucl.Phys. B* **823** (2009) 269 [[0907.2120](#)].
- [193] Y. Maezawa and P. Petreczky, *Quark masses and strong coupling constant in 2+1 flavor QCD*, *Phys. Rev. D* **94** (2016) 034507 [[1606.08798](#)].
- [194] P. Petreczky and J. Weber, *Strong coupling constant and heavy quark masses in (2+1)-flavor QCD*, *Phys. Rev. D* **100** (2019) 034519 [[1901.06424](#)].
- [195] J.H. Kühn, M. Steinhauser and C. Sturm, *Heavy quark masses from sum rules in four-loop approximation*, *Nucl. Phys. B* **778** (2007) 192 [[hep-ph/0702103](#)].



- [196] K. Chetyrkin, J. Kuhn, A. Maier, P. Maierhofer, P. Marquard et al., *Charm and Bottom Quark Masses: An Update*, *Phys.Rev.* **D80** (2009) 074010 [[0907.2110](#)].
- [197] D. Boito and V. Mateu, *Precise determination of  $\alpha_s$  from relativistic quarkonium sum rules*, *JHEP* **03** (2020) 094 [[2001.11041](#)].
- [198] [HPQCD 13A] R. Dowdall, C. Davies, G. Lepage and C. McNeile,  *$V_{us}$  from  $\pi$  and  $K$  decay constants in full lattice QCD with physical  $u$ ,  $d$ ,  $s$  and  $c$  quarks*, *Phys.Rev.* **D88** (2013) 074504 [[1303.1670](#)].
- [199] L. Chimirri and R. Sommer, *Investigation of the Perturbative Expansion of Moments of Heavy Quark Correlators for  $N_f = 0$* , *PoS LATTICE2021* (2022) 354 [[2203.07936](#)].
- [200] R. Sommer, L. Chimirri and N. Husung, *Log-enhanced discretization errors in integrated correlation functions*, *PoS LATTICE2022* (2023) 358 [[2211.15750](#)].
- [201] M. Lüscher and P. Weisz, *Perturbative analysis of the gradient flow in non-abelian gauge theories*, *JHEP* **02** (2011) 051 [[1101.0963](#)].
- [202] Z. Fodor, K. Holland, J. Kuti, D. Nogradi and C.H. Wong, *A new method for the beta function in the chiral symmetry broken phase*, *EPJ Web Conf.* **175** (2018) 08027 [[1711.04833](#)].
- [203] D. Boito and V. Mateu, *Precise  $\alpha_s$  determination from charmonium sum rules*, *Phys. Lett. B* **806** (2020) 135482 [[1912.06237](#)].
- [204] S. Zafeiropoulos, P. Boucaud, F. De Soto, J. Rodríguez-Quintero and J. Segovia, *Strong Running Coupling from the Gauge Sector of Domain Wall Lattice QCD with Physical Quark Masses*, *Phys. Rev. Lett.* **122** (2019) 162002 [[1902.08148](#)].
- [205] [FLAG 21] Y. Aoki et al., *FLAG Review 2021*, *Eur. Phys. J. C* **82** (2022) 869 [[2111.09849](#)].
- [206] [ETM 13D] B. Blossier et al., *High statistics determination of the strong coupling constant in Taylor scheme and its OPE Wilson coefficient from lattice QCD with a dynamical charm*, *Phys.Rev.* **D89** (2014) 014507 [[1310.3763](#)].
- [207] [ETM 12C] B. Blossier, P. Boucaud, M. Brinet, F. De Soto, X. Du et al., *The strong running coupling at  $\tau$  and  $Z_0$  mass scales from lattice QCD*, *Phys.Rev.Lett.* **108** (2012) 262002 [[1201.5770](#)].
- [208] [ETM 11D] B. Blossier, P. Boucaud, M. Brinet, F. De Soto, X. Du et al., *Ghost-gluon coupling, power corrections and  $\Lambda_{\overline{\text{MS}}}$  from lattice QCD with a dynamical charm*, *Phys.Rev.* **D85** (2012) 034503 [[1110.5829](#)].
- [209] K. Nakayama, H. Fukaya and S. Hashimoto, *Lattice computation of the Dirac eigenvalue density in the perturbative regime of QCD*, *Phys. Rev.* **D98** (2018) 014501 [[1804.06695](#)].
- [210] K.G. Chetyrkin, G. Falcioni, F. Herzog and J.A.M. Vermaseren, *Five-loop renormalisation of QCD in covariant gauges*, *JHEP* **10** (2017) 179 [[1709.08541](#)], [Addendum: JHEP 12, 006 (2017)].

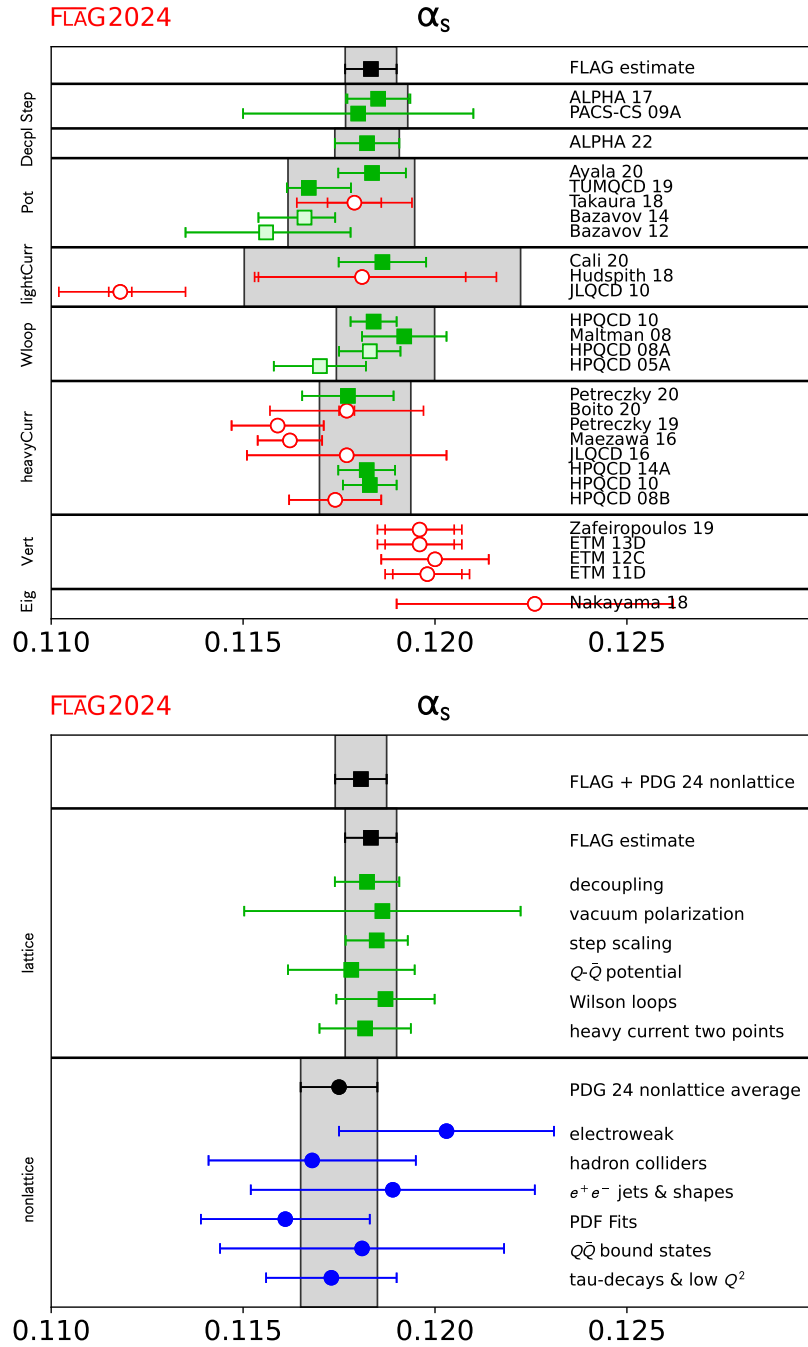


Figure 40:  $\alpha_{\overline{\text{MS}}}^{(5)}(M_Z)$ , the coupling constant in the  $\overline{\text{MS}}$  scheme at the  $Z$ -boson mass. Top: lattice results, pre-ranges from different calculation methods, and final average. Bottom: Comparison of the lattice pre-ranges and average with the nonlattice ranges and average. The first PDG 24 entry gives the outcome of their analysis excluding lattice results. At the very top we display the weighted average of PDG 24 nonlattice and FLAG lattice estimates, with the error taken from the FLAG estimate (statistics dominated), see Sec. 9.10.3.